THE EFFECT OF SAMPLING PROCEDURES ON ORGANIC AEROSOL MEASUREMENT

Stephen Robert McDow
B.A., University of California, Santa Cruz, 1980

A dissertation submitted to the faculty
of the Oregon Graduate Center
in partial fulfillment of the
requirements for the degree
Doctor of Philosophy
in
Environmental Science

January 1986

The dissertation "The Effect of Sampling Procedures on Organic Aerosol Measurement" by Stephen Robert McDow has been examined and approved by the following Examination Committee.

James J. Huntzicker, Thesis Advisor
Professor

James F. Pankow
Professor

Richard L. Johnson
Assistant Professor

Douglas F. Barofsky
Associate Professor, Oregon State University

DEDICATION

To my mother and father

ACKNOWLEDGEMENTS

I would like to extend my sincere thanks and appreciation to Dr. James Huntzicker for his guidance and support in all aspects of this research and of my education at Oregon Graduate Center.

John Rau, Lorne Isabelle and Fred Thone provided much needed advice and assistance in the construction of the sampler. I am also indebted to John Rau and Bob Cary for their instruction in operation of the carbon analyzer.

For advice and assistance regarding the use of gas chromatography/mass spectrometry I am grateful to Dr. James Pankow and Mary Ligocki and especially to Lorne Isabelle who provided hours of excellent instruction and encouragement.

The Oregon Department of Environmental Quality provided the sampling site. I am especially indebted for this to Dennis Duncan and Mike Keller.

Thanks to Ken Hart and Barbara Turpin for hours of technical discussion about possible explanations of the results.

I am grateful for the efforts of Dorothy Malek and Carol Hendrickson.

The constant inspiration and support of Professors James Pankow and Douglas Barofsky have been greatly appreciated throughout my time as a student at OGC.

Finally, special thanks to Bill Asher, Ken Hart, Henry Kalinoski, Emily Heyerdahl, Mike Rosen, Ge Su, Allison Bollman, Trish Quinn and Lorne Isabelle for their encouragement and friendship.

CONTENTS

LIST OF TABLES

LIST OF FIGURES

ABSTRACT

THE EFFECT OF SAMPLING PROCEDURES ON
ORGANIC AEROSOL MEASUREMENT

Stephen Robert McDow, Ph.D.
Oregon Graduate Center, 1986

Dissertation Advisor: Dr. J. J. Huntzicker

The effects of face velocity, sampling duration and filter type on apparent concentrations of atmospheric particulate organic matter have been investigated. This was accomplished by collection of ambient samples with a low volume sampling apparatus capable of collecting six simultaneous samples. Samples were analyzed by thermal-optical analysis for organic and elemental carbon.

All of the sampling parameters investigated had a significant effect on the measured concentration of organic aerosol. The apparent concentration of organic aerosol collected by quartz fiber filters decreased with increasing face velocity by 1.2 to 2.5 $\mu gC/m^3$ for the face velocity range 15-150 cm/s and organic carbon concentrations of 3.1 to 15.0 $\mu g/m^3$. Apparent organic carbon concentrations were an average of 19% higher for samples collected for 24 hour than for 48 hour sampling durations.

Adsorption of organic vapor by the filter medium is the most reasonable explanation for the observed differences in apparent organic carbon concentration. The adsorption artifact was estimated from carbon collected on quartz fiber back-up filters behind either quartz fiber or Teflon membrane primary aerosol filters. More than 80% of

the variation in apparent concentration with face velocity was accounted for by estimates of adsorption artifact. Adsorbed vapor also accounted for a significantly higher fraction of organic mass collected for 24 than for 48 hour sampling durations, and more organic vapor was observed on quartz fiber than on simultaneously sampled Teflon membrane filters.

For samples collected on quartz fiber filters at a face velocity of 40 cm/s for a 24 hour sampling period, adsorbed vapors accounted for a lower limit of 10-15% of the collected organic carbon for a typical organic aerosol concentration of about 7 $\mu g/m^3$. At lower concentrations and lower face velocities this percentage was significantly higher, and in some cases more carbonaceous vapor than aerosol was collected. A simple fluid dynamics-adsorption kinetics model is presented in order to explain the observations. n-Alkanes ranging from tetradecane (C-14) to tetracosane (C-24) are among the compounds responsible for organic vapor adsorption.

The observation of a significant adsorption artifact suggests that organic aerosol concentrations may be seriously overestimated by conventional aerosol sampling techniques, especially at low organic aerosol concentrations. Adsorption can be minimized by using high face velocities, long sampling durations and/or Teflon membrane filters in place of glass or quartz fiber filters.

CHAPTER I - INTRODUCTION

Since the discovery of the carcinogenic properties of benzene-extractable particulate matter (Leiter and Shear, 1942), substantial research has been focused on the characterization of organic aerosol. The observation of the potent carcinogen, benzo-(a)pyrene (Hieger, 1946) and other polycyclic aromatic hydrocarbons (PAHs) (Hoffman and Wynder, 1968) in atmospheric aerosol initiated extensive research on atmospheric PAHs.

As the scope of interest in atmospheric aerosols has increased to include studies on physical, chemical, and biological properties of suspended particulate matter in general, it has become practical for many applications to consider the organic fraction without further specification of its composition. Techniques for rapid analysis of particulate organic carbon have recently been developed (Grosjean, 1975; Appel et al., 1976; Cadle et al., 1980; Huntzicker et al., 1982; Johnson et al., 1982; Tanner et al., 1982).

Two major artifact errors are associated with the application of conventional high volume sampling to collection of particulate organic matter. These relate to the volatilization of particulate organic matter during sampling and adsorption of ambient organic vapors on filter materials. An inadequate understanding of these phenomena still impedes progress toward the capability of accurate measurement of organic aerosol concentrations.

A. Volatilization of Collected Particulate Matter

Early investigations into the efficiency of PAH collection by filtration using glass fiber material revealed that significant volatilization from samples occurred during prolonged exposure to particle-free laboratory air (Commins, 1962; Rondia, 1965). This phenomenon has subsequently been referred to as the "blow-off" effect (Brodding et al., 1980; Konig et al., 1980; Van Vaeck et al., 1984). PAH volatilization however was not observed from smoke samples on which strong adsorption by collected "soot" might occur (Commins, 1962; Thomas et al., 1968). Volatilization of n-alkanes and carboxylic acids after exposure to a stream of nitrogen has also been observed (Van Vaeck et al., 1984). The magnitude of volatilization loss for some compounds can be as high as 70% (Van Vaeck et al., 1984). It is not clear from "blow-off" experiments on the various organic species what fraction of the total organic mass collected is affected by "blow-off".

Since PAHs and other organic compounds susceptible to loss by volatilization have been observed in the vapor phase in the atmosphere (Cautreels and Van Cauwenberghe, 1978; Van Vaeck et al., 1984; Ligocki et al., 1985), it is likely that their condensation or adsorption on collected particulate matter serves to replace material volatilized during sampling. Consequently, experiments in which samples are exposed to cleaner laboratory air or nitrogen probably represent an upper limit to volatilization during sampling, but it is not clear from these types of experiments whether volatilization

should be expected during typical ambient conditions.

The possibility of volatilization during sampling has thus given rise to a number of investigations to determine the effect of sampling conditions on collection of particulate organic matter. Della Fiorentina et al. (1975) demonstrated an inverse relationship between sampling face velocity and apparent concentration of non-volatile hydrocarbons measured by infrared absorbance and concluded that extensive volatilization of sample occurred at higher face velocities. Observations of an inverse relationship between apparent concentrations of solvent-extractable particulate matter and duration of sampling period have been observed and interpreted to indicate that sampling efficiency of particulate organic matter decreases with longer sampling periods (Appel et al., 1979; Schwartz et al., 1981). An average of 21% more total extractable mass was collected over seven two-hour sampling periods than from a simultaneous fourteen-hour sampling period (Appel et al., 1979). However, for non-polar compounds apparent concentrations generally increased with duration of sampling period. Adsorption of organic vapors on collected particulate matter has been offered as a possible explanation for this observation (Schwartz et al., 1981; Appel et al., 1979).

Chemical reactions can constitute an important sampling error which can potentially be confused with volatilization loss. Peters and Seifert (1980) compared two PAHs of differing volatility, benzo(a)pyrene and coronene, and demonstrated that chemical reaction was a more important loss mechanism than volatilization for the more

volatile benzo(a)pyrene. Nitration (Pitts et al., 1978) and epoxidation (Pitts et al., 1980) of some PAHs have been observed during sampling and might be catalyzed by filter substrates (Pitts et al., 1978; Lee et al., 1980). Although reaction artifacts can affect the measurement of individual species or classes of organic compounds (Schwartz et al., 1981), loss of total organic carbon measured by thermal analysis should not be expected unless reaction products are more volatile than their precursors. This is not likely for oxidation or nitration reactions. However, not all of the observed losses of PAHs from samples can be attributed to chemical reactions. Konig et al., (1980) have observed that the correlation between variations in apparent concentrations with sampling duration is more pronounced for PAHs of lower volatility. They concluded that reaction artifact could be ruled out as an explanation for differences in apparent concentration with sampling period for relatively volatile PAHs.

Theoretical aspects of volatilization during sampling have received limited attention. Klippel and Warneck (1980) postulated that atmospheric vapor-particulate equilibria are generally established rapidly. They maintained that at atmospheric equilibrium the only mechanism which could be responsible for volatilization loss is the disturbance of equilibrium during a particle's collision with the filter and that large disturbances of equilibrium during sampling were unlikely.

Pupp et al., (1974) predicted significant losses of five PAHs on the basis of their equilibrium vapor concentration. However,

these estimates were substantially higher than experimental volatilization losses observed by Commins (1962) and Rondia (1965). Pupp et al. proposed two possible explanations for the differences. First, the partitioning of a species between a condensed phase in collected particulate matter and a vapor phase in air passing through the filter might not be at equilibrium. This condition would be expected for species with slow vaporization rates from ambient particulate matter. In this case, volatilization from the sample would be governed by the kinetics of sublimation. At slow flow rates, equilibrium vapor concentrations could be attained in the air stream passing through the filter, and the rate of volatilization would be limited by flow rate. At flow rates too fast for attainment of equilibrium vapor concentrations, the volatilization rate would be limited by sublimation rate. The second possibility is that the system reaches equilibrium rapidly, but that observed volatilization loss is less than expected because adsorption on aerosol surfaces is not included in equilibrium calculations.

Consideration of the extent to which volatilized material is replaced by vapor adsorption on collected particles has received less attention. In the vapor-particulate equilibrium state, it is not clear why equilibrium should be altered during sampling to promote volatilization. Alternatively, non-equilibrium conditions of enrichment in either the vapor or particulate phase are equally likely. Yet comparisons of apparent concentrations of organic particulate matter at different face velocities and sampling durations consistently indicate lower apparent concentrations for higher face velocities and

longer sampling periods. Consequently, the explanation of these observations might require other considerations in addition to vapor-particulate phase distribution.

B. Adsorption of Organic Vapor

Inorganic vapor phase constituents have long been noted as possible interferents during collection of aerosol by glass fiber filters (Scaringelli and Rehme, 1969). Spicer and Schumacher (1977) estimated that the mass of artifact nitrate was as much as ten to twenty times actual particulate nitrate collected. Coutant (1977) estimated that from 0.3 to 3 $\mu g/m^3$ of sulfate collected on glass fiber filters resulted from sorption and subsequent oxidation of sulfur dioxide. Witz and Wendt (1981) compared sulfate mass between glass, Teflon-coated glass, and quartz fiber filters for 24 hour samples over approximately a two month period and reported average artifact sulfate and nitrate concentrations of 2.0 and 8.3 $\mu g/m^3$, respectively.

Stevens et al. (1980) included total carbon measurements in estimates of vapor adsorption artifacts on glass fiber filters and found artifact concentrations of 0.3 to 1.1 $\mu g/m^3$. These results were used by Witz et al. (1983) as a possible explanation for an average difference of 8.6 $\mu g/m^3$ in aerosol mass concentration between two types of glass fiber filters of different alkalinities after accounting for sulfate and nitrate differences. They suggested that neutral quartz fiber filters could possibly be used to prevent adsorption. Kawamura et al. (1985) have since observed that quartz fiber filters

are inefficient collectors of atmospheric formic acid. In contrast, Cadle et al. (1983) have reported that adsorbed vapor accounted for an average of 15% of organic carbon collected on quartz fiber filters. Their comparison of vapor carbon artifact between several filter types indicated significant organic vapor artifact for glass fiber and silver membrane filters also. Adsorbed formaldehyde (Klippel and Warneck, 1980) and n-alkanes (Eichmann et al., 1979) have been observed on glass fiber filters.

C. Sampling Considerations

A variety of solutions have been proposed to avoid or minimize sampling artifacts. Filters have been impregnated with glycerol-tricaprylate in order to increase collection efficiency (Brockhaus, 1974; Konig et al., 1980). Adsorbents such as polyurethane foam (Thrane and Mikalsen, 1981) and Tenax-GC (Van Vaeck et al., 1984) have been mounted downstream of aerosol filters to collect organic vapors not collected or retained by filters. While these sampling methods may provide more accurate measurements of total atmospheric concentrations, their use for obtaining information about the physical state of samples in the atmosphere requires additional specialized sampling procedures and careful interpretation (Van Vaeck et al., 1984; Van Vaeck and Van Cauwenberghe, 1985). For collection of particulate matter only, sampling at low face velocities (Della Fiorentina et al., 1975; De Wiest and Della Fiorentina, 1976) and frequent filter replacement, as with the automatic procedure devised by Van Vaeck et al. (1984), have been advocated as a means of minimizing volatiliza-

tion. Tu (1984) reported that sample volatilization could be largely avoided by the use of an ultra-high volume liquid electrostatic aerosol precipitator sampler. Organic vapor adsorption has been avoided by diffusion stripping (Appel et al., 1983), but this could promote aerosol volatilization by disruption of the vapor-particulate equilibrium.

Although the possibility of both positive and negative artifacts during sampling poses a major difficulty in the selection of sampling procedures for organic aerosol, no comparison of the relative importance of volatilization and adsorption is available. Because compounds susceptible to volatilization during sampling generally have an atmospheric vapor phase component (Van Vaeck et al., 1984), it is possible that these compounds might be partially responsible for adsorption of organic vapors observed on filter material. Consequently, adsorption on the filter substrate should also be considered in explanations of variations in apparent particulate phase concentrations with sampling period and face velocity.

The results of early experiments on PAH volatilization (Commins, 1962; Rondia, 1965) have been used extensively in explanations of possible loss mechanisms for particulate organic matter (Appel et al., 1979; Schwartz et al., 1981) and many specific organic compounds (Pupp et al., 1974; Della Fiorentia et al., 1975; De Wiest and Della Fiorentina, 1975; Broddin et al., 1980; Konig et al., 1980; Van Vaeck et al., 1984) during ambient sampling. The consideration of an organic vapor adsorption artifact complicates the interpretation of results of these early volatilization experiments.

Commins (1962) and Rondia (1965) were more concerned with the collection efficiency than with the physical state of PAHs. This distinction may not have always seemed important since PAHs had not been detected in the vapor phase when they were first observed in atmospheric particulate matter (Commins, 1962). However, PAH "loss" reported from filters has sometimes been used to refer to the sum of vapor phase material not collected by filtration and loss of condensed material, since it is not always possible to distinguish between these two PAH "loss" mechanisms (Pupp et al., 1974; Konig et al., 1980). These considerations suggest that it is not valid to assume that loss from aerosol filters consists only of organic material volatilized from particulate matter. It may also include volatilization of vapors adsorbed on the filter itself.

These considerations underscore the need for a systematic comparison of the relative importance of sampling artifacts under a variety of sampling conditions. The development of an optimum organic aerosol sampling procedure requires not only a comparison of apparent concentrations of particulate organic matter under a variety of sampling conditions, but also an explanation of observed differences based on investigations of the role of both positive and negative sampling artifacts. Observations and explanations of the effects of face velocity, filter type and sampling period on apparent concentration of organic particulate matter, on organic vapor adsorption, and on volatilization of collected particulate organic matter are presented here.

CHAPTER II - SAMPLING AND ANALYSIS METHODS

A. Sampling Apparatus

A sampling apparatus was constructed with which six samples could be collected simultaneously from a common manifold (Fig. 2.1). Each of the six sampling ports was equipped with 1) a 60 cm tall, 4.45 cm diameter aluminum delivery tube, 2) a 47 mm aluminum filter holder, 3) a regulating valve and 4) a Dwyer VFB-67 rotameter (Dwyer Instruments, Inc., Michigan City, Indiana) connected in series. Air was pumped through the six sampling ports with three Gast 0522 rotary vane oilless vacuum pumps (Gast Manufacturing Corp., Benton Harbor, Michigan). Viton O-rings were used to seal connections between sampling tubes and filter holders and to seal the filter holders during sampling.

The delivery tubes were enclosed in a cylindrical aluminum manifold, 2 m in height and 20 cm in diameter. The sampling manifold was covered by an aluminum rain cap. The primary air flow in the manifold was maintained by drawing (unsampled) air through it with a Grainger 2C782 shaded pole blower (Grainger Manufacturing, Medway, Massachusetts). This arrangement required that the blower and filter holders be mounted at the base of the sampling manifold in close proximity. Consequently, long delivery tubes were attached to the filter holders to minimize the effect of blower induced streamline changes at the sampling port entrance (See Fig. 2.1).

Figure 2.2 depicts a schematic of the filter holders which were located at the bottom of the delivery tubes. Filters were pressed

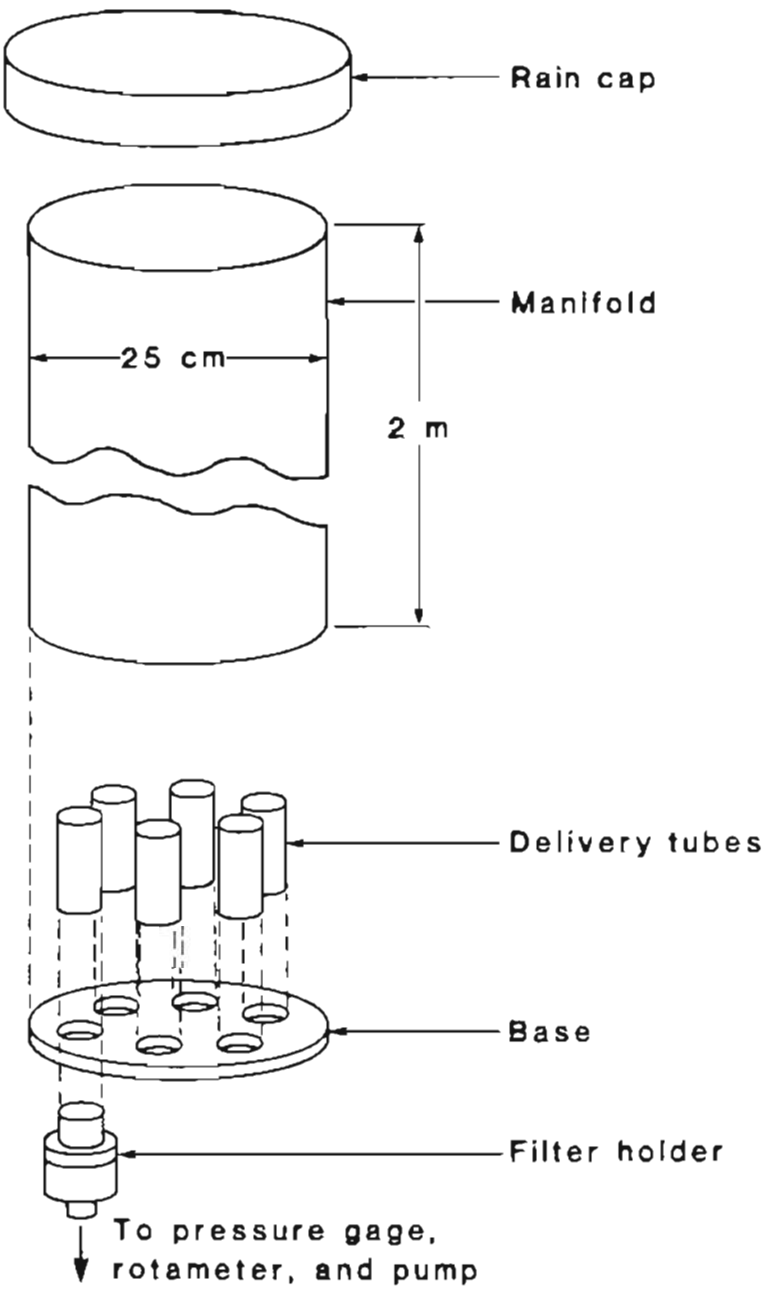

Figure 2.1. Sampling manifold

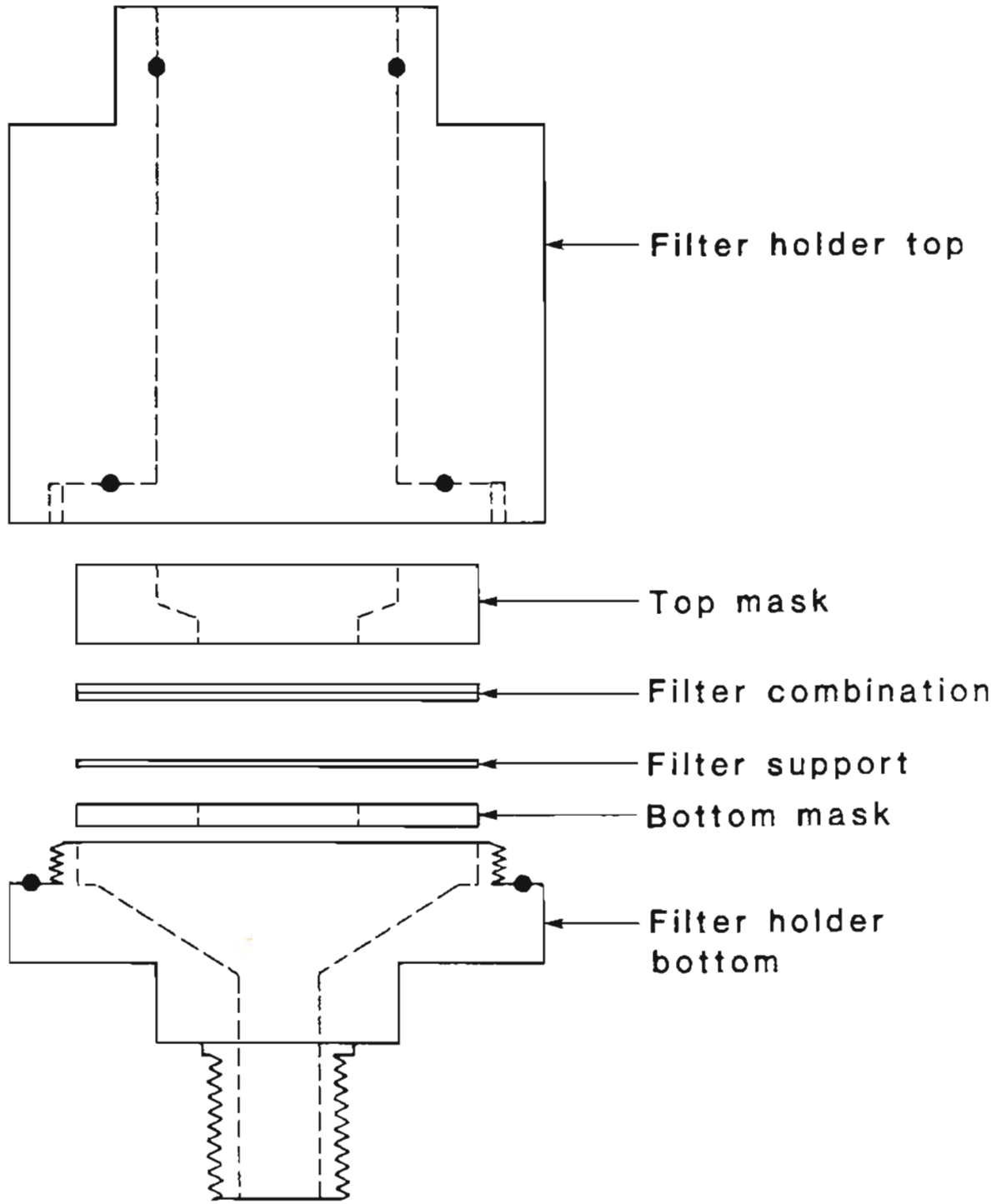

Figure 2.2. Aerosol filter holder with annular masks. The solid black circles are O-rings.

between two masks with a tight seal achieved by a Viton O-ring between the top mask and the filter holder. The masks were annular constructions of aluminum which served to obstruct flow through an outer portion of the filter. Flow was diverted only through the central unmasked portion of the filter. For all experiments the volumetric flow was the same for all six ports, and the filter face velocity was varied between sampling ports by using masks with different inner diameters.

A tee and snap valve upstream of the regulating valve and rotameter in each sampling port provided optional connection to any of four Dwyer Magnehelic pressure gauges (Dwyer Instruments Inc., Michigan City, Indiana) with removable Tygon tubing. Pressure gauges with a variety of ranges were selected for measurement of a wide range of pressure drops with a high degree of relative precision.

A 1 μm impactor was placed at the entrance to each delivery tube to minimize possible optical interferences associated with coarse particles during carbon analysis (see Section II.E.). The effect on the collection of organic aerosol was expected to be minimal since particulate organic matter is predominantly associated with fine particles (Appel et al., 1976; Van Vaeck and Van Cauwenberghe, 1978).

The multiple sampling port configuration permitted the investigation of the effects of face velocity, sampling duration and sampling media on the collection of organic particulate matter. In the sampling duration experiments the first set of three sampling ports was operated for a period of between six and forty-eight hours without replacing filters. The second set of three filters was subdivided into two parts by replacing the filters half-way through the sampling period. The sum

of the mass collected during the two shorter sampling periods was compared to mass collected with the longer sampling period.

For filter type comparisons, Pallflex QAOT quartz fiber (Pall Corporation, Glen Cove, New York), Gelman A/E glass fiber (Gelman Sciences, Ann Arbor, Michigan), and Membrana Zefluor Teflon backed Teflon membrane filters (Membrana Corp., Pleasanton, California) were used.

All ambient samples were collected on the roof of the Central Fire Station at 55 S.W. Ash Street in downtown Portland, Oregon. For all ambient samples the flow rate through each sampling port was set to within 0.1 l/min of 8.9 l/min. This was accomplished by calibrating the rotameters with a dry test meter while simulating the pressure drop across impactors, face velocity masks, and filters with a regulating valve between the dry test meter and rotameter. In general, flow rates were set at the commencement of sampling and remained constant throughout the sampling period. For a few samples, the pressure drop across the filter increased during sampling, causing a decrease in flow rate. For these samples rotameters were calibrated at flow rates and pressure drops corresponding to those observed at the end as well as the beginning of the sampling period, and the initial and final flow rates were averaged.

The sampling apparatus was designed to accommodate more than one filter in each filter holder. Analysis of back-up filters provided estimates of the mass of carbonaceous vapor adsorbed. This technique has been used by Stevens et al. (1980) and Cadle et al. (1983).

To investigate volatilization of collected organic matter from aerosol filters during sampling, sampling ports were connected to an Aadco Model 737 High Volume Pure Air Generator capable of generating air with less than 5 ppb of hydrocarbons and less than 300 ppb of carbon dioxide. The purified air was blown through previously collected ambient samples (Fig. 2.3).

B. Thermal-Optical Carbon Analysis

Before sampling, quartz fiber filters were baked for at least two hours at 500°C. No improvement in blank levels was observed for longer baking periods. Filters were stored at -10°C within 30 minutes after sampling. A blank filter, designated as the storage blank, was also baked with each sample set and was immediately stored. The storage blank was analyzed at the same time as the samples.

Samples were analyzed by thermal-optical carbon analysis using the OGC carbon analyzer (Johnson et al., 1982; Huntzicker et al., 1982; Johnson, 1981). In normal operation a two part procedure is used to measure both organic and elemental carbon. This method compares favorably with other methods of analysis for both organic and elemental carbon (Johnson, 1981; Japar et al., 1984).

Between one and six 0.25 cm^2 disks were removed from sample filters and inserted into a temperature programmable oven. The amount of sample analyzed depended on the amount of unmasked filter available. In the first phase, organic carbon was removed from samples in helium in two or more temperature steps from 300 to 650°C. This was followed by 1) oxidation to carbon dioxide in a packed manganese

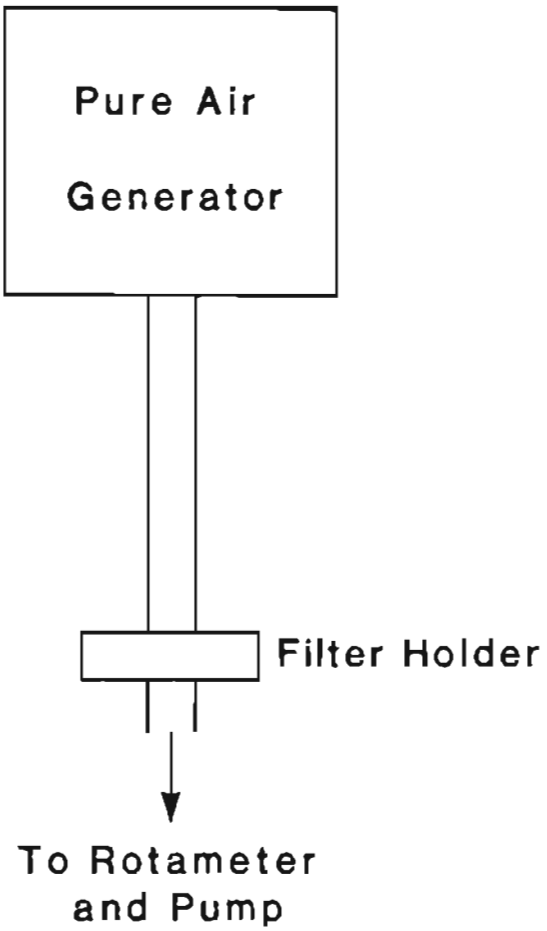

Figure 2.3. Volatilization apparatus

dioxide bed, and 2) methanation using a firebrick supported nickel catalyst. In the second phase the process was repeated for elemental carbon combustion in a gas mixture of 2% oxygen in helium and removal temperatures stepped from 400 to 750°C. The resultant methane was measured by a flame ionization detector. Each run was individually calibrated by injection of a known amount of methane. The flame ionization detector is not susceptible to significant interference from inorganic compounds generated from samples during analysis (McNair and Gonelli, 1968) and exhibits linear sensitivity over a wide concentration range (David, 1974). Masses of organic and elemental carbon were calculated after analog to digital conversion of the detector signal.

Formation of elemental carbon by pyrolysis during analysis of organic carbon is a common problem associated with thermal organic carbon analysis (Cadle and Groblicki, 1982; Huntzicker et al., 1982). Correction for this pyrolytically generated elemental carbon was accomplished by continuously monitoring the accompanying decrease in the reflectance of the filter to 633 nm He-Ne laser light during organic carbon analysis. The mass of elemental carbon oxidized before the reflectance returned to its initial value during the elemental carbon oxidation was considered organic carbon. Sample analysis was accomplished in 1660 seconds. This mode of operation, which is designated as the "normal analysis mode," was used for primary (or aerosol) filters.

Back-up filters, which were used to collect adsorptive organic vapors, were analyzed for total carbon only by oxidation at 750°C

for 140 seconds. This type of analysis is designated as the "total carbon mode." This method provided improved precision over the normal analysis mode for lightly loaded samples. All carbon measured was considered organic. This assumption was verified by analyzing one back-up filter from each experiment for both organic and elemental carbon. These samples are listed in Table 2.1. The mean elemental carbon value was indistinguishable from blank values.

For primary aerosol filters two sets of 0.25 cm^2 discs were removed from the sample filters and analyzed. Results were reported as mean values of the replicate analyses. Prior to May 25, 1985, this procedure was not followed for samples collected at 150 cm/s face velocity because the exposed filter area was too small. Subsequent high face velocity samples were collected at 140 cm/s. The mask required for this face velocity exposed enough filter area to permit duplicate analyses. For back-up filters, replicate analysis was only feasible for low face velocity samples. The boundary between the sampled and masked-off portions was more difficult to distinguish than for primary filters because both the masked and unmasked portions of the filter were the same color. Also a greater portion of the filter was required for analysis.

The average storage blank (i.e., as a result of organic vapor adsorption during storage) was estimated from the data in Tables 2.2 and 2.3. Instrument blanks were obtained by measuring analytical response of the instrument in the absence of sample or blank filters. Instrument blanks averaged 0.18 ± 0.62 and 0.13 ± 0.12 μgC for the normal analysis and total carbon modes, respectively (see Tables 2.4 and

TABLE 2.1 - ORGANIC AND ELEMENTAL CARBON LOADINGS ($\mu gC/cm^2$) ON BACK-UP FILTERS

SAMPLE	ORGANIC CARBON	ELEMENTAL CARBON	TOTAL CARBON*
1	2.88	0.03	2.91
2	0.74	-0.20	0.53
3	1.49	0.03	1.52
4	1.03	0.01	1.04
5	2.12	0.08	2.20
6	0.63	-0.11	0.52
7	1.44	0.02	1.46
8	2.90	0.03	2.93
9	0.95	-0.06	0.89
10	2.56	0.08	2.64
11	2.00	-0.05	1.95
12	1.35	0.00	1.35
13	1.93	0.00	1.93
14	1.52	0.00	1.51
15	2.43	-0.21	2.22
16	2.35	0.30	2.65
MEAN	1.77	0.00	1.77
STANDARD DEV.		0.12	

*ORGANIC + ELEMENTAL CARBON

TABLE 2.2 - STORAGE BLANKS ($\mu gC/cm^2$) FOR NORMAL ANALYSIS MODE

BLANK	ORGANIC CARBON	ELEMENTAL CARBON	TOTAL CARBON
1	0.11	0.00	0.11
2	0.06	0.10	0.16
3	0.00	0.03	0.03
4	0.30	0.00	0.30
5	0.86	0.42	1.29
6	0.03	0.00	0.03
7	0.30	0.17	0.47
8	0.38	0.00	0.38
9	0.02	0.01	0.03
10	0.10	0.00	0.10
11	0.00	0.03	0.03
12	0.07	0.01	0.08
13	0.10	0.00	0.10
14	0.57	0.00	0.57
15	0.54	0.00	0.55
16	0.45	0.36	0.81
17	0.19	0.21	0.40
18	-0.02	0.00	-0.02
19	0.61	0.00	0.61
20	-0.04	-0.03	-0.08
21	-0.32	-0.15	-0.47
22	0.02	0.03	0.05
23	-0.11	-0.13	-0.24
24	-0.18	-0.29	-0.47
25	0.04	-0.16	-0.12
26	0.03	0.18	0.20
27	0.40	0.44	0.85
MEAN	0.17	0.05	0.21
STANDARD DEV.	0.27	0.17	0.40

TABLE 2.3 - STORAGE BLANKS ($\mu gC/cm^2$) FOR TOTAL CARBON MODE

BLANK	REPLICATE #1	#2	AVERAGE
1	0.11		0.11
2	0.28		0.28
3	0.17		0.17
4	0.13		0.13
5	0.19		0.19
6	0.48		0.48
7	0.16		0.16
8	0.33		0.33
9	0.15		0.15
10	0.14		0.14
11	0.17		0.17
12	0.42		0.42
13	0.18		0.18
14	0.36		0.36
15	0.27		0.27
16	0.09		0.09
17	0.23		0.23
18	0.13	0.15	0.14
19	0.09		0.09
20	0.06		0.06
21	0.13	0.06	0.10
22	0.16		0.16
23	0.11		0.11
24	0.10		0.10
25	0.93	0.31	0.62
26	0.16	0.46	0.31
27	0.08		0.08
28	0.09	0.33	0.21
29	0.08		0.08
30	0.07		0.07
31	0.13		0.13
32	0.11		0.11
33	0.07		0.07
MEAN			0.19
STANDARD DEV.			0.13

TABLE 2.4 - INSTRUMENT BLANKS (μgC) FOR NORMAL ANALYSIS MODE

DATE	ORGANIC CARBON	ELEMENTAL CARBON	TOTAL CARBON
5/13/83	0.01	0.09	0.10
5/16/83	0.00	0.01	0.01
5/17/83	0.06	0.18	0.24
5/19/83	0.69	0.67	1.36
	0.00	0.05	0.05
9/14/83	1.19	0.00	1.19
	0.24	0.36	0.60
	1.64	0.00	1.64
	-0.39	-0.10	-0.49
	0.09	0.09	0.18
	0.64	-0.01	0.63
	0.12	0.25	0.37
	0.00	0.05	0.05
	0.20	0.19	0.39
	0.13	0.08	0.21
	-0.03	0.05	0.02
	-0.21	-0.08	-0.29
	0.05	0.16	0.21
	-0.23	-0.07	-0.30
	0.26	0.30	0.55
	0.29	0.27	0.56
9/15/83	-0.27	-0.26	-0.53
	0.64	0.40	1.04
	-0.10	-0.11	-0.21
	-0.28	0.00	-0.28
	-0.04	0.00	-0.04
	0.85	-0.01	0.84
	-0.19	0.00	-0.19
	-0.81	-0.01	-0.82
	-0.33	-0.01	-0.34
	0.20	0.00	0.20
	0.21	0.01	0.20
	0.22	-0.01	0.21
	0.88	-0.01	0.87
	-0.18	-0.32	-0.50
	0.38	-0.01	0.37
	0.33	-0.01	0.32
	-0.44	-0.01	-0.45
	-0.66	-0.01	-0.67
	-0.15	-0.01	-0.16
	-0.34	-0.01	-0.35
	-1.03	-0.01	-1.04
	-0.62	-0.59	-1.21
5/14/84	0.98	0.04	1.02
	0.13	-0.01	0.12

TABLE 2.4 - INSTRUMENT BLANKS (μgC) FOR NORMAL ANALYSIS MODE

(Continued)

DATE	ORGANIC CARBON	ELEMENTAL CARBON	TOTAL CARBON
5/14/84	0.37	0.13	0.50
	0.95	0.22	1.17
	0.47	0.01	0.48
5/16/84	-0.05	-0.02	-0.07
	0.85	0.31	1.16
5/24/84	0.72	0.07	0.79
	0.05	-0.13	-0.08
	0.15	-0.16	-0.01
6/21/84	-0.04	-0.52	-0.56
6/26/84	0.22	-0.15	0.07
10/31/84	0.06	0.01	0.07
11/8/84	-0.33	-0.16	-0.49
2/14/85	-0.42	-0.39	-0.81
2/17/85	0.58	0.01	0.59
2/18/85	0.77	0.01	0.78
3/20/85	0.36	0.02	0.38
3/21/85	0.43	-0.01	0.42
3/22/85	0.01	0.00	0.01
4/5/85	1.05	0.01	1.06
8/22/85	-0.01	0.04	-0.03
8/25/85	0.31	0.00	0.31
8/26/85	-0.13	-0.20	-0.33
8/28/85	0.28	0.00	0.28
8/30/85	0.00	-0.01	-0.01
MEAN	0.16	0.01	0.17
STANDARD DEV.	0.48	0.19	0.67

2.5). For both the normal analysis and total carbon modes t-tests indicated that storage blanks were not significantly different from instrument blanks ($p = 0.05$). Uncertainties refer to one standard deviation. In addition, three experiments were conducted in which clean filters were transported to and from the sampling site, without sampling. These travel blanks were analyzed for total carbon only and are listed in Table 2.6. A t-test indicated that they were not significantly different from storage blanks ($p = 0.05$).

For all experiments comparing the effects of sampling period and face velocity, Pallflex QAOT quartz fiber filters were used. These exhibited greater thermal stability during analysis, and lower storage blanks than glass fiber filters.

C. Precision

Apparent concentrations are derived from organic, elemental, or total carbon mass loading using equation 2.1:

$$C = (M-X)A/Qt = (M-X)/vt \qquad 2.1$$

where C represents the apparent carbon concentration, M is the mass of carbon collected per unit area of filter and is generally obtained as the mean of replicate analyses, X is the average storage blank, A is the unmasked area of the filter, Q is the flow rate, t is the duration of the sampling period, and v, the face velocity, is defined as Q/A.

Propagation of errors associated with equation 2.1 leads to equation 2.2:

$$\left(\frac{s_C}{C}\right)^2 = \left(\frac{s_M}{M-X}\right)^2 + \left(\frac{s_X}{M-X}\right)^2 + \left(\frac{s_A}{A}\right)^2 + \left(\frac{s_Q}{Q}\right)^2 + \left(\frac{s_t}{t}\right)^2 \qquad 2.2$$

TABLE 2.5 - INSTRUMENT BLANKS (µgC) FOR TOTAL CARBON MODE

DATE	TOTAL CARBON	DATE	TOTAL CARBON
6/26/84	0.10	11/28/84	0.01
6/26/84	0.13	12/7/84	0.14
6/26/84	0.08	12/8/84	0.05
7/3/84	0.18	1/6/85	0.10
7/4/84	0.27	1/6/85	0.05
7/4/84	0.14	1/23/85	0.13
7/4/84	0.28	1/24/85	0.06
7/12/84	0.56	1/29/85	0.16
7/12/84	0.07	2/5/85	0.03
7/15/84	0.22	2/5/85	0.05
7/15/84	0.29	2/14/85	0.00
7/15/84	0.21	3/7/85	0.09
7/17/84	0.27	2/21/85	-0.05
7/17/84	0.35	4/29/85	0.08
7/17/84	0.19	5/4/85	0.07
7/18/84	0.25	5/20/85	0.04
7/18/84	0.35	6/3/85	-0.06
7/18/84	0.16	6/12/85	0.03
7/18/84	0.12	6/23/85	0.01
7/18/84	0.28	7/17/85	0.02
9/25/84	0.16	7/16/85	0.01
9/26/84	0.20	7/14/85	-0.01
10/10/84	-0.05		
10/16/84	0.05	MEAN	0.13
10/26/84	0.18	STANDARD DEV.	0.12
10/27/84	-0.04		
10/27/84	0.12		
11/26/84	0.20		

TABLE 2.6 - TRAVEL BLANKS ($\mu gC/cm^2$)

SAMPLE SET	SAMPLING PORT	PRIMARY FILTER	BACK-UP FILTER
2.1	1	0.28	0.16
	2	0.12	0.14
	3	0.18	0.16
2.2	1	0.20	0.13
	2	0.19	0.09
	3	0.50	0.32
2.3	1	0.07	0.04
	2	0.10	0.06
	3	0.38	0.26
MEAN		0.22	0.16
STANDARD DEV.		0.14	0.09

where s_i represents the standard deviation of the ith parameter of equation 2.1. Uncertainties in apparent concentration have been estimated from this equation. The various terms of equation 2.2 have been determined as follows.

The mass uncertainty term of Equation 2.2, $\left(\frac{s_M}{M-X}\right)^2$ can be derived from the detector response. For a flame ionization detector a linear response to concentration is observed, which can be expressed with Equation 2.3:

$$\phi R = \phi T + \phi B \qquad 2.3$$

where ϕ is the signal response per unit mass analyzed, ϕR is the total signal response, ϕT is the signal response to analyte, ϕB is the background signal and R is mass of carbon in the sample.

Carbon mass is obtained by rearranging Equation 2.3 and dividing by ϕ, the signal response per unit mass of carbon analyzed.

$$T = R - B \qquad 2.4$$

The uncertainty in carbon mass analyzed can be obtained by propagating the error from Equation 2.4:

$$s_T^2 = s_R^2 + s_B^2 \qquad 2.5$$

where

T = total mass analyzed

s_T = standard deviation for total mass analyzed

s_R = standard deviation in signal response to analyte.

s_B = standard deviation in background signal response (i.e., instrument blank)

The uncertainty in background response refers to random fluctuations associated with the flame ionization detector signal and associated electronics. Uncertainties in analyte response can be caused by non-uniformity in filter deposit, variations in analysis temperature, volume of calibration gas injected and area of filter analyzed, and variation in the reproducibility of correction for pyrolytically generated elemental carbon (Johnson, 1981). These analyte response uncertainties are probably independent of concentration. In contrast, the relative importance of background uncertainties is inversely related to the carbon mass analyzed. If the uncertainty for α, the filter area analyzed, is negligible, the uncertainty in carbon mass per unit area in Equation 2.2 can be expressed in terms of the uncertainty in total mass analyzed.

$$\left(\frac{s_M}{M-X}\right)^2 = \left(\frac{s_{T/\alpha}}{M-X}\right)^2 = \left(\frac{s_{B/\alpha}}{M-X}\right)^2 + \left(\frac{s_{R/\alpha}}{M-X}\right)^2 \qquad 2.6$$

Equation 2.6 allows the convenient distinction between concentration dependent and concentration independent components of the collected mass uncertainty. α was usually 1 cm^2.

Typically, observed carbonaceous aerosol concentrations were within the range for which uncertainties due to both background and analyte response contributed significantly to the total analytical uncertainty. Consequently, the relative uncertainty was expected to decrease with increasing concentration and it was not valid to apply a single value for relative uncertainty to all samples.

Uncertainties in both background and analyte response have

been estimated and a total uncertainty which varies with concentration has been calculated using Equation 2.6. s_B has been estimated for both the normal analysis mode and total carbon mode from instrument blanks listed in Tables 2.5 and 2.6.

Relative error in analyte response has been estimated from replicate analyses listed in Tables 2.7 and 2.8. For each sample, the difference in replicate analyses was expressed as a fraction of the average value. The replicate variance was computed from Equation 2.7, which assumes equal variance for each replicate data set (Davies and Goldsmith, 1972).

$$V = \frac{\Sigma \left(x_1-\bar{x}_1\right)^2 + \Sigma \left(x_2-\bar{x}_2\right)^2 + \ldots + \Sigma \left(x_k-\bar{x}_k\right)^2}{N - k} \qquad 2.7$$

where:

V = variance

x_i = ith sample mass

k = number of samples

N = total number of observations.

When all replicate analyses were included, the variance was a strong function of concentration. This was probably due to large relative background response errors for samples with low concentrations. However, when samples with mass loadings lower than $10s_B$ were excluded, regressions of variances calculated for each replicate against mean mass loadings showed no significant correlations for organic, elemental, or total carbon measured using the normal analysis mode, or for total carbon only. The absence of these correlations was

TABLE 2.7 - RELATIVE PRECISION FOR NORMAL ANALYSIS MODE

	ORGANIC CARBON	ELEMENTAL CARBON	TOTAL CARBON*
NUMBER OF SAMPLES	59	53	60
STANDARD DEV.	4.1%	6.1%	3.2%
CORRELATION WITH CONCENTRATION CORRELATION COEFF. (R)	0.11	0.00	0.00
VARIANCE ACCOUNTED FOR BY CONCENTRATION (R^2)	1.2%	0.0%	0.0%

*ORGANIC + ELEMENTAL CARBON

TABLE 2.8 - RELATIVE PRECISION FOR TOTAL CARBON MODE

NUMBER OF SAMPLES	47
STANDARD DEV.	5.4%
CORRELATION WITH CONCENTRATION CORRELATION COEFF. (r)	0.19
VARIANCE ACCOUNTED FOR BY CONCENTRATION (r^2)	3.9%

used to verify the assumption of equal variances. Even at $10s_B$, the standard deviation for background response should be 10% of the total signal. Consequently, the analyte response uncertainties estimated in Tables 2.7 and 2.8 could also include some background response error and should be considered conservative estimates. However, the coefficients of correlation between precision and sample concentration suggested that differences in concentration accounted for only a small fraction of the variance.

Uncertainties in flow rates were estimated from replicate calibrations, usually repeated three times for each rotameter reading. s_Q represents the average standard deviation obtained with this method. For samples which experienced changes in flow rates over the course of the sampling period, the magnitude of this change was added to the average flow rate uncertainty.

The uncertainty in exposed filter area, s_A, was estimated from repeated measurements of the highest face velocity mask, for which relative uncertainties would be the greatest. The uncertainty in sampling duration, s_t, was generally less than five minutes.

Uncertainties used in Equation 2.2 are summarized in Table 2.9. Relative uncertainties are expressed as a percentage of concentration. The relative uncertainties in flow rate, filter area, and sampling period are considered independent of carbon mass collected. Relative uncertainties in carbon mass collected correspond to the analytical uncertainties of Equation 2.5 and are composed of a carbon mass independent component based on analyte response uncertainty and

TABLE 2.9 - RELATIVE UNCERTAINTIES IN TERMS USED IN CONCENTRATION CALCULATIONS

TERM	UNCERTAINTY (ONE STANDARD DEVIATION) INDEPENDENT	DEPENDENT ON MASS COLLECTED	DEPENDENT ON MASS ANALYZED
(Equation 2.2)		($\mu gC/cm^2$)	(μgC)
MASS LOADING ($S_M/M-X$)	$\left(\frac{s_R/a}{M-X}\right)$		(s_B)
Organic Carbon	4.1%		0.48
Elemental Carbon	6.1%		0.19
Total Carbon*	3.2%		0.62
Total Carbon Mode	5.4%		0.12
STORAGE BLANK		(s_X)	
Organic Carbon		0.27	
Elemental Carbon		0.17	
Total Carbon		0.40	
Total Carbon Mode		0.13	
FLOW RATE (s_Q/Q)	1.7%		
FILTER AREA (s_A/A)	0.5%		
SAMPLING PERIOD (s_t/t)	0.4%		
TOTAL INDEPENDENT UNCERTAINTY** (Equation 2.6)	(Δ)		
Organic Carbon	4.5%		
Elemental Carbon	6.4%		
Total Carbon	3.7%		
Total Carbon Mode	5.7%		

*organic + elemental carbon from normal analysis mode

**square root of sum of squares of independent uncertainty terms

a carbon mass dependent component which corresponds to the instrument blank uncertainty. Relative storage blank uncertainties are dependent on carbon mass collected.

Uncertainties are evaluated in Table 2.9. From these values and Equations 2.5 and 2.6, Equation 2.2 can be expressed as:

$$\left(\frac{s_C}{C}\right)^2 = \Delta^2 + \left(\frac{s_X}{M-X}\right)^2 + \left(\frac{s_B/\alpha}{M-X}\right)^2 \qquad 2.8$$

where Δ^2 represents the sum of the squares of the relative uncertainties independent of carbon mass collected. This equation has been used to calculate the reported uncertainties in apparent concentrations.

Precision in organic carbon measurements between sampling ports was tested by operating each port under identical conditions. Results of these experiments are given in Table 2.10. Expressed as one standard deviation of the six samples collected, relative precision was within 5% for both experiments. Relative precision for elemental carbon could not be adequately determined because mass loadings in both experiments were below the limit of quantitation. However, similar uncertainties have been obtained for elemental carbon in other experiments (see section 2.E).

D. Analytical Modifications for Glass and Teflon Filters

Modifications in the analytical procedure were required for analysis of glass fiber and Teflon membrane filters. For glass fiber filters, temperatures were only programmed up to 600°C because the filters melted at higher temperatures. At this temperature, complete

TABLE 2.10 - ORGANIC CARBON SAMPLING PRECISION MEASURED BETWEEN SAMPLING PORTS

SAMPLE SET	SAMPLING PORT	ORGANIC CARBON ($\mu gC/cm^2$)
2.4	1	10.06
	2	9.55
	3	10.01
	4	9.36
	5	10.52
	6	10.26
	MEAN	9.96
	STD. DEV.	0.43 (4.4%)
2.5	1	4.43
	2	4.76
	3	4.46
	4	4.35
	5	4.47
	6	4.37
	MEAN	4.47
	STD. DEV.	0.15 (3.4%)

removal was not accomplished for elemental carbon. This could be concluded from the gray color remaining on the filter after analysis. It is also possible that a lower percentage of organic carbon was removed from glass than from quartz fiber filters. Storage blank measurements for glass fiber filters are summarized in Table 2.11. These can be compared to storage blanks for quartz fiber filters in Table 2.3. Two experiments were conducted in which six quartz and six glass fiber filters were baked, then stored for several weeks. For both experiments a t-test showed that glass storage blanks were significantly higher than quartz storage blanks ($p=.05$). Blank values for the two experiments are given in Table 2.12. For one sample set, one of each filter type was analyzed immediately after heat cleaning and resulted in blank values of 0.10 and 0.20 $\mu gC/cm^2$ for quartz and glass fiber filters respectively. This indicates that both filter types are satisfactorily cleaned by baking at 500°C, but that glass fiber filters exhibit poorer organic carbon blank stability than quartz fiber filters during storage.

For Teflon membrane filters, samples were analyzed at 275°C in O_2-He for total carbon only. No elemental carbon is removed at this temperature. Higher temperatures caused significant bleeding of the organic filter material. At 275°C an average of three blanks was 0.21 $\mu g/cm^2$. The quartz fiber filters used in filter type comparisons were also analyzed under these conditions. These comparisons involve the assumption that temperatures required for removal of organic carbon are similar between filter types. However, for adsorbed vapors,

TABLE 2.11 - STORAGE BLANKS FOR GLASS FIBER FILTERS

BLANK	MASS COLLECTED ($\mu gC/cm^2$)
1	0.27
2	1.09
3	1.61
4	1.51
5	1.25
6	1.24
7	1.36
8	1.29
9	1.93
10	1.93
11	1.78
12	1.75
13	1.71
14	1.25
15	1.22
NO. BLANKS	15
MEAN	1.41
STANDARD DEV.	0.42

TABLE 2.12 - BLANK COMPARISON BETWEEN GLASS AND QUARTZ FIBER FILTERS

SAMPLE SET	STORAGE PERIOD	NO. SAMPLES	MEAN ($\mu gC/cm^2$)	STANDARD DEV. ($\mu gC/cm^2$)
2.6				
GLASS	28 DAYS	6	1.38	0.15
QUARTZ		6	0.10	0.05
2.7				
GLASS	50 DAYS	6	1.73	0.25
QUARTZ		6	0.16	0.04
SAMPLING BLANK				
GLASS	9 DAYS	1	1.28	
	20 DAYS	1	1.15	
QUARTZ	9 DAYS	1	0.13	
	20 DAYS	1	0.15	

removal temperatures required are probably a straightforward function of heats of adsorption of filter material. Moreover, the role of filter type in pyrolysis of organic to elemental carbon is poorly understood. Consequently, filter type comparisons based on thermal-optical carbon analysis must be considered qualitative at best.

E. Quality Assurance Using Elemental Carbon

Because elemental carbon is not volatile, it is not susceptible to the artifact errors associated with organic aerosol. Consequently, variations in apparent concentration with face velocity, sampling period, and filter type observed for particulate organic carbon should not be observed for elemental carbon. It can therefore be used to test whether variations in collected organic mass between sampling ports were unique to the organic fraction rather than symptomatic of general aerosol sampling problems.

The reproducibility of elemental carbon concentrations was tested by comparing elemental carbon collected at different face velocities under conditions in which apparent organic carbon concentrations were expected to vary with face velocity. A carbonaceous aerosol was produced with a combustion aerosol generator (Fig. 2.4). The aerosol generator consisted of a propane source, needle valve, rotameter and burner in series. The flame from the burner was drawn into the sampling apparatus through a 16 cm diameter flexible aluminum tube. The ratio of organic to elemental carbon was controlled by varying the fuel flow rate with the needle valve. A significant elemental carbon

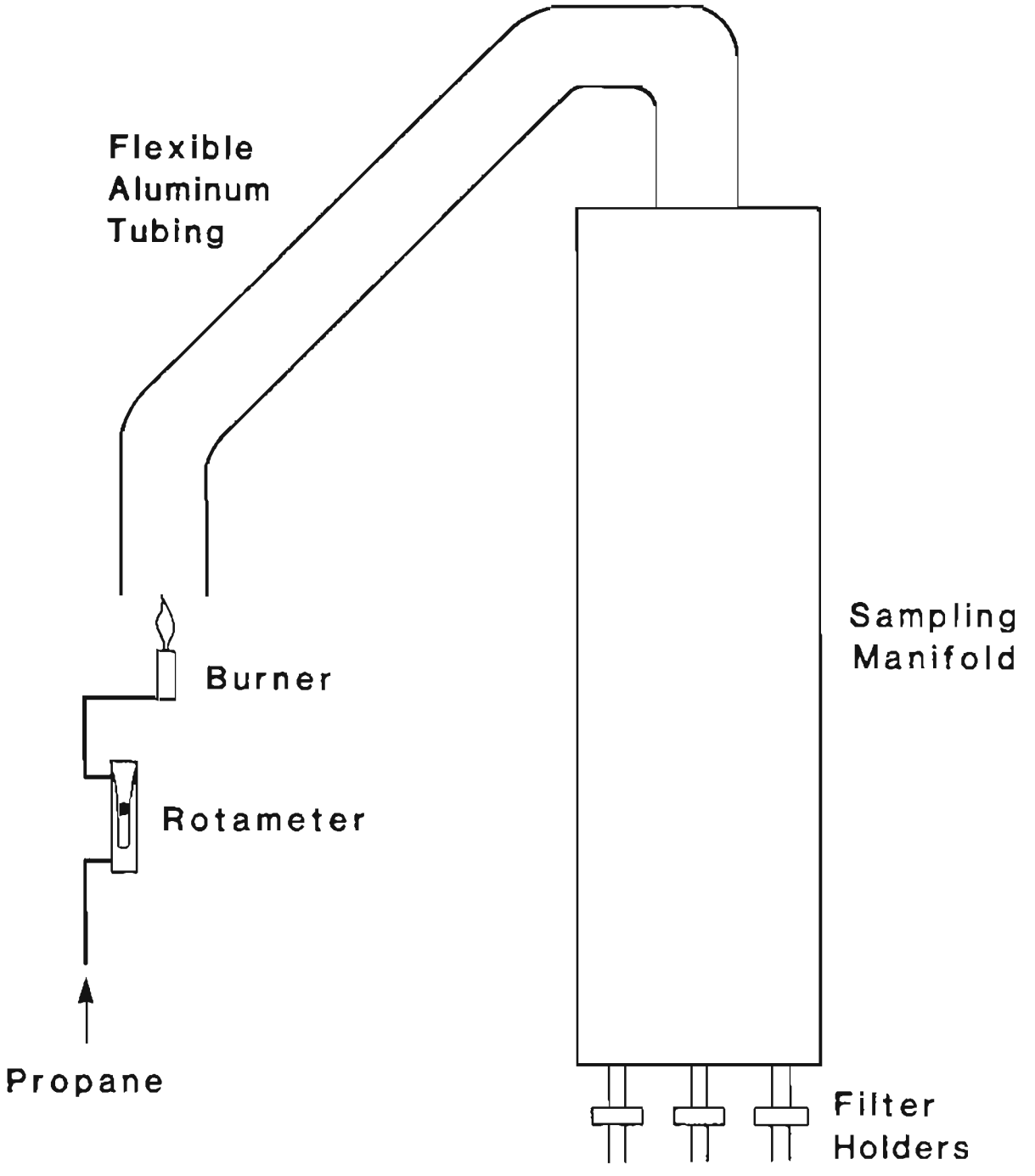

Figure 2.4. Combustion aerosol generator

fraction could only be produced with the burner completely closed off to air.

Four sets of combustion samples were collected at varying face velocities (Figs. 2.5 through 2.8). For Sample Set 2.6 the aerosol generated was almost pure elemental carbon. In Sample Sets 2.7, 2.8 and 2.9, (Figs. 2.6, 2.7 and 2.8) a significant fraction of carbonaceous aerosol was organic. Symbols represent mean values of mass loadings indicated. Uncertainties for Sample Sets 2.6 through 2.8 (Figs. 2.5 through 2.7) were propagated from carbon mass, filter area and storage blank uncertainties listed in Table 2.9. For Sample Set 2.9 (Fig. 2.8) the uncertainties in correction for pyrolysis of elemental carbon were much higher than predicted from uncertainties observed for samples with lower elemental carbon concentrations. For these samples symbols represent measurements from each analysis and the connecting lines represent the range between replicate analyses.

Sample Sets 2.6 and 2.7 (Figs. 2.5 and 2.6) confirmed that elemental carbon mass collected did not vary with face velocity. Table 2.13 shows that the standard deviation of the six samples were within expected error limits and poor correlations of elemental carbon with face velocity were observed.

Sample Sets 2.8 and 2.9 (Figs. 2.7 and 2.8), however, illustrate the limitations of using elemental carbon for quality assurance. For high mass loadings changes in reflectance become less responsive to changes in mass. Consequently, random fluctuations in reflectance can grossly affect uncertainties in the correction for pyrolytically

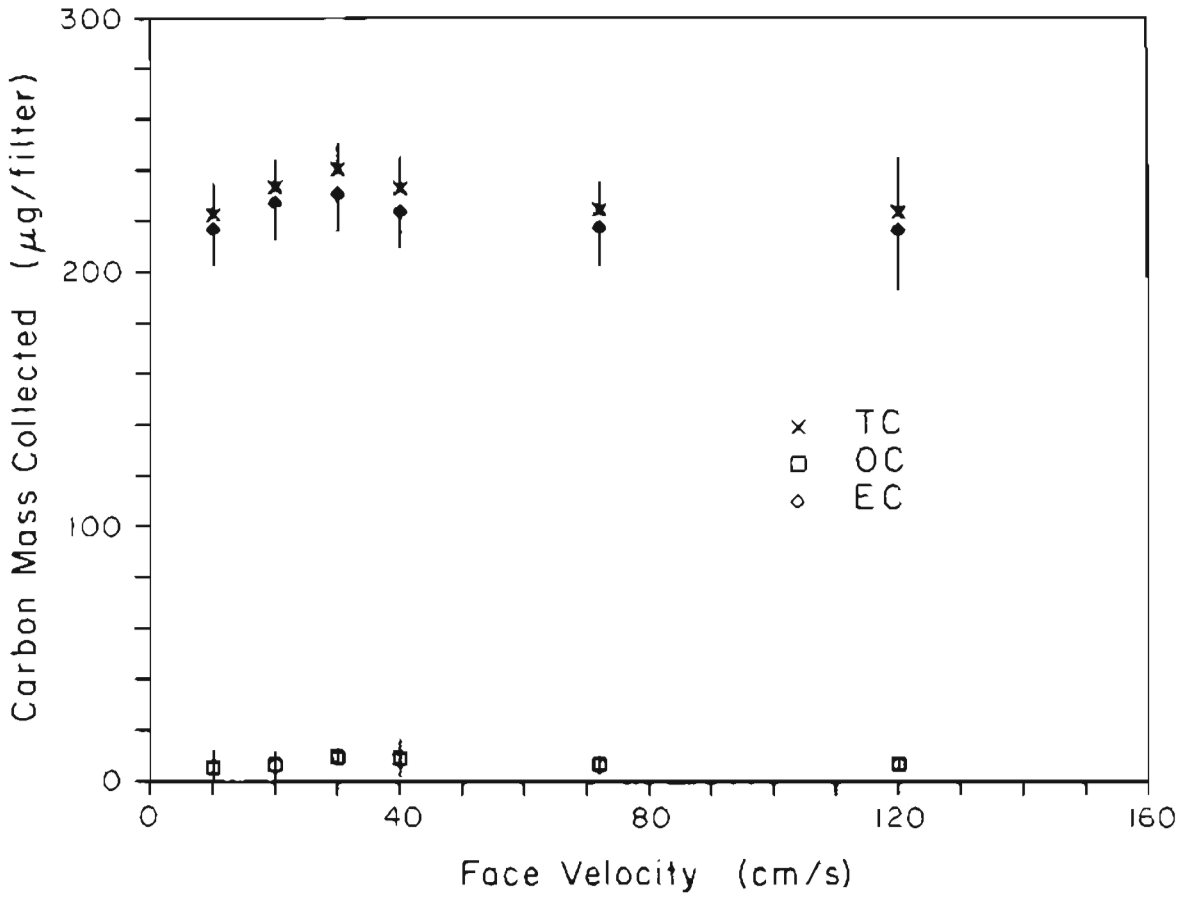

Figure 2.5. Variation of organic, elemental and total carbon mass loading with face velocity for sample set 2.6.

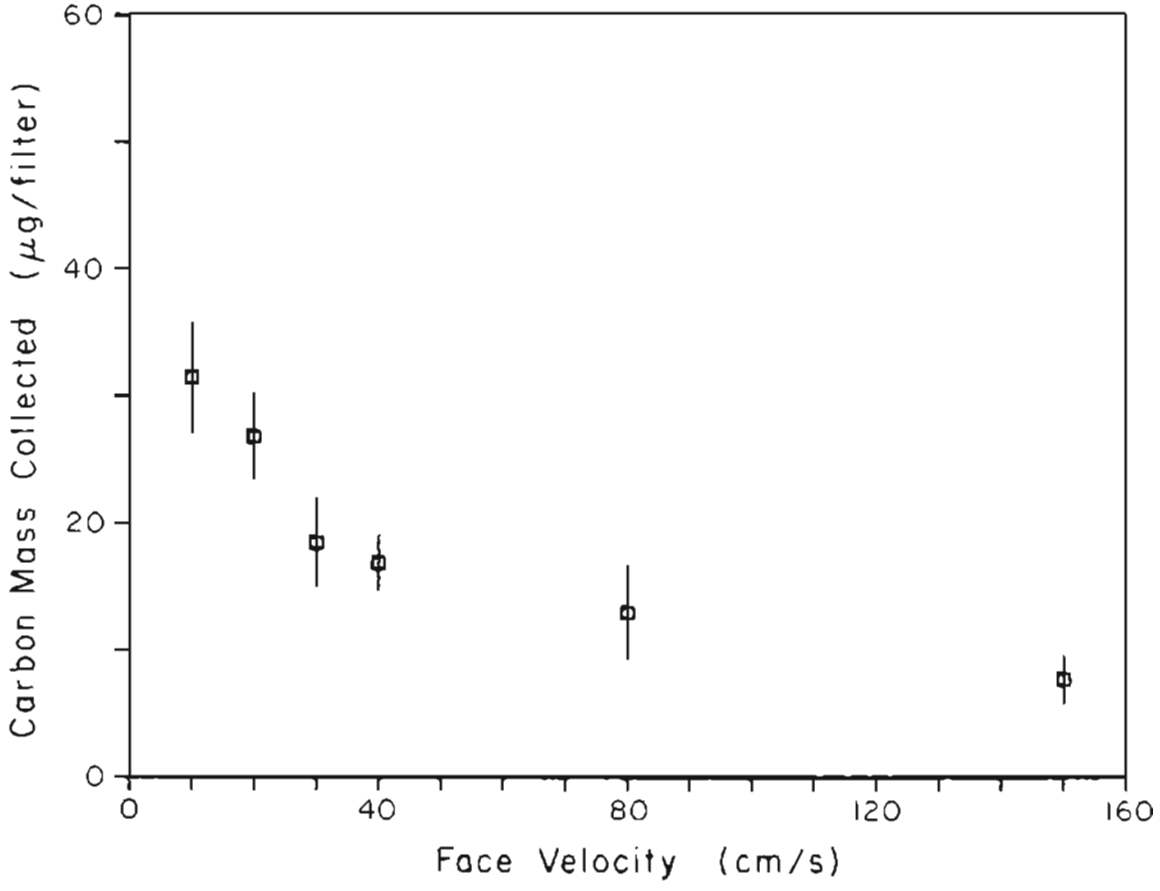

Figure 2.6a. Variation of organic carbon mass loading with face velocity for sample set 2.7.

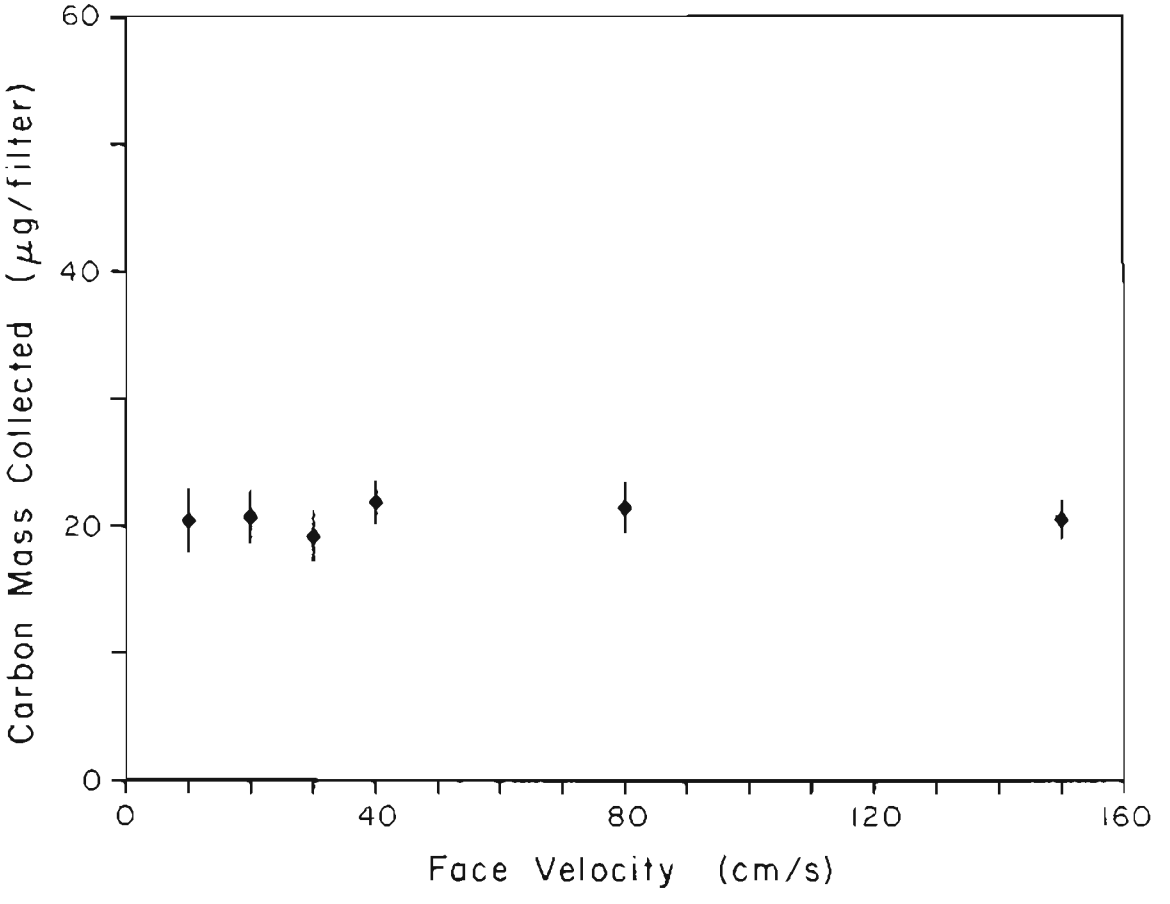

Figure 2.6b. Variation of elemental carbon mass loading with face velocity for sample set 2.7.

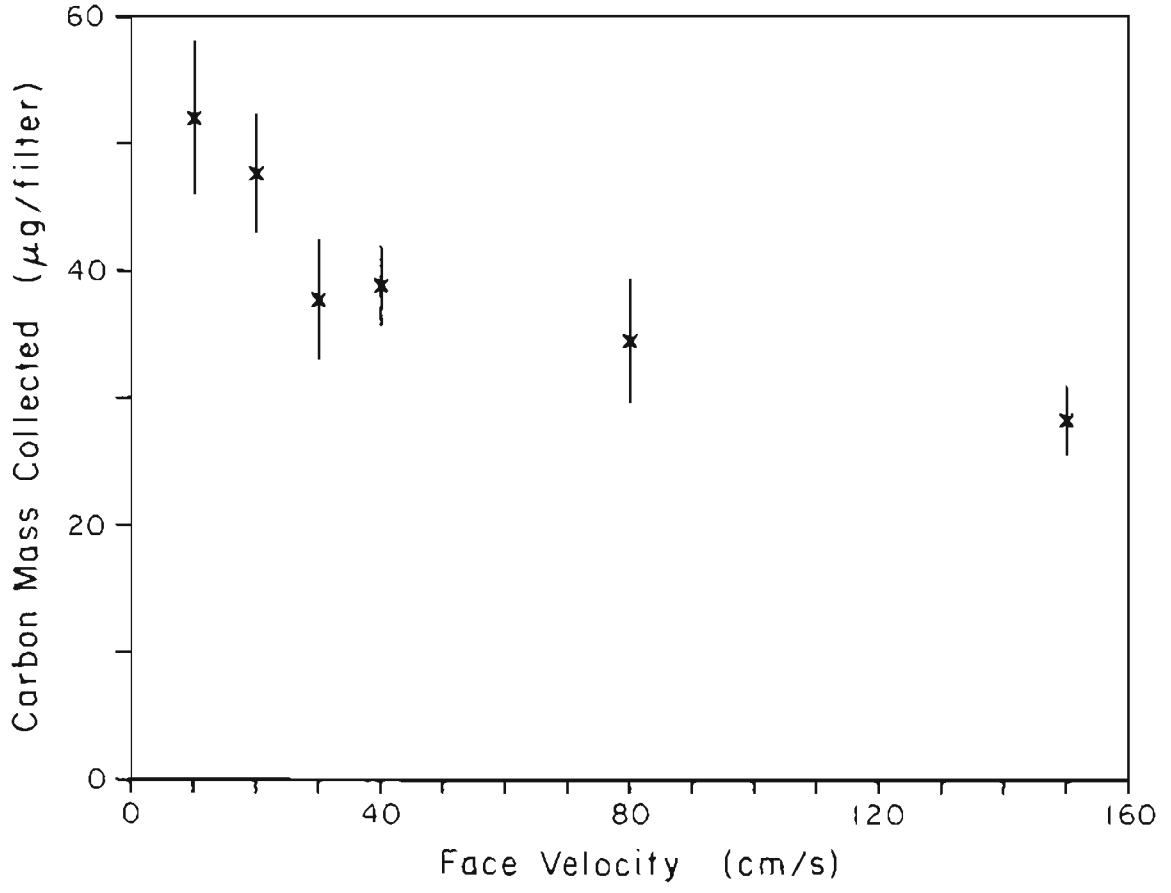

Figure 2.6c. Variation of total carbon mass loading with face velocity for sample set 2.7.

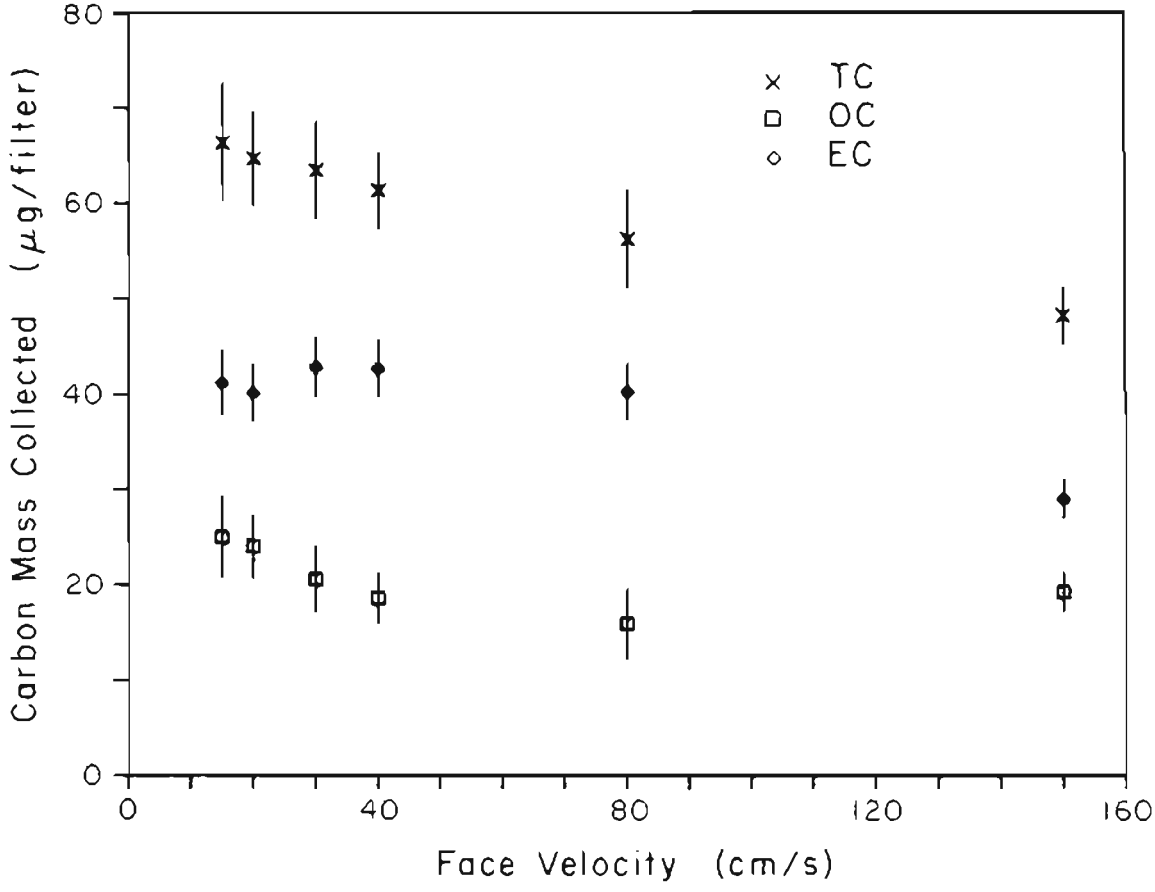

Figure 2.7. Variation of organic, elemental and total carbon mass loading with face velocity for sample set 2.8.

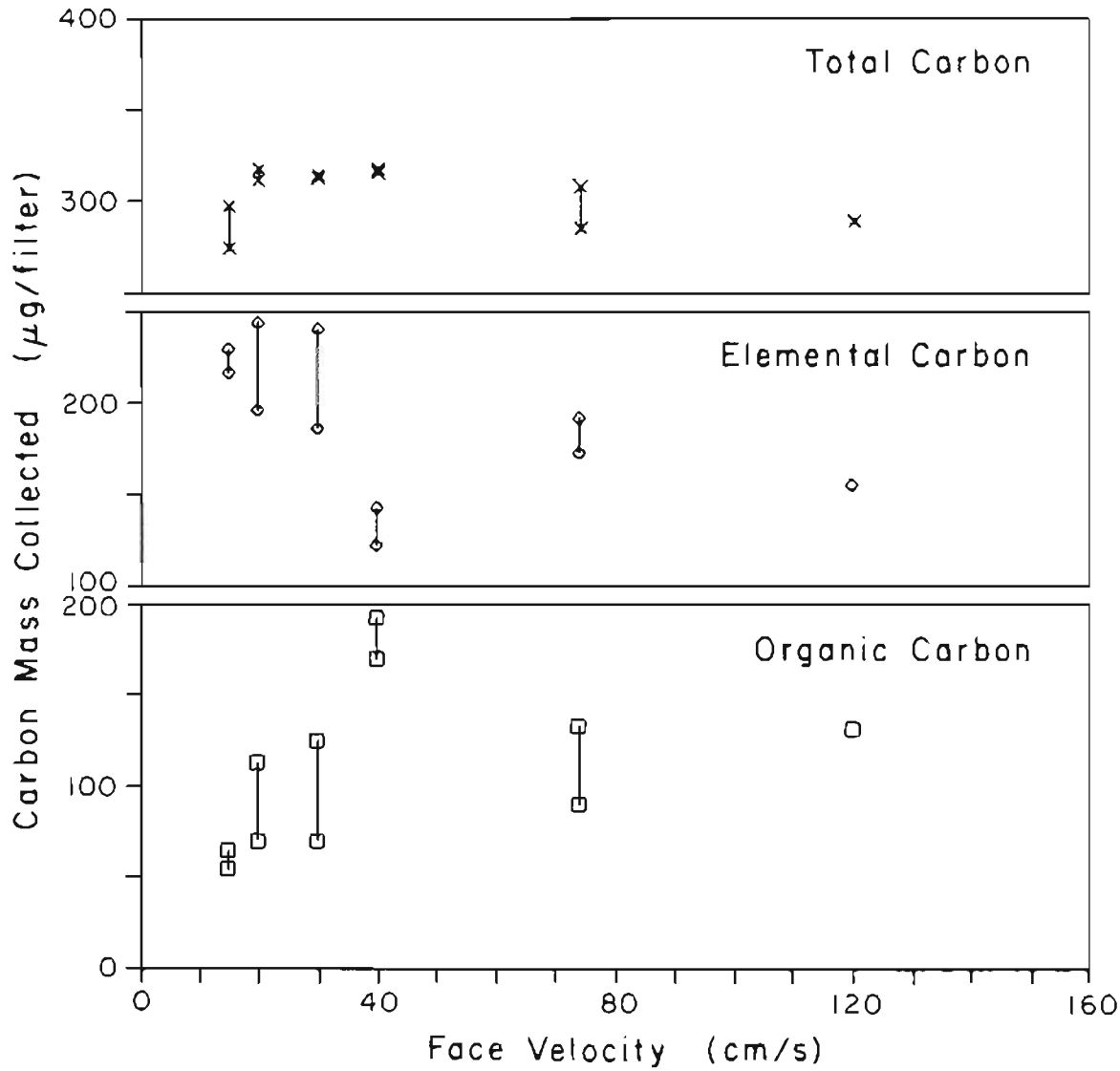

Figure 2.8. Variation of organic, elemental and total carbon mass loading with face velocity for sample set 2.9.

TABLE 2.13 - RELATIVE PRECISION AND CORRELATION COEFFICIENTS FOR COMBUSTION GENERATED ELEMENTAL CARBON

SAMPLE SET	STANDARD DEVIATION	CORRELATION WITH FACE VELOCITY (r)
2.6	2.8%	0.31
2.7	4.1%	0.00

generated elemental carbon. This occurred in the propane combustion samples with mass loadings greater than 30 $\mu g/cm^2$. In Sample Set 2.8 (Fig. 2.7) it affected only the sample with the highest mass loading (i.e., highest face velocity). For Sample Set 2.9 (Fig. 2.8), mass loadings were sufficiently high that results were not reproducible. This was not a problem in Sample Set 2.6 (Fig. 2.5) in spite of the high mass loadings observed because not enough organic carbon was available to promote significant pyrolytic generation of elemental carbon. The threshold value of 30 $\mu g/cm^2$ might not be the same in atmospheric conditions since physical characteristics of elemental carbon are highly variable (Goldberg, 1985). Elemental carbon mass loadings greater than 30 $\mu g/cm^2$ were generally not observed for ambient samples even at high face velocities.

A second possible problem in reflectance measurements is the presence of inorganic aerosol constituents capable of absorbing visible radiation. Poor elemental carbon agreement was obtained for samples on which red color was observed after analysis. The interferent was probably iron oxide associated with coarse particles and analytical results were improved after 1 μm impactors were included as components of the sampling ports.

Elemental carbon is consequently capable of providing a valuable quality assurance parameter for investigating artifacts in sampling of organic fine particulate matter for all but the most heavily loaded samples.

CHAPTER III - VARIATIONS OF APPARENT ORGANIC AEROSOL CONCENTRATION AND ADSORPTION ARTIFACT WITH SAMPLING PROCEDURES

A. Experimental Description

A.1. Overview

Samples were collected using one of the three filter arrangements shown in Fig. 3.1. Configuration A (Fig. 3.1a) consisted of two quartz fiber filters in series: Primary filters (A1Q) for aerosol collection, and back-up filters (A2Q) for adsorption artifact estimates. In configuration B (Fig. 3.1b), two quartz fiber filters were placed in series behind a Teflon membrane prefilter (B1T). The carbon mass collected on the furthest upstream quartz fiber filter (B2Q) was used to estimate the mass of carbon adsorbate which would be collected on a primary filter (i.e., the A1Q filter of Fig. 3.1a) under the same sampling conditions (i.e., the same face velocity, filter type and sampling duration). A second quartz fiber filter (B3Q) was also included in configuration B. Configuration C consisted of two Teflon membrane filters (C1T,C2T) followed by two quartz fiber filters (C3Q,C4Q) in series.

Ambient sampling experiments are summarized in Table 3.1. In the first column, experiments are categorized according to their primary purpose: the investigation of the effects of face velocity, sampling duration or filter type. The next three columns indicate the particular face velocities, sampling durations and filter types employed in each experiment. If a particular sampling parameter was varied, all of the varied conditions are included.

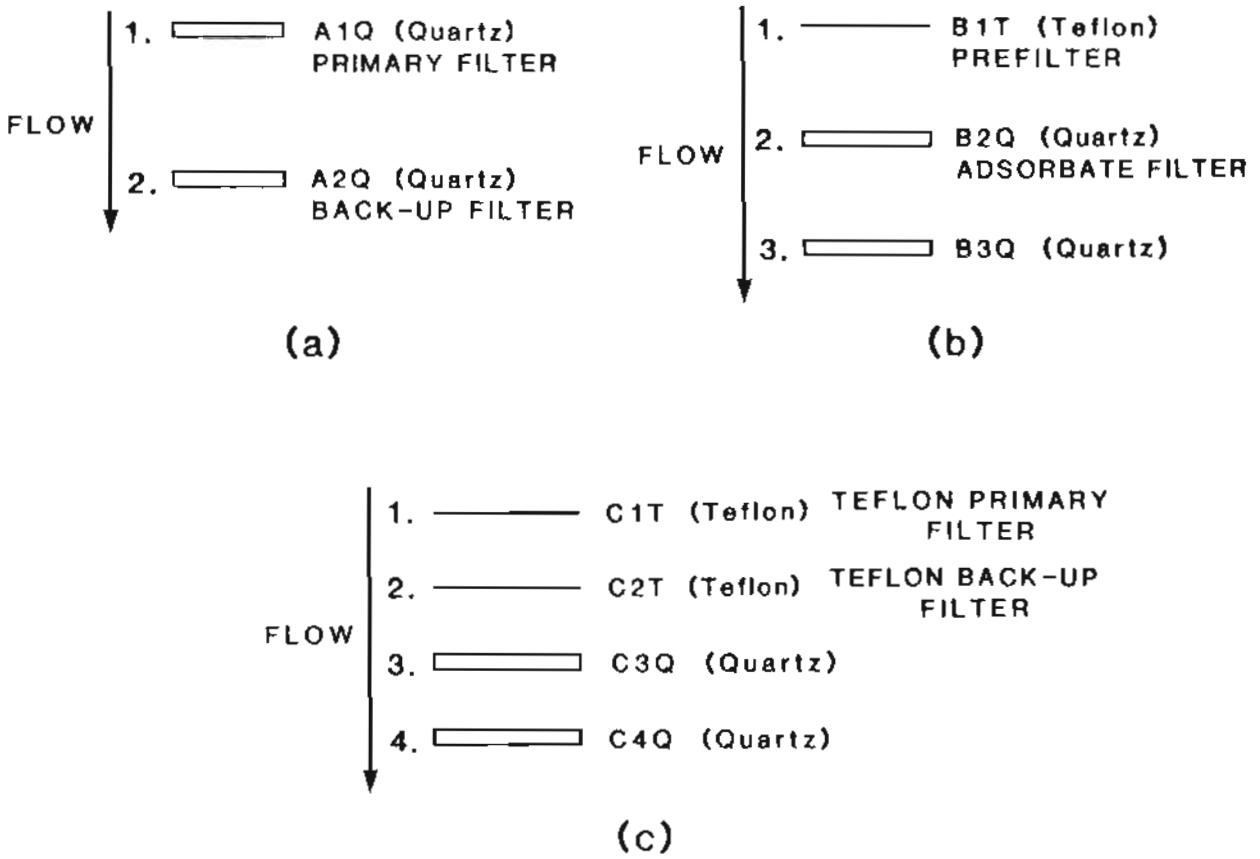

Figure 3.1. Filter configurations during sampling

TABLE 3.1 - SUMMARY OF EXPERIMENTS

EXPERIMENT	FACE VELOCITY (cm/s)	SAMPLING DURATION (hr.)	PRIMARY FILTER TYPE	APPARENT CONCENT.	ADSORBED VAPOR Behind Teflon Prefilter	ADSORBED VAPOR Behind Quartz Prefilter
FACE VELOCITY						
Variation in Apparent Concentration						
3.1	15,20,30,40,80,150	24	Quartz	X		X
3.2	15,20,30,40,80,150	24	Quartz	X		X
3.3	15,20,30,40,80,150	24	Quartz	X		X
3.4	15,20,30,40,80,150	24	Quartz	X		X
Variation in Adsorption Artifact						
3.5	15,40,80	24	Quartz,Teflon	X	X	X
3.6	15,40,80	24	Quartz,Teflon	X	X	X
3.7	15,40,140	24	Quartz,Teflon	X	X	X
3.8	15,40,140	8.75	Quartz,Teflon	X	X	X
Variation in Volatilization						
3.9	15,20,30,40,80,140	24	Quartz	X		
3.10	15,20,30,40,80,140	24	Quartz	X		
VOLATILIZATION						
Adsorbate Volatilization						
3.11	40	24	Quartz	X	X	
SAMPLING DURATION						
Variation in Apparent Concentration						
3.12	15,40,80	3,6	Quartz	X		X
3.13	15,40,140	24,48	Quartz	X		X
3.14	15,40,140	24,48	Quartz	X		X
FILTER TYPE						
Quartz and Glass Apparent Concentrations						
3.15	10	24	Quartz,Glass	X		
3.16	10	24	Quartz,Glass	X		
Quartz and Glass Adsorption Artifact						
3.17	15,40,80	24	Quartz,Glass		X	
Quartz and Teflon Apparent Concentration						
3.18	15,40,80	24	Quartz,Teflon	X		X
3.19	15,40,80	24	Quartz,Teflon	X		X

In the last three columns an X indicates quantities for which the samples were analyzed. "Apparent" concentration refers to the particulate organic carbon concentration derived from the carbon mass collected on a primary filter (A1Q of Fig. 3.1a) using Equation 2.1, and represents the sum of true organic aerosol and adsorbed organic vapors. The concentration of adsorbed organic vapors is defined as the mass of organic carbon adsorbed per unit volume sampled, and was determined from back-up filters (B2Q or A2Q).

Distinction is made between two methods of estimating the vapor adsorption artifact: the carbon concentration as measured on a quartz fiber filter (B2Q) behind a Teflon prefilter or on a quartz fiber filter (A2Q) behind a quartz fiber prefilter. The former will be shown to provide a better estimate of organic vapor adsorption on quartz fiber aerosol filters.

A.2. Face Velocity Experiments

Four experiments were conducted in which apparent concentrations were compared between samples collected at six different face velocities (Experiments 3.1 through 3.4). Filter configuration A (Fig. 3.1a) was used in all sampling ports, and all samples were collected for 24 hours. Apparent particulate organic carbon concentrations were determined from carbon mass collected on primary filters (A1Q) and adsorbed vapor concentrations from carbon mass collected on the A2Q back-up filters (i.e., behind quartz fiber prefilters).

The variation of adsorption artifact with face volocity was further explored in Experiments 3.5 through 3.8. Samples were collected at three different face velocities, with one pair of sampling ports operated at each face velocity. In each pair one of the sampling ports contained filters arranged in configuration A (Fig. 3.1a), and apparent particulate organic carbon concentration was derived from the carbon mass collected on primary filters (A1Q). In the second sampling port filters were arranged in configuration B (Fig. 3.1b), and adsorbed vapor concentrations were estimated from carbon mass collected on the B2Q back-up filters (i.e., behind Teflon prefilters). Controllable sampling conditions were otherwise identical for each sampling port pair.

A.3. Volatilization Experiments

Two experiments were conducted in which the variation of volatilization of collected organic carbon with face velocity was investigated (Experiments 3.9 and 3.10). High-volume samples were collected for 24 hours on quartz fiber filters. 47 mm disks were removed from the high-volume filters and placed in sampling ports connected to the volatilization apparatus (Fig. 2.3). Samples were exposed to purified air for 24 hours. The original apparent concentrations were derived from high-volume samples. Volatilization artifact is defined as the mass of carbon lost per unit volume of purified air throughput and was estimated from the difference in carbon mass observed between the original sample and the exposed 47mm disk after volatilization.

The volatilization of organic vapor adsorbed during sampling was investigated in Experiment 3.11 by drawing purified air through previously collected filters (see Section II.B). Two pairs of samples were collected in four sampling ports. One pair of samples was stored and designated as the reference sample. The other samples were exposed to purified air at a face velocity of 40 cm/s for 24 hours using the volatilization apparatus. Filter configuration A (Fig. 3.1a) was used in one sampling port from each pair. Configuration B (Fig. 3.1b) was used in the other sampling port. Apparent concentrations and artifact concentrations were determined in the same manner as described for the adsorption artifact experiments (Experiments 3.5 through 3.8). This procedure was also applied to a freshly baked blank filter. Volatilization loss was calculated for both primary (A1Q) and adsorbate (B2Q) filters. These quantities were used to estimate the vapor fraction of total organic carbon lost from the primary filter.

A.4. Sampling Duration Experiments

In three experiments (3.12 through 3.14) sampling durations were varied. In all sampling ports filters were arranged in configuration A (Fig. 3.1a). In Experiment 3.12, samples in three sampling ports were collected for six hours. In the other three ports filters were replaced after three hours. As a result two samples were collected for three hours each in these sampling ports. The six-hour samples are referred to as long duration samples and the three-hour samples as short duration samples. One pair of short and long duration samples was collected at each of three different face velocities.

The same procedure was followed for the other two experiments, but with short and long duration samples of 24 and 48 hours, respectively. Both apparent particulate organic carbon concentrations and adsorbed vapor concentration were compared between sampling periods. For short duration samples these quantities were derived from the average of the two samples collected.

A.5. Filter Type Experiments

The collection of organic carbon on quartz and glass fiber filters was compared with all sampling ports operated at a face velocity of 10 cm/s (Experiments 3.15 and 3.16). Filters were arranged in configuration A (Fig. 3.1a) but with glass replacing quartz filters in three of the six sampling ports.

Adsorbed organic vapor concentrations were compared between quartz and glass fiber filters in a separate experiment (Experiment 3.17). Filters were arranged in all sampling ports in configuration B (Fig. 3.1b), but with glass replacing quartz fiber filters in three sampling ports. One of each filter type was used to collect samples at each of three face velocities. The B2Q filters were used to compare adsorbed vapor collected between filter types at each face velocity.

In two experiments (3.18 and 3.19), apparent organic aerosol concentration and adsorbed organic vapor concentrations were compared between quartz fiber and Teflon membrane filters. Quartz samples were collected with filters arranged in configuration A (Fig. 3.1a) and Teflon samples with filters arranged in configuration C (Fig. 3.1c).

Apparent concentrations were derived from the primary filters (A1Q,C1T) and adsorption artifact from the back-up filters (A2Q,C2T) for each filter type.

The utility of the data obtained from these nineteen experiments was such that results from many of them could be used to illustrate variations with sampling procedures other than those for which they were primarily intended to investigate. For example, information about variations of apparent concentration with face velocity could be obtained from the experiments designed principally to investigate sampling duration effects. Consequently, in some cases results are reported based on several types of experiments. Unless otherwise indicated, reported uncertainties in concentration are calculated from Equation 2.2.

B. Variations with Face Velocity

B.1. Results: Apparent Particulate Carbon Concentrations

Apparent carbonaceous aerosol concentrations from Experiments 3.1 through 3.4 are plotted against face velocity in Figs. 3.2a-3.2d. For Experiment 3.1, 10 μm impactors were used instead of 1 μm impactors. Also in Experiment 3.1, the 20 cm/s sample is excluded from data analysis because of contamination from rain. A decreasing trend of apparent organic carbon concentration with increasing face velocity was observed in all four experiments.

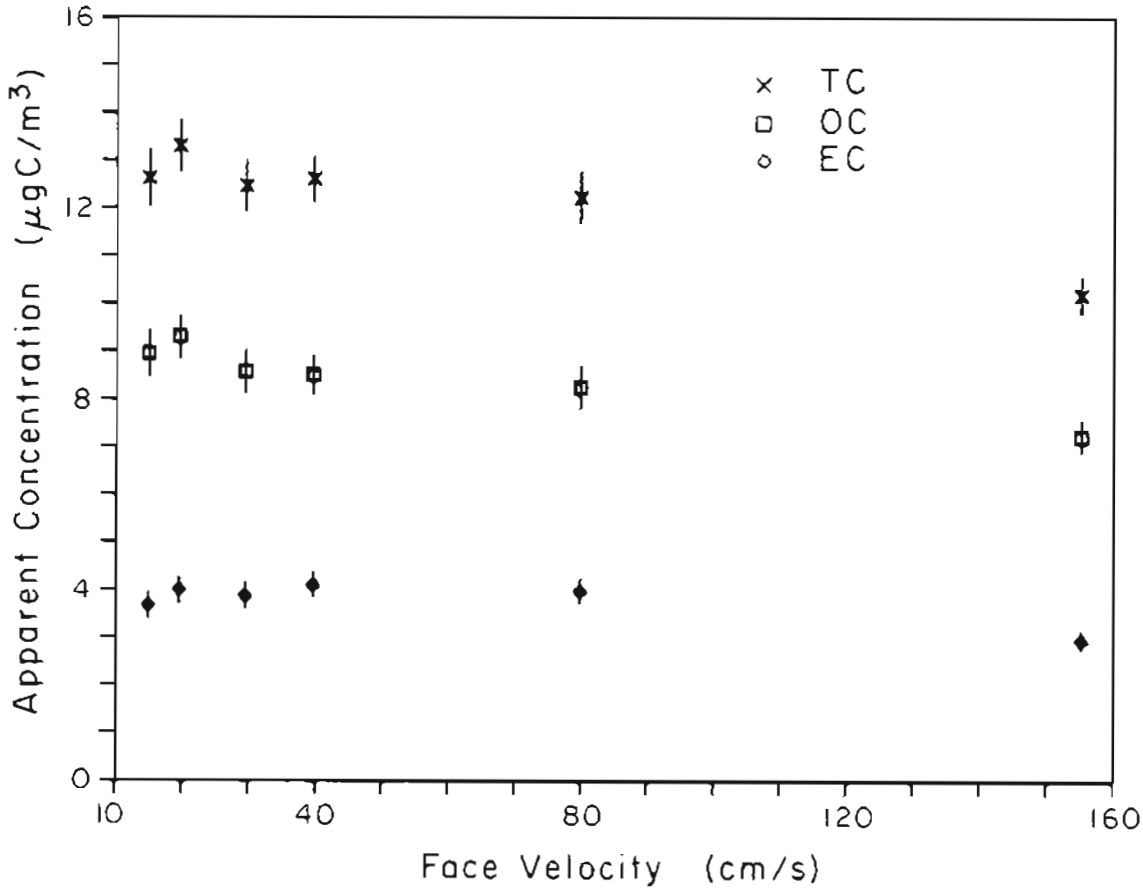

Figure 3.2a. Variation of apparent organic, elemental and total particulate carbon concentration with face velocity for Experiment 3.1.

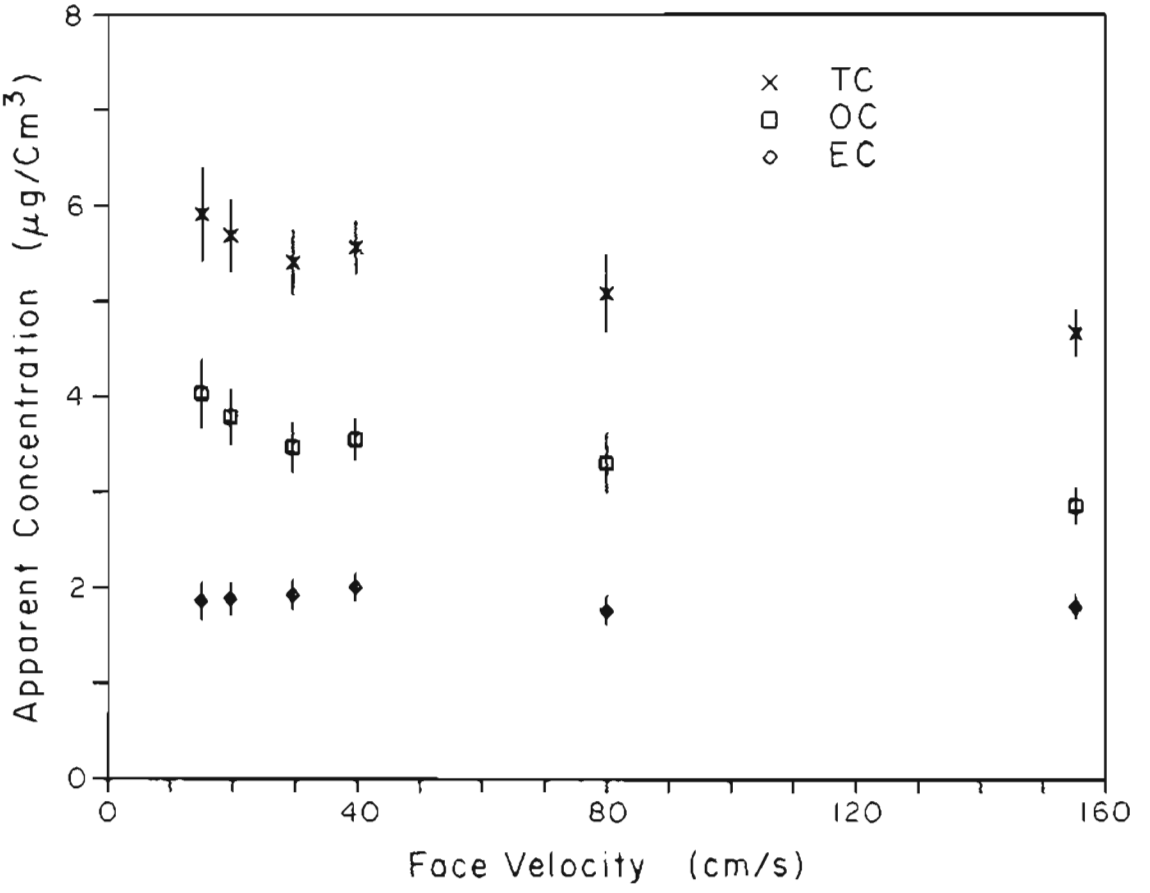

Figure 3.2b. Variation of apparent organic, elemental and total particulate carbon concentration with face velocity for Experiment 3.2.

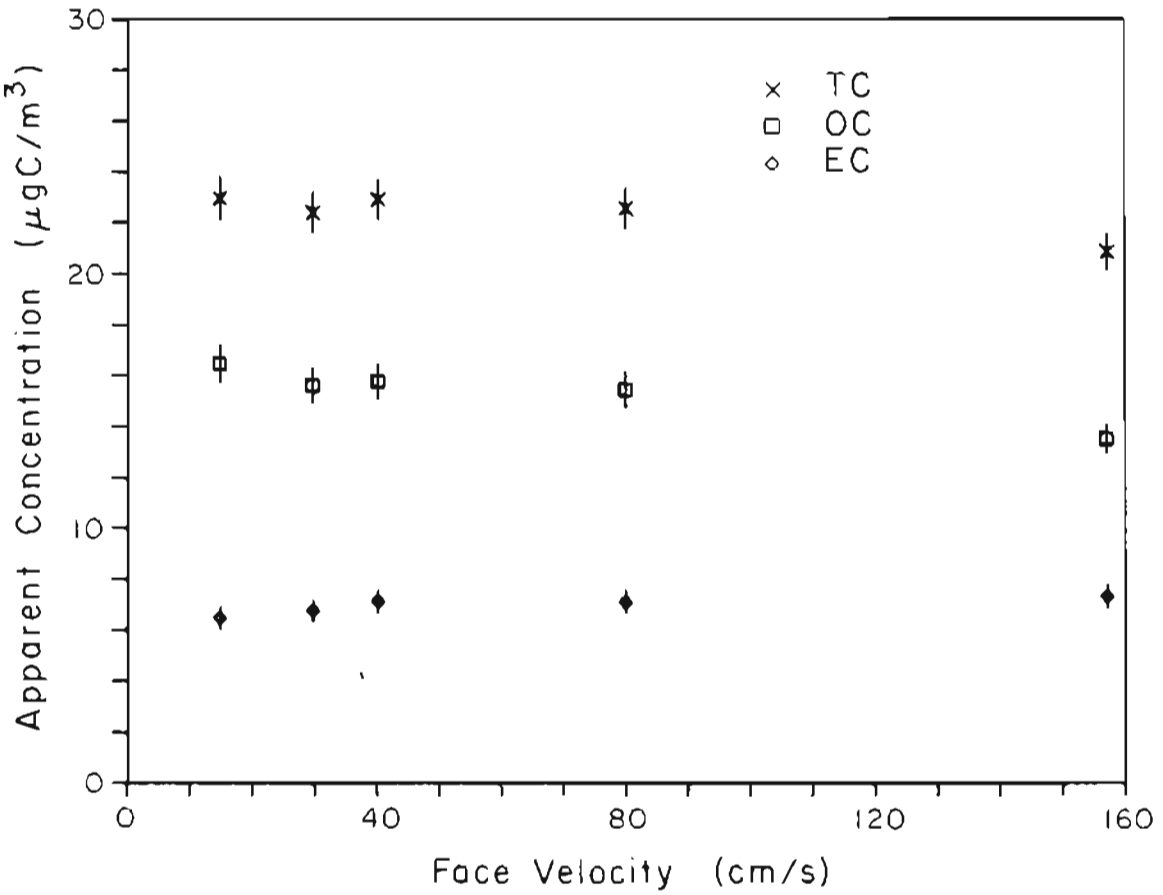

Figure 3.2c. Variation of apparent organic, elemental and total particulate carbon concentration with face velocity for Experiment 3.3.

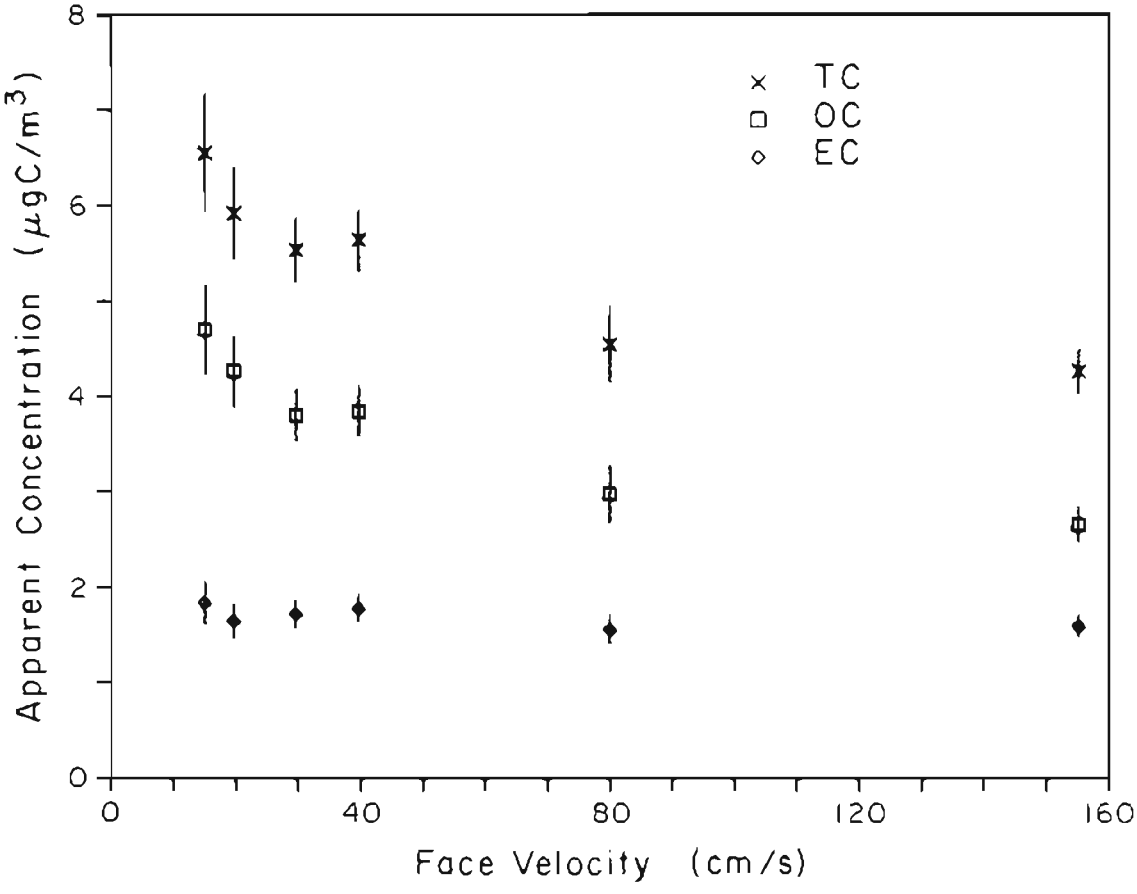

Figure 3.2d. Variation of apparent organic, elemental and total particulate carbon concentration with face velocity for Experiment 3.4.

The differences in apparent concentration between 15 cm/s and 150 cm/s face velocity samples are given in Table 3.2. Strong correlations were observed for each experiment between apparent organic carbon concentration and face velocity. Correlation coefficients were significant (p=0.05) for all four experiments.

The difference between concentrations calculated from the samples at the highest and lowest face velocities ranged from -1.2 to -3.0 $\mu gC/m^3$. This corresponded to 22-76% of the concentration calculated from the samples collected at 150 cm/s face velocity. Variations with face velocity were a larger fraction of apparent concentration at lower concentrations.

Correlations between elemental carbon concentration and face velocity were not significant (p=0.05) and the differences in elemental carbon concentrations between the samples collected at the highest and lowest face velocity were much smaller than those for organic carbon. Differences less than 1.0 $\mu gC/cm^2$ and under 20% of the mean elemental carbon concentration were observed for all sample sets.

For Experiment 3.1 elemental carbon appeared to increase with face velocity. Red color was observed on the filter after analysis. This was probably due to coarse iron oxide-containing particles which might have interfered with the correction for pyrolytically generated elemental carbon. These were apparently able to pass through the 5 µm impactors used in collection of the samples. Subsequent experiments used 1 µm impactors.

The mean uncertainties in Table 3.2 refer to one standard deviation calculated from the observed differences. Uncertainties

TABLE 3.2 - VARIATION OF APPARENT CONCENTRATION WITH FACE VELOCITY

APPARENT CONCENTRATION ($\mu gC/m^3$)	EXPERIMENT 3.1 ---	3.2 ---	3.3 ---	3.4 ---	MEAN ---
ORGANIC CARBON					
AT 15 cm/s	16.48	4.03	8.96	4.71	
AT 150 cm/s	13.52	2.87	7.23	2.66	
DIFFERENCE	-2.96	-1.16	-1.73	-2.05	-1.98
(uncertainty)	(0.94)	(0.41)	(0.59)	(0.50)	(0.75)
CORRELATION (r^2)	0.925	0.865	0.906	0.837	
ELEMENTAL CARBON					
AT 15 cm/s	6.48	1.87	3.67	1.84	
AT 150 cm/s	7.32	1.81	2.96	1.60	
DIFFERENCE	0.84	-0.06	-0.71	-0.24	-0.04
(uncertainty)	(0.62)	(0.24)	(0.34)	(0.25)	(0.65)
CORRELATION (r^2)	0.654	0.323	0.587	0.436	

individual experiments were propagated from those of the high and low face velocity values.

The decreasing trend of apparent aerosol organic carbon concentration with increasing face velocity was also supported by data from all experiments with 24-hour sampling duration in which face velocities were varied (Experiments 3.1 through 3.7, 3.13, 3.14, 3.18 and 3.19). For Experiments 3.13 and 3.14 both 24-hour sample sets were used from each experiment. Results are expressed in Fig. 3.3a as ratios of the mass collected for each sample to the mass collected simultaneously at 15 cm/s face velocity. A total of 13 separate 24-hour sample sets were obtained. Uncertainties refer to one standard deviation of the ratios observed at each face velocity. The results confirmed the strong decreasing trend of apparent aerosol organic carbon with increasing face velocity. 61% more organic carbon was collected at 15 cm/s than at 150 cm/s face velocity. Elemental carbon exhibited little variation with face velocity (Fig. 3.3b).

A significant decreasing trend of apparent aerosol organic carbon with increasing face velocity can be concluded. The magnitude of the difference in apparent concentration between samples collected at face velocities of 15 cm/s and 150 cm/s corresponds to a significant fraction of the apparent concentration. The absence of a similar decreasing trend for elemental carbon indicates that the phenomenon is not associated with general aerosol sampling problems (e.g. leaks, inlet effects, etc.).

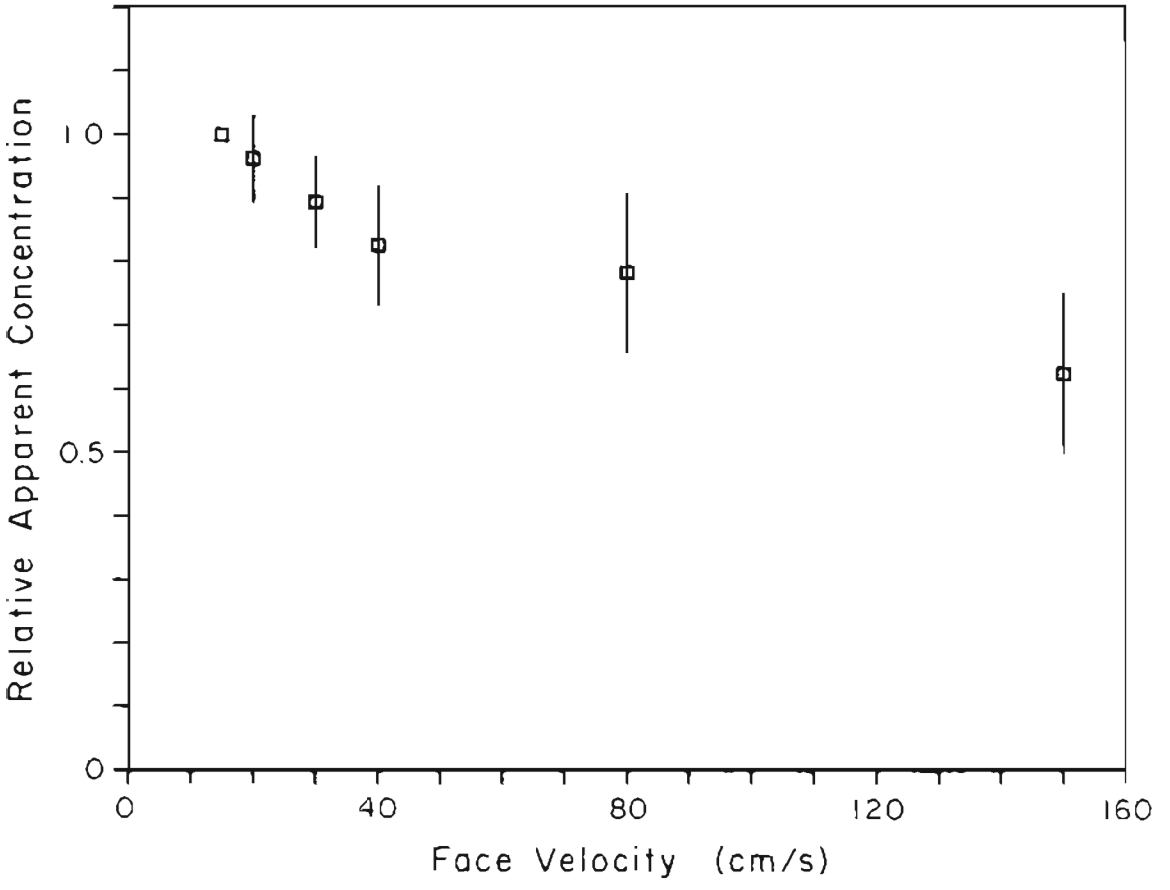

Figure 3.3a. Variation of apparent particulate organic carbon concentration with face velocity for 13 sets of samples. The average apparent concentration at 15 cm/s was 6.9 $\mu g/m^3$. Relative apparent concentration for a given face velocity sample to that of the sample collected at 15 cm/s.

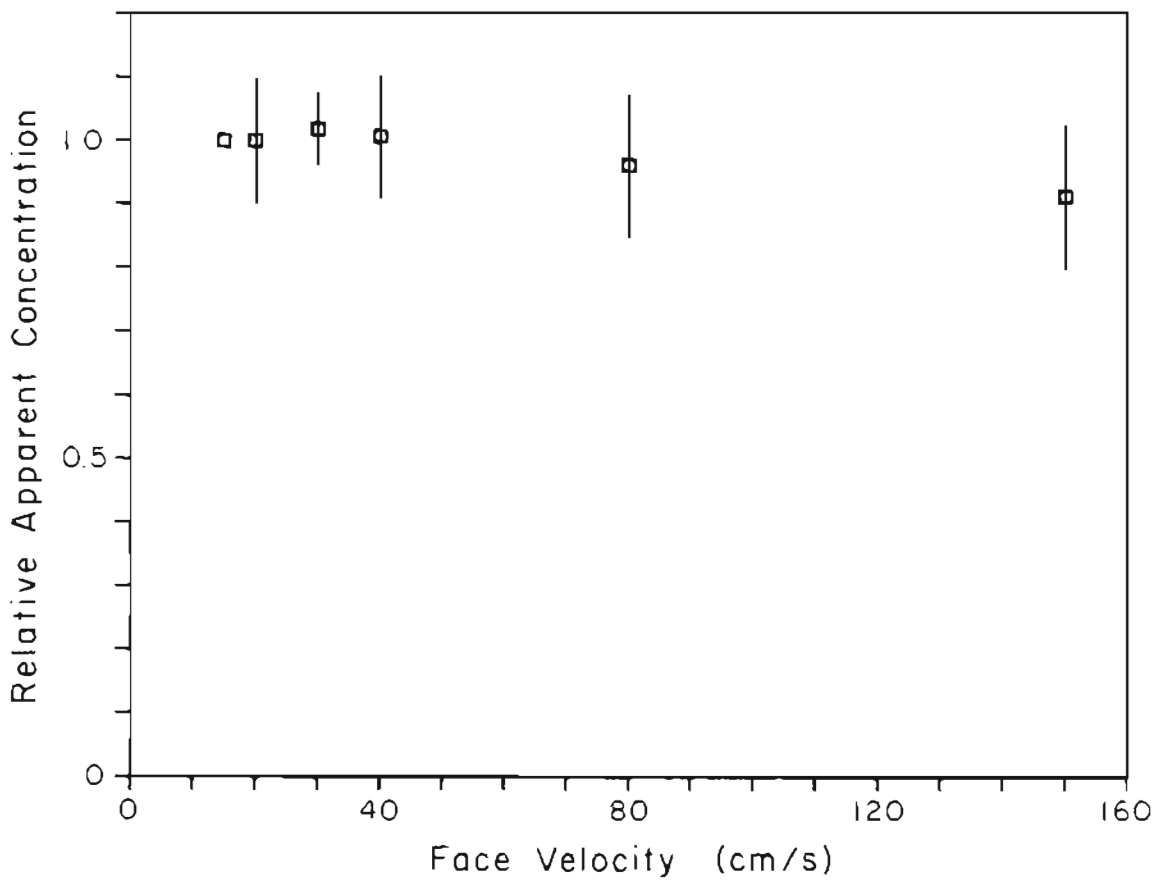

Figure 3.3b. Variation of apparent particulate elemental carbon concentration with face velocity for 13 sets of samples. The average apparent concentration at 15 cm/s was 2.7 $\mu g/m^3$. Relative apparent concentration refers to the ratio of the apparent concentration for a given face velocity sample to that of the sample collected at 15 cm/s.

B.2. Results: Adsorption Artifact

Figures 3.4a - 3.4d show the variation with face velocity of the adsorbed organic vapor concentrations estimated from the back-up filters (A2Q, behind quartz primary filters) of Experiments 3.1 through 3.4. A decreasing trend of concentration with increasing face velocity was observed. This relationship was similar to that between apparent organic aerosol concentration and face velocity. The face velocity dependence is especially pronounced at the lower face velocities.

Differences in the adsorbed vapor concentration between the 15 cm/s and 150 cm/s face velocity samples for Experiments 3.1 through 3.4 are given in Table 3.3. As with apparent organic aerosol concentrations, a strong negative correlation with face velocity was observed for the adsorbed organic vapor concentration. The correlation was significant ($p=.05$) for all experiments.

Differences in adsorbed organic vapor concentration between the highest and lowest face velocity ranged from 0.4 to 0.8 $\mu gC/m^3$. These were not as great as differences in apparent organic aerosol concentrations. This could be because the primary filters were depleting the sampled air of adsorptive vapor (see Chapter V). Nonetheless, 84-185% higher adsorbed organic vapor artifact concentrations were observed for back-up filter samples collected at 15 cm/s than for those collected at 150 cm/s in the same four experiments. The strong negative correlation of adsorption artifact with face velocity suggests

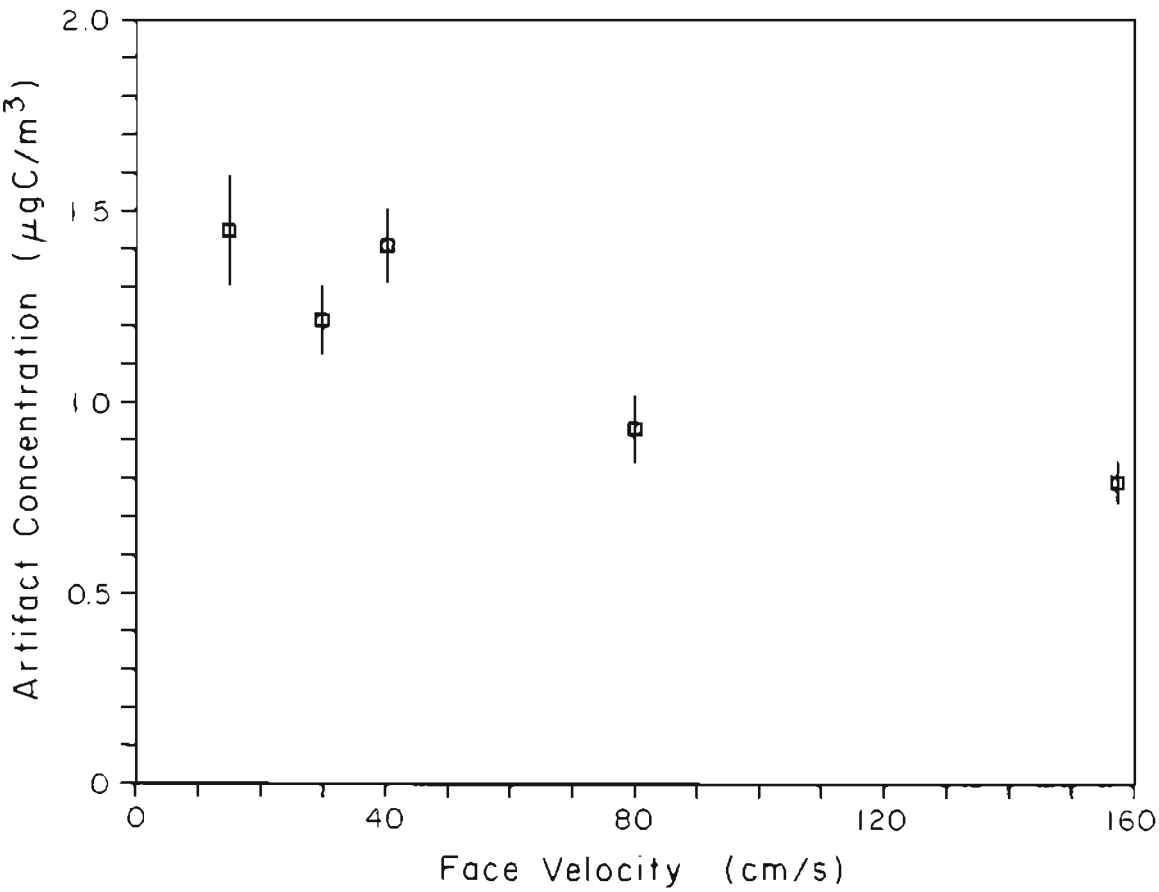

Figure 3.4a. Variation of adsorption artifact concentration with face velocity for Experiment 3.1. Artifact concentrations were estimated from carbon collected on quartz back-up filters behind quartz primary filters.

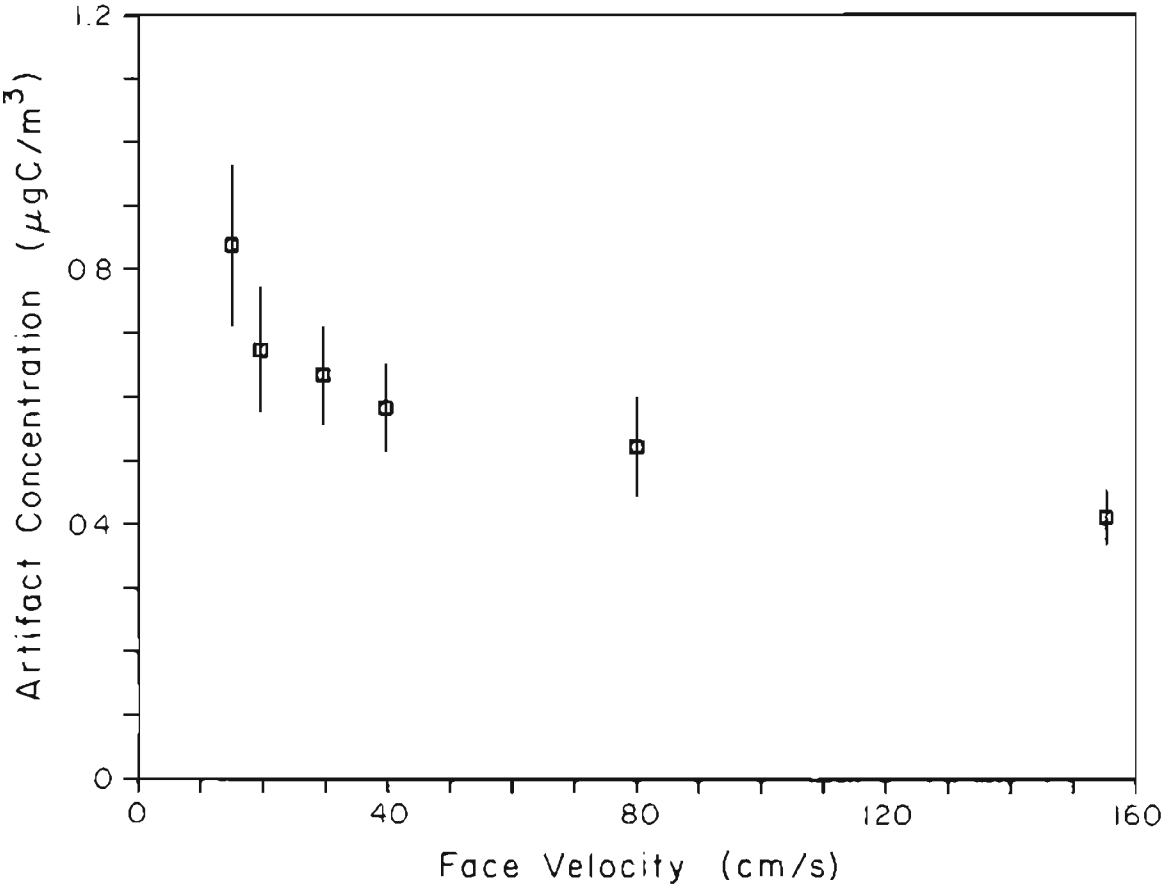

Figure 3.4b. Variation of adsorption artifact concentration with face velocity for Experiment 3.2. Artifact concentrations were estimated from carbon collected on quartz back-up filters behind quartz primary filters.

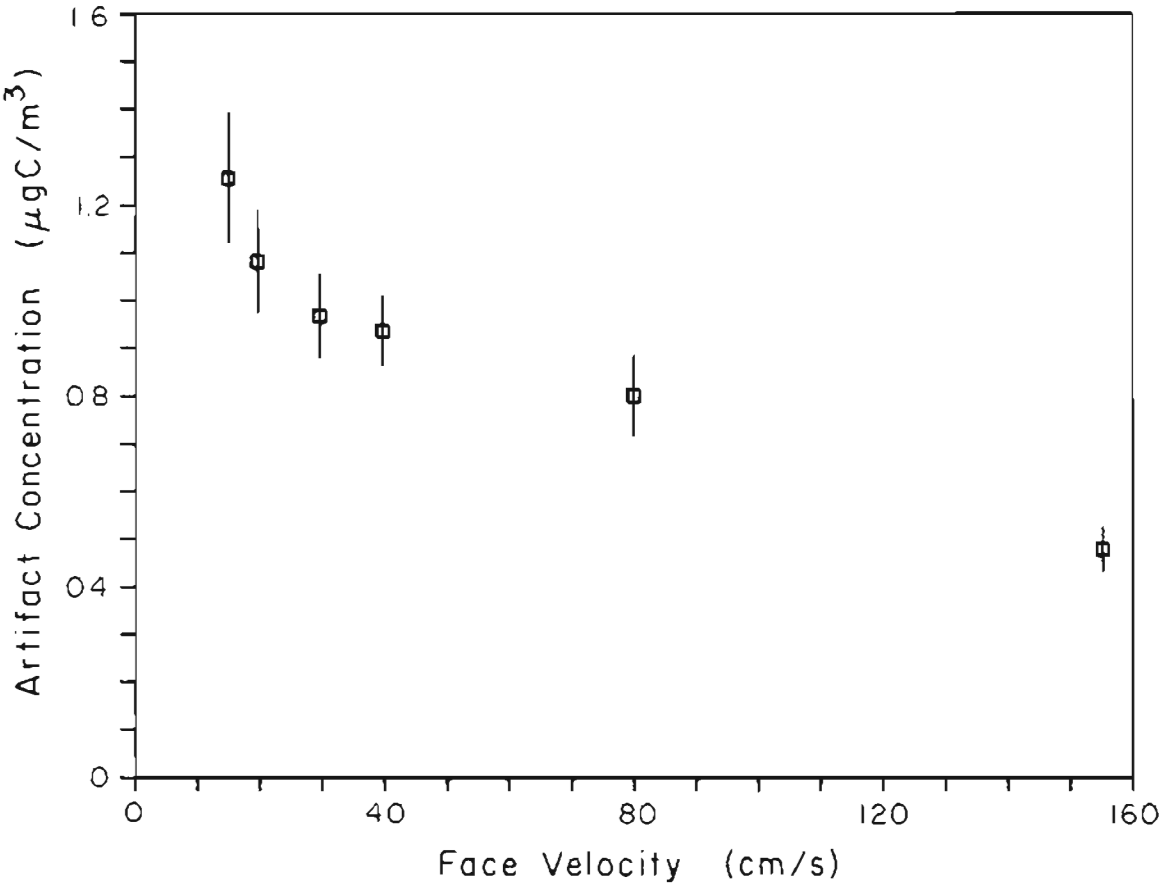

Figure 3.4c. Variation of adsorption artifact concentration with face velocity for Experiment 3.3. Artifact concentrations were estimated from carbon collected on quartz back-up filters behind quartz primary filters.

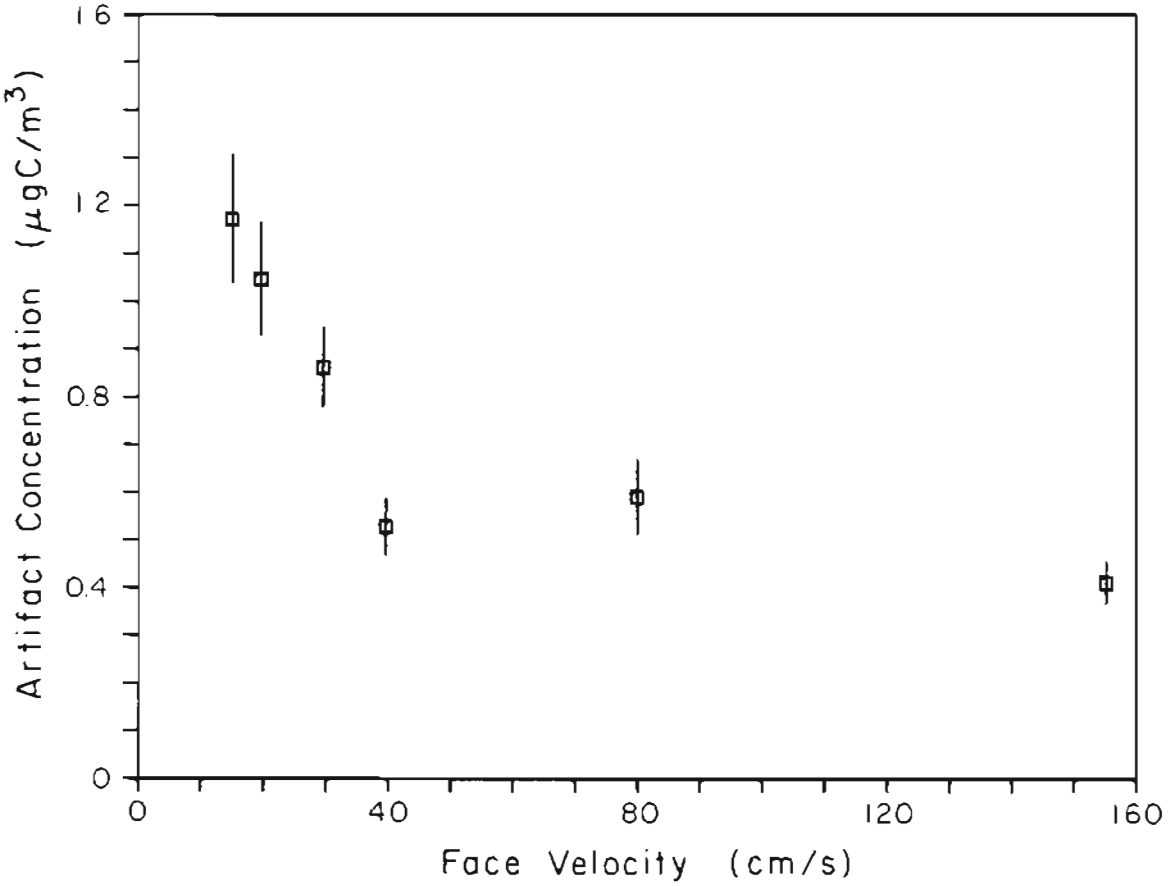

Figure 3.4d. Variation of adsorption artifact concentration with face velocity for Experiment 3.4. Artifact concentrations were estimated from carbon collected on quartz back-up filters behind quartz primary filters.

TABLE 3.3 - VARIATION OF ARTIFACT CONCENTRATION (FROM A2Q FILTERS) WITH FACE VELOCITY

	EXPERIMENT				
CARBON MASS ADSORBED PER CUBIC METER OF AIR SAMPLED ($\mu gC/m^3$)	3.1 ---	3.2 ---	3.3 ---	3.4 ---	MEAN ---
AT 15 cm/s	1.45	0.84	1.26	1.17	
AT 150 cm/s	0.79	0.41	0.48	0.41	
DIFFERENCE (uncertainty)	-0.66 (0.15)	-0.43 (0.13)	-0.78 (0.14)	-0.76 (0.14)	-0.66 (0.16)
CORRELATION (r^2)	0.824	0.752	0.916	0.642	

that organic vapor adsorption is at least partially responsible for the variation of apparent aerosol organic carbon with face velocity. In Table 3.3 uncertainties in the differences in apparent concentration between the 15 cm/s and 150 cm/s face velocity were determined in the same manner as for Table 3.2.

The decreasing trend of adsorbed organic vapor concentration with increasing face velocity is supported by data from back-up filters from the same experiments used in Figs. 3.3a-d. Results are expressed as the ratios of the mass collected for each sample to the mass collected simultaneously at 15 cm/s in Fig. 3.5. Uncertainties refer to one standard deviation of ratios observed at each face velocity.

The mass loading of carbon on the back-up filter per unit area of filter is plotted against face velocity for the same four experiments in Figs. 3.6a - 3.6d. Here an increasing trend in carbon mass collected with increasing face velocity is consistently observed, and there is no conclusive evidence of any saturation phenomenon.

Experiments 3.5 through 3.8 (i.e., quartz back-up filters behind Teflon and quartz primary filters) were conducted to estimate the fraction of apparent organic aerosol concentration differences which can be explained by vapor adsorption. A decreasing trend of apparent organic aerosol concentration calculated from the quartz primary filter with increasing face velocity was also observed in these experiments, as described by Figs. 3.7a - 3.7d and Table 3.4. Elemental carbon does not appear to vary with face velocity. Table 3.4 shows that apparent organic carbon concentration differences

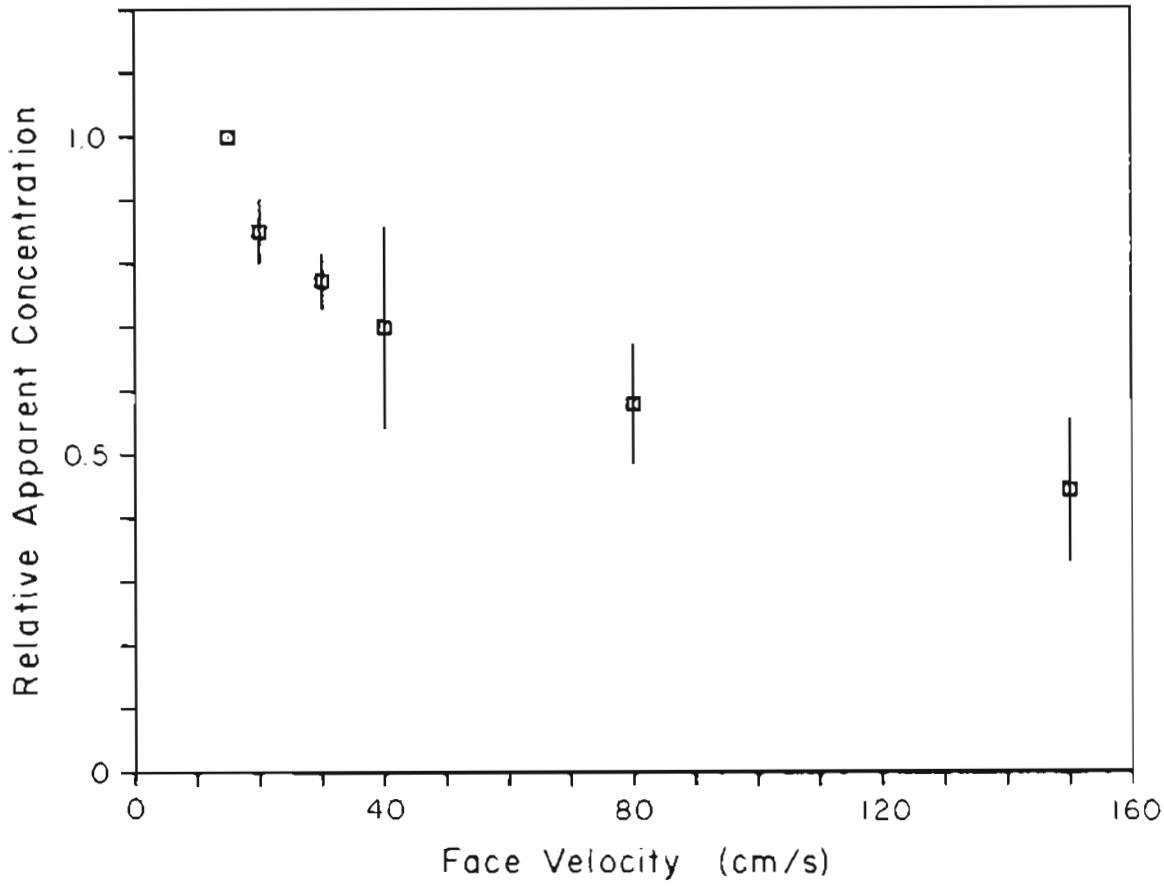

Figure 3.5. Variation of adsorption artifact concentration with face velocity for 13 sets of samples. The average artifact concentration at 15 cm/s was 1.21 $\mu g/m^3$. Adsorption artifact concentrations were estimated from carbon collected on quartz back-up filters behind quartz primary filters. Relative artifact concentration refers to the ratio of the artifact concentration for a given face velocity sample to that of the sample collected at 15 cm/s.

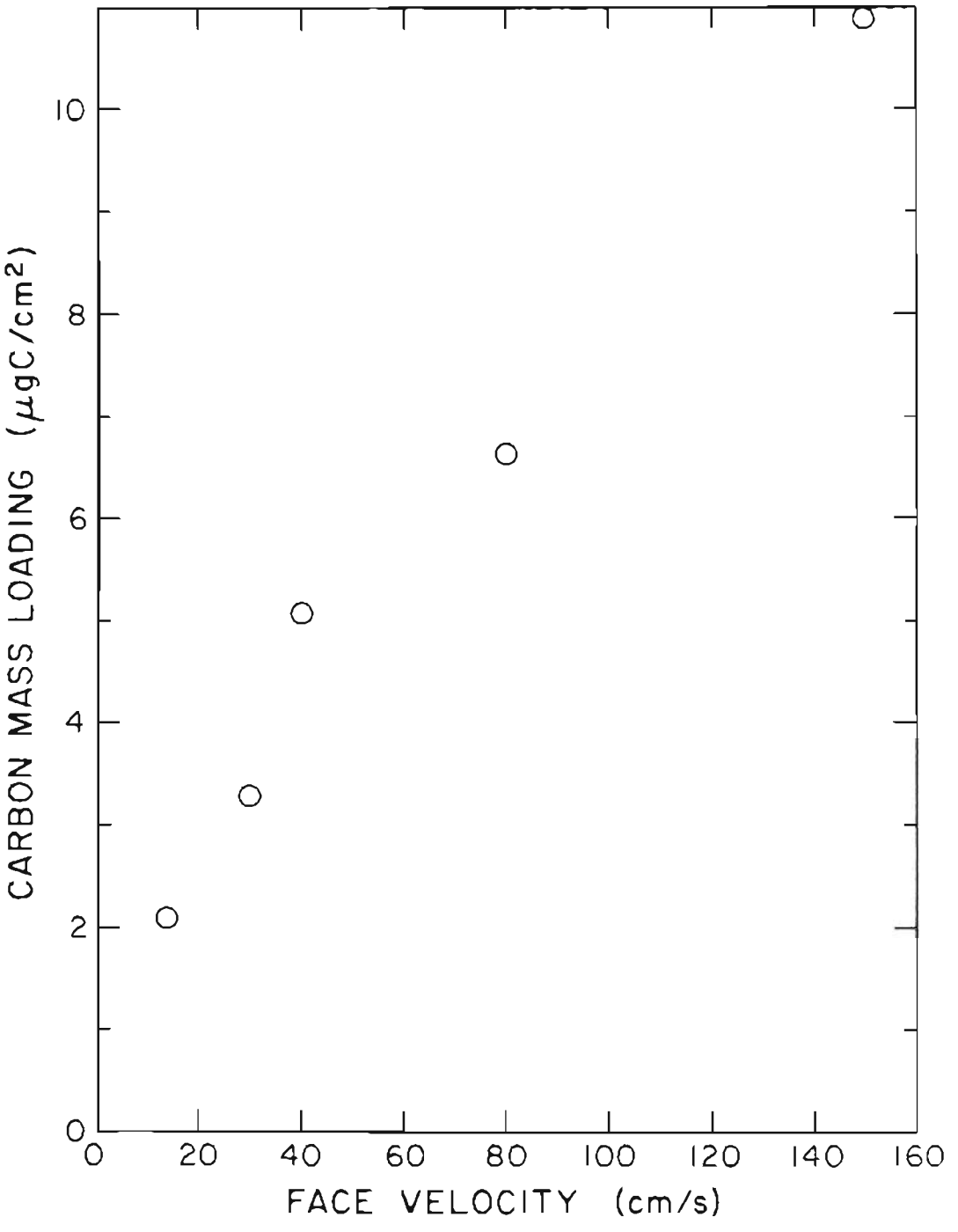

Figure 3.6a. Carbon mass collected per unit area of back-up filter for Experiment 3.1.

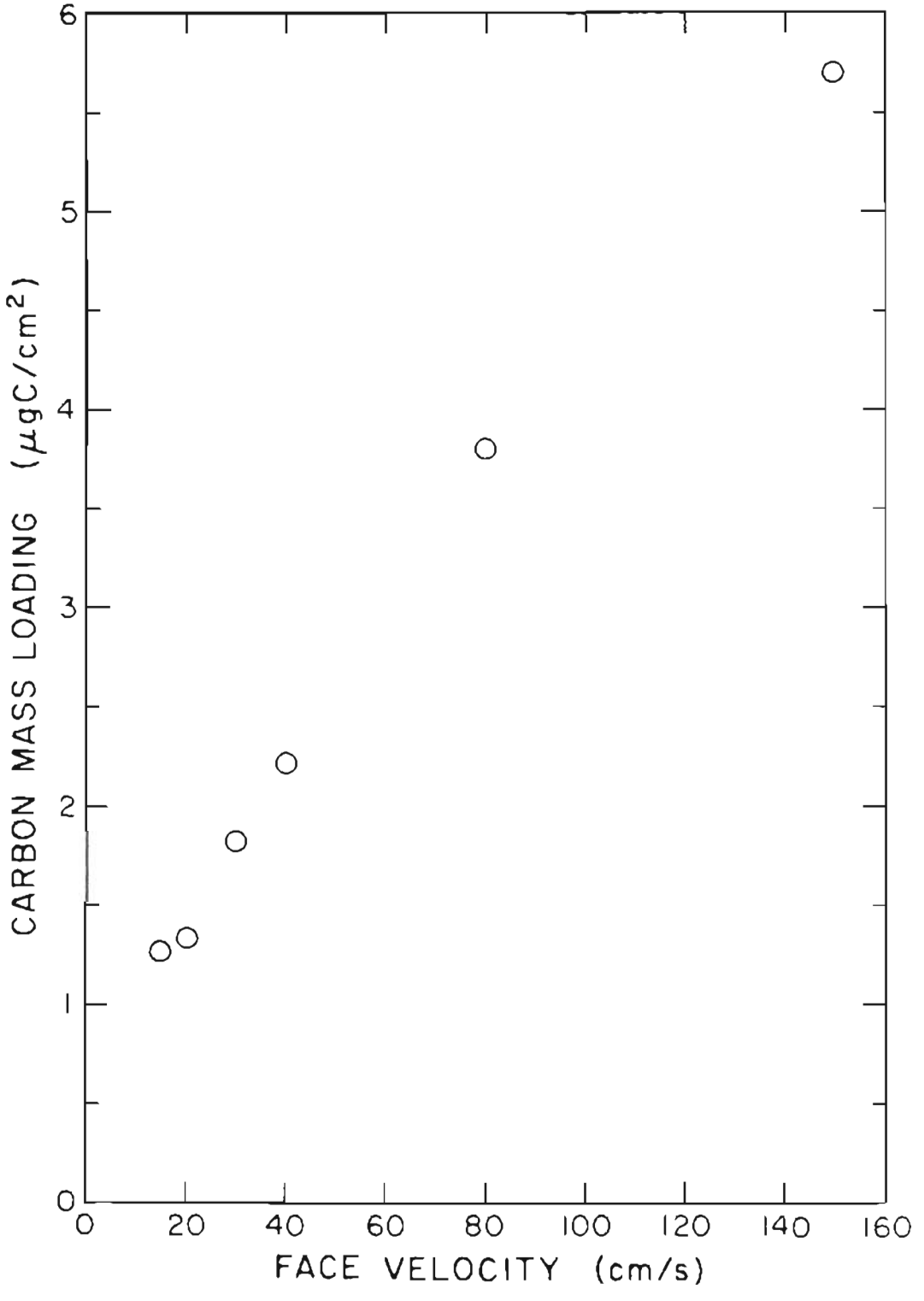

Figure 3.6b. Carbon mass collected per unit area of back-up filter for Experiment 3.2.

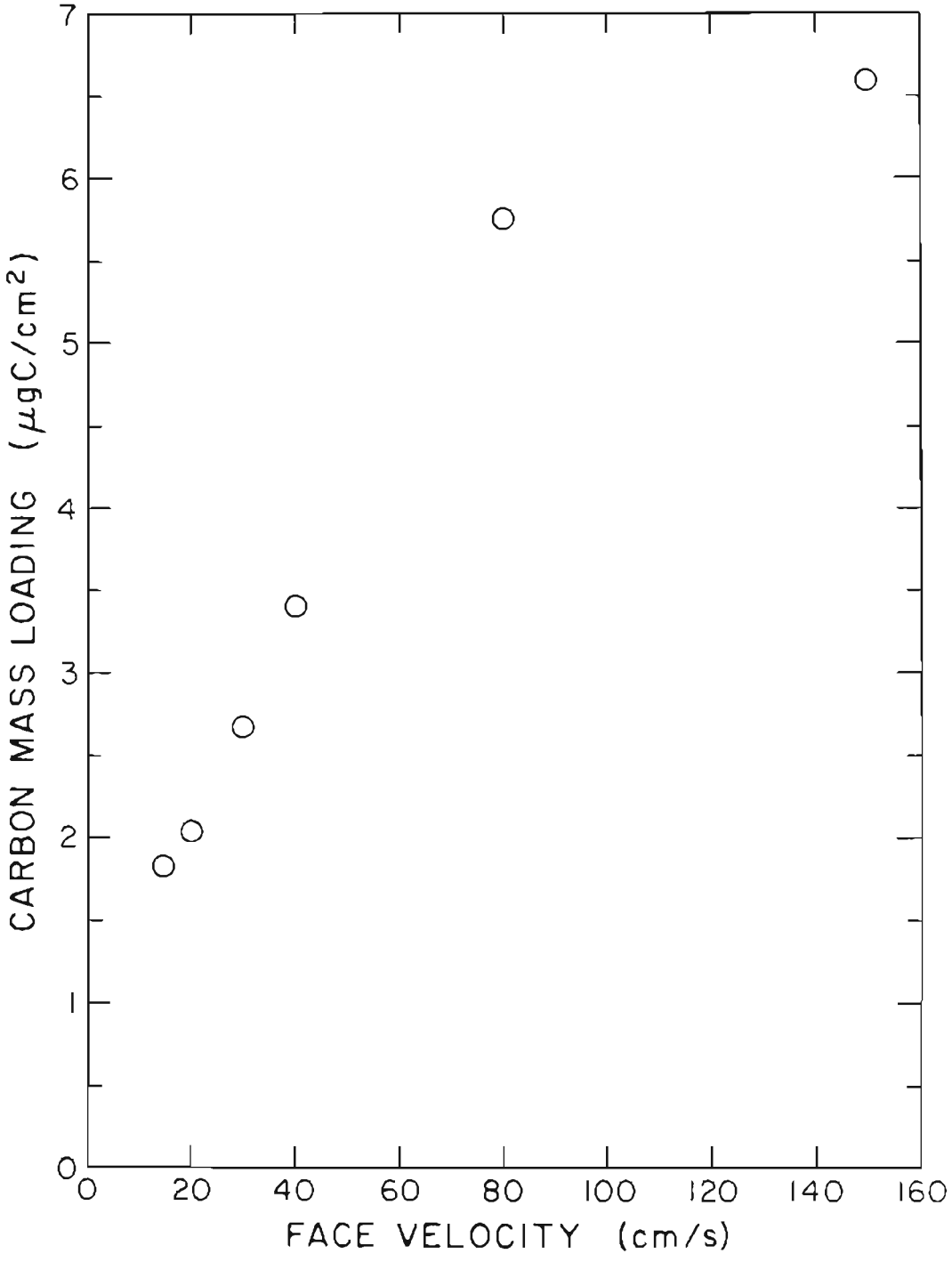

Figure 3.6c. Carbon mass collected per unit area of back-up filter for Experiment 3.3.

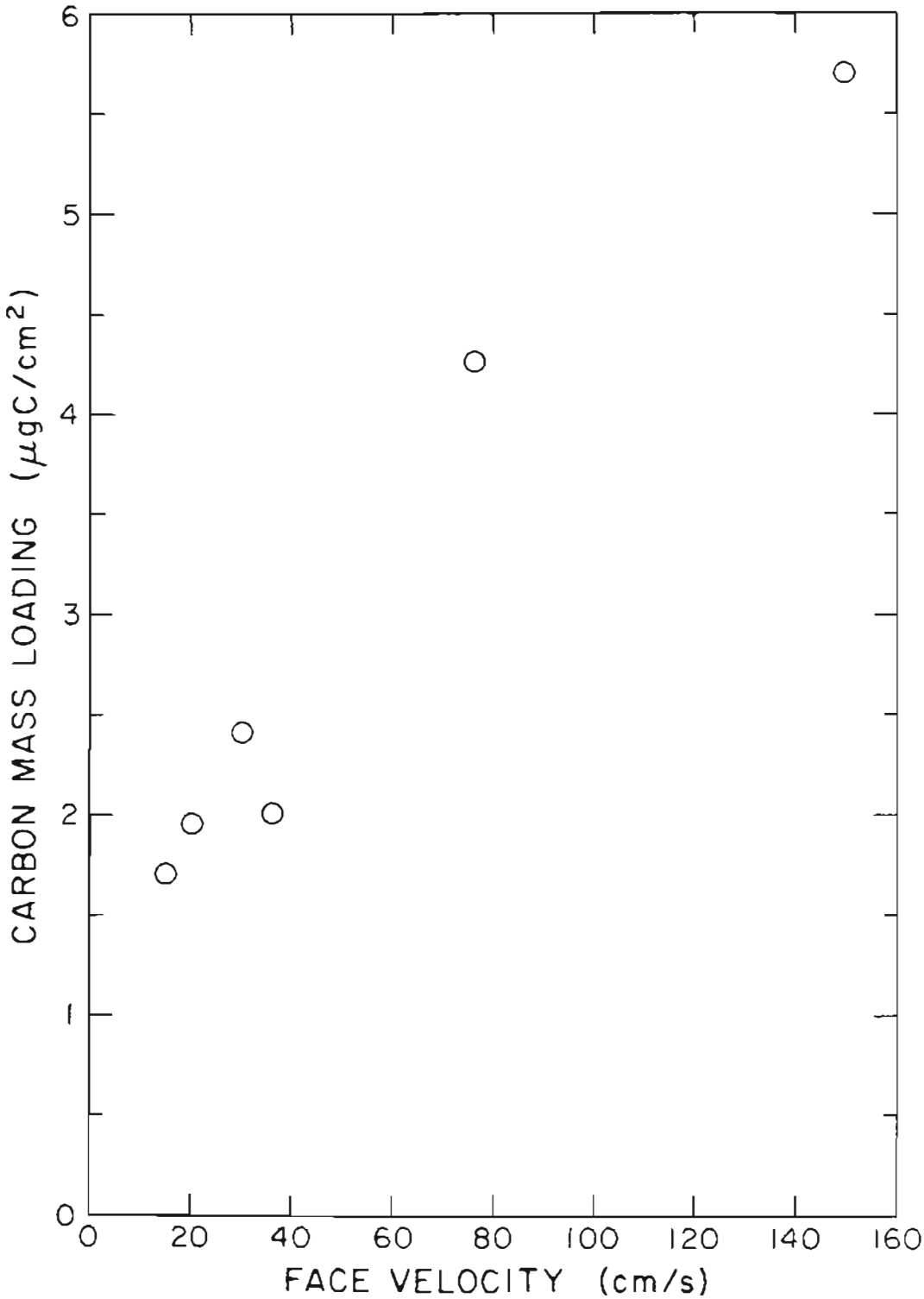

Figure 3.6d. Carbon mass collected per unit area of back-up filter for Experiment 3.4.

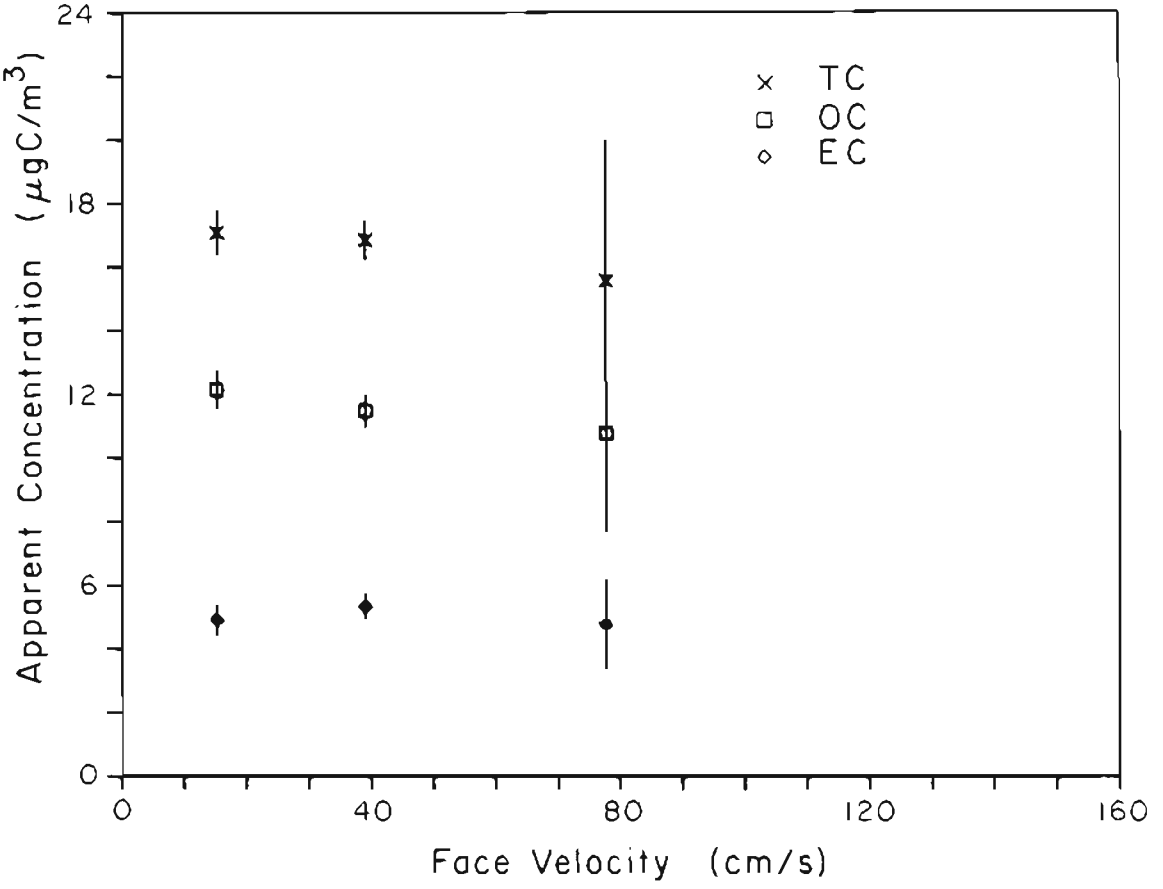

Figure 3.7a. Variation of apparent particulate organic carbon concentration with face velocity for Experiment 3.5.

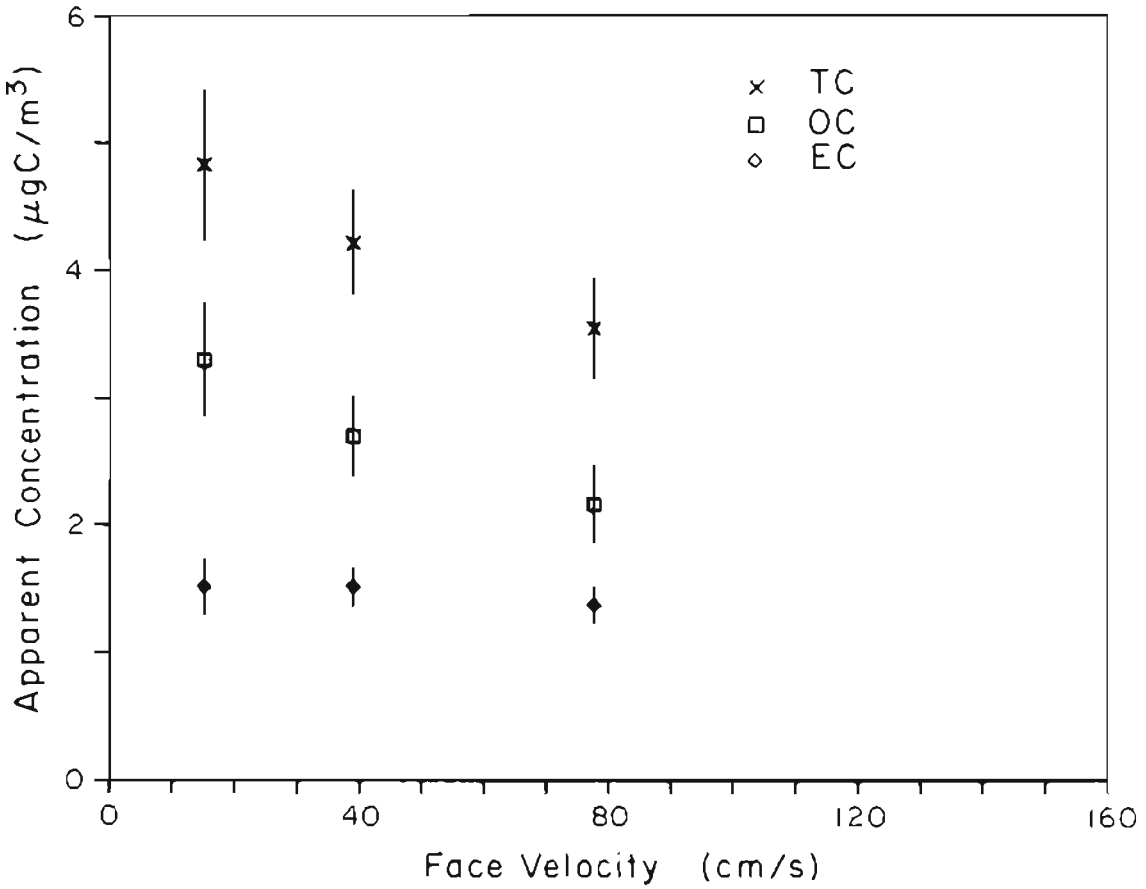

Figure 3.7b. Variation of apparent particulate organic carbon concentration with face velocity for Experiment 3.6.

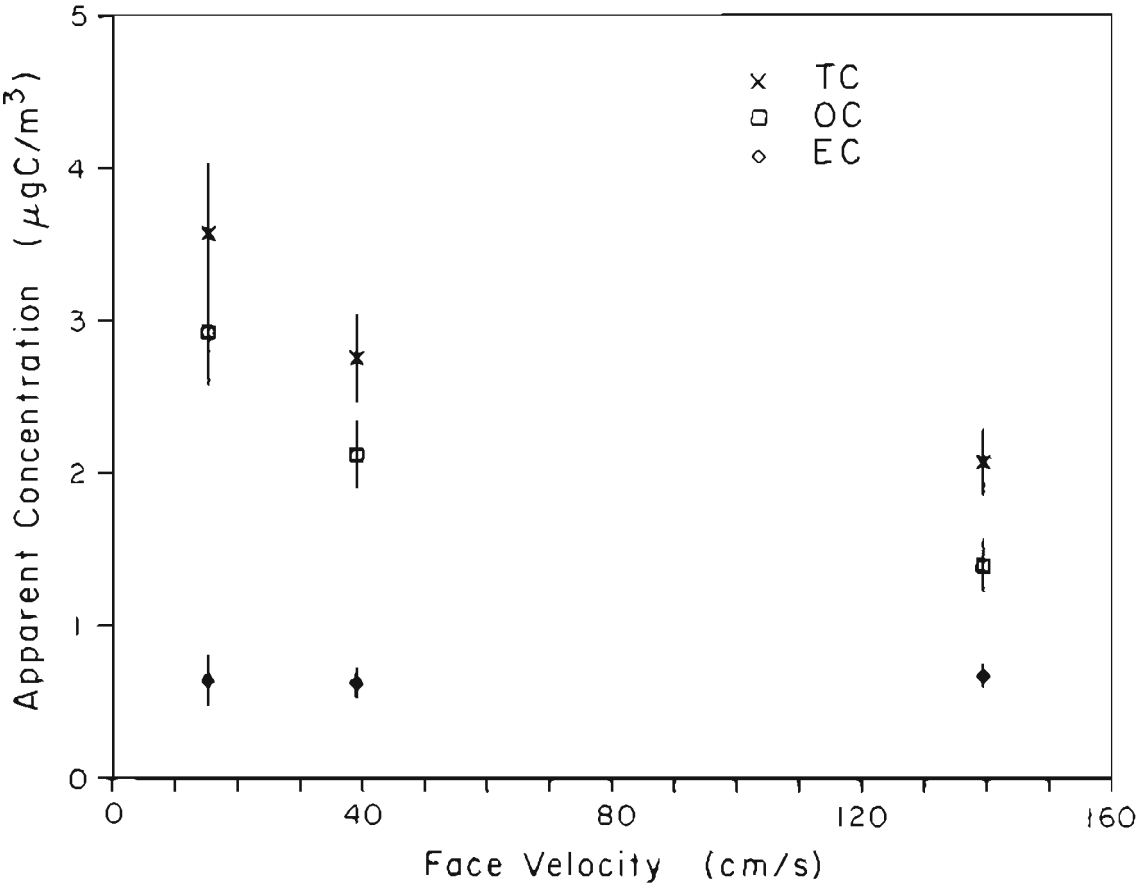

Figure 3.7c. Variation of apparent particulate organic carbon concentration with face velocity for Experiment 3.7.

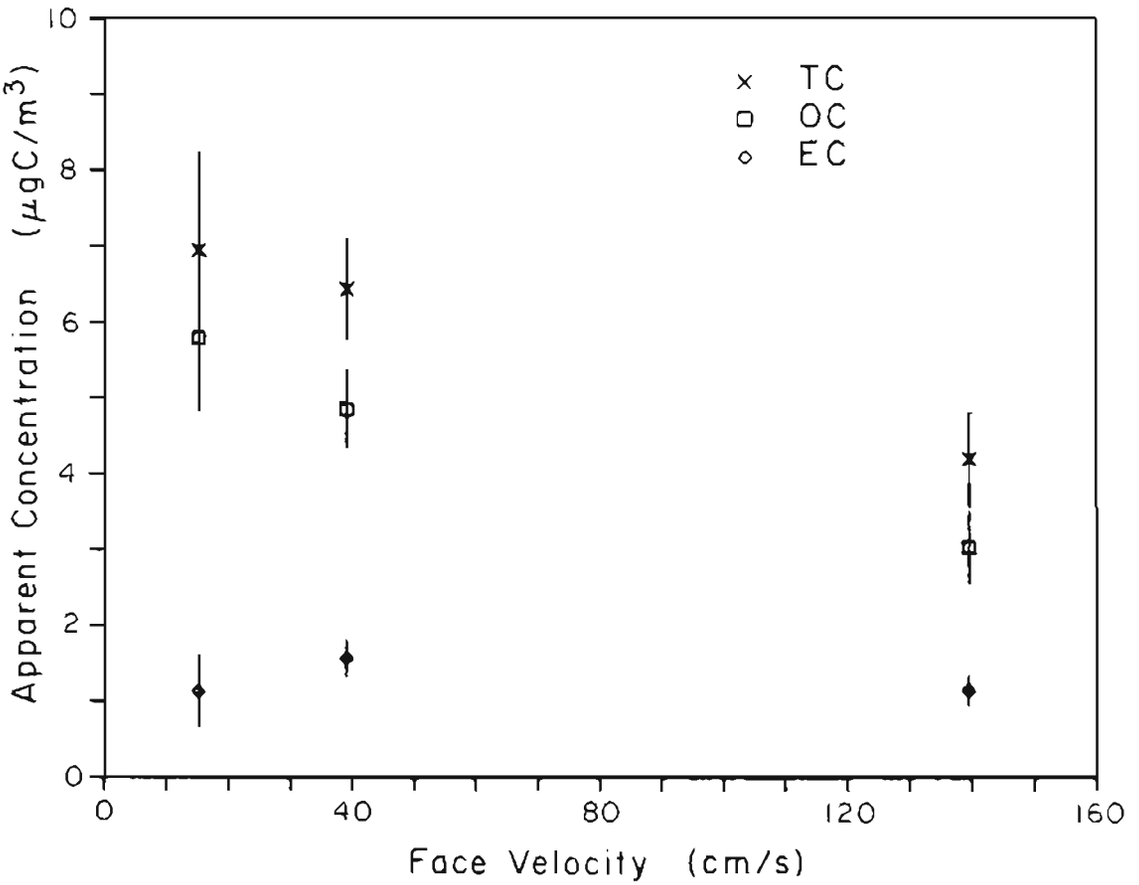

Figure 3.7d. Variation of apparent particulate organic carbon concentration with face velocity for Experiment 3.8.

TABLE 3.4 - VARIATION OF APPARENT ORGANIC CARBON CONCENTRATION WITH FACE VELOCITY FOR QUARTZ PRIMARY FILTERS

	EXPERIMENT				
	3.5	3.6	3.7	3.8	MEAN
SAMPLING PERIOD (hrs.)	24	24	24	8.75	
APPARENT ORGANIC CARBON ($\mu gC/m^3$)					
LOWEST FACE VELOCITY*	12.15	3.30	2.92	5.80	
HIGHEST FACE VELOCITY**	10.77	2.17	1.40	3.00	
DIFFERENCE	-1.38	-1.13	-1.52	-2.77	-1.70
(uncertainty)	(3.12)	(0.55)	(0.38)	(1.16)	(0.73)

* 15 cm/s for all experiments

** 80 cm/s for Experiments 3.5 and 3.6; 140 cm/s for 3.7 and 3.8.

between the highest and lowest face velocities averaged -1.7 $\mu gC/m^3$ and ranged from -1.1 to -2.8 $\mu gC/m^3$. If only the 24-hour sampling periods are included the average is -1.3 $\mu gC/m^3$. Uncertainties reported in Table 3.4 were determined in the same manner as for Table 3.2.

In all four experiments a decreasing trend with increasing face velocity is also observed for the adsorbed organic vapor concentrations derived from quartz fiber filters (B2Q) behind Teflon prefilters. This is shown in Figs. 3.8a - 3.8d. It is similar to the relationship with face velocity of adsorbed organic vapor concentration estimated from the A2Q filters in Figs. 3.4a - 3.4d, but is greater in magnitude. Table 3.5 lists the differences in adsorption artifact estimates between the highest and lowest face velocities employed for Experiments 3.5 through 3.8. The average difference in adsorption artifact between the highest and lowest face velocity was 1.5 $\mu gC/m^3$. Uncertainties reported in Table 3.5 were determined in the same manner as for Table 3.2.

Table 3.6 compares the concentrations of adsorbed organic carbon on quartz fiber back-up filters behind Teflon and quartz prefilters for Experiments 3.5 - 3.8. In all cases more organic carbon was collected on the back-up filters behind the Teflon prefilters than behind the quartz fiber prefilters. This suggests that organic carbon on the quartz fiber back-up filter behind the Teflon prefilter is a better estimate of organic vapor adsorption on a quartz fiber aerosol filter than would be obtained from a quartz fiber back-up filter behind a quartz fiber primary filter.

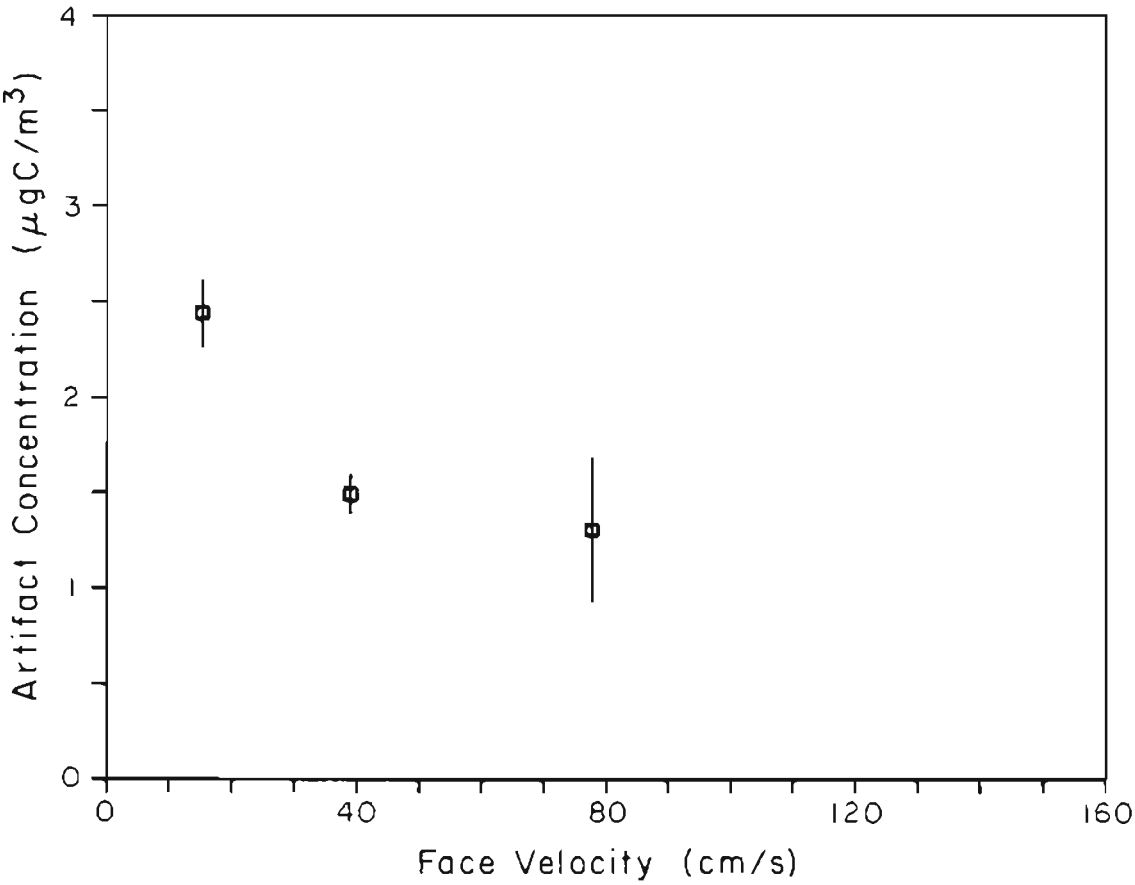

Figure 3.8a. Variation of adsorption artifact concentration with face velocity for Experiment 3.5. Adsorption artifact concentrations were estimated from carbon collected on quartz filters behind Teflon prefilters.

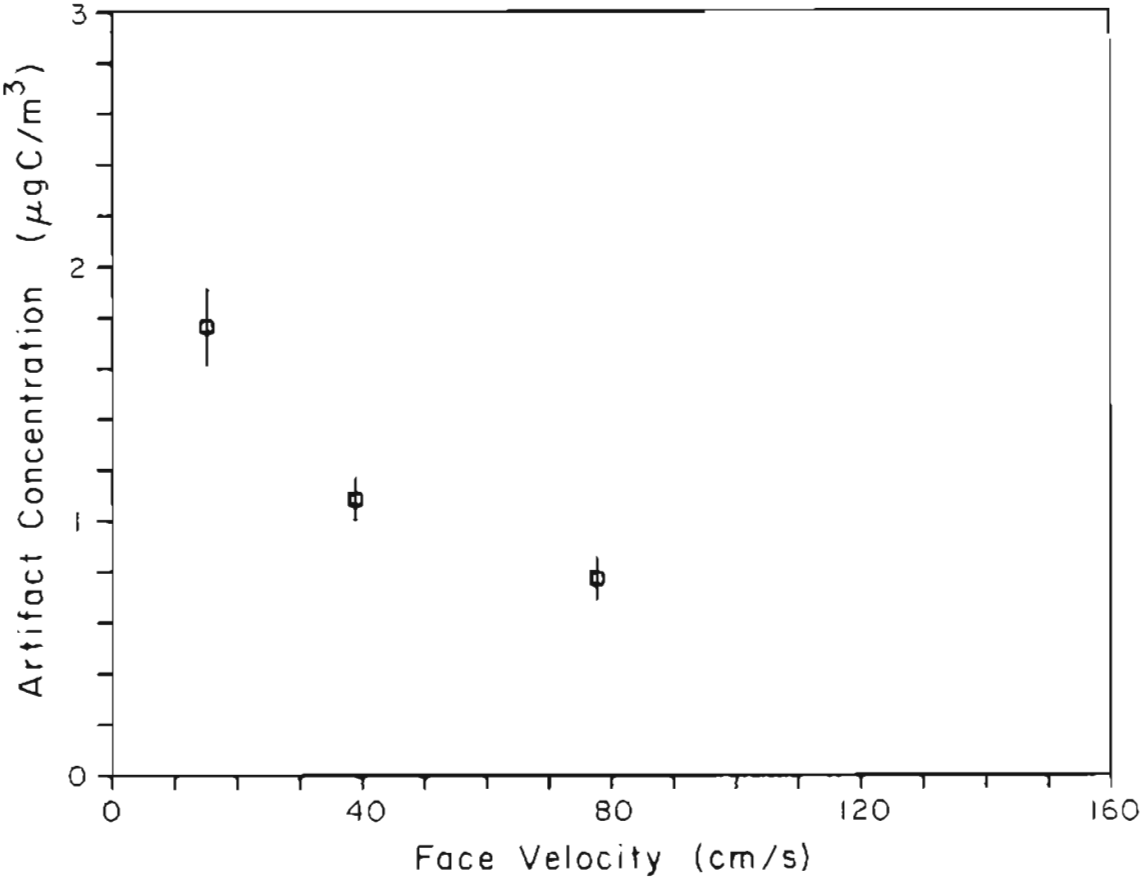

Figure 3.8b. Variation of adsorption artifact concentration with face velocity for Experiment 3.6. Adsorption artifact concentrations were estimated from carbon collected on quartz filters behind Teflon prefilters.

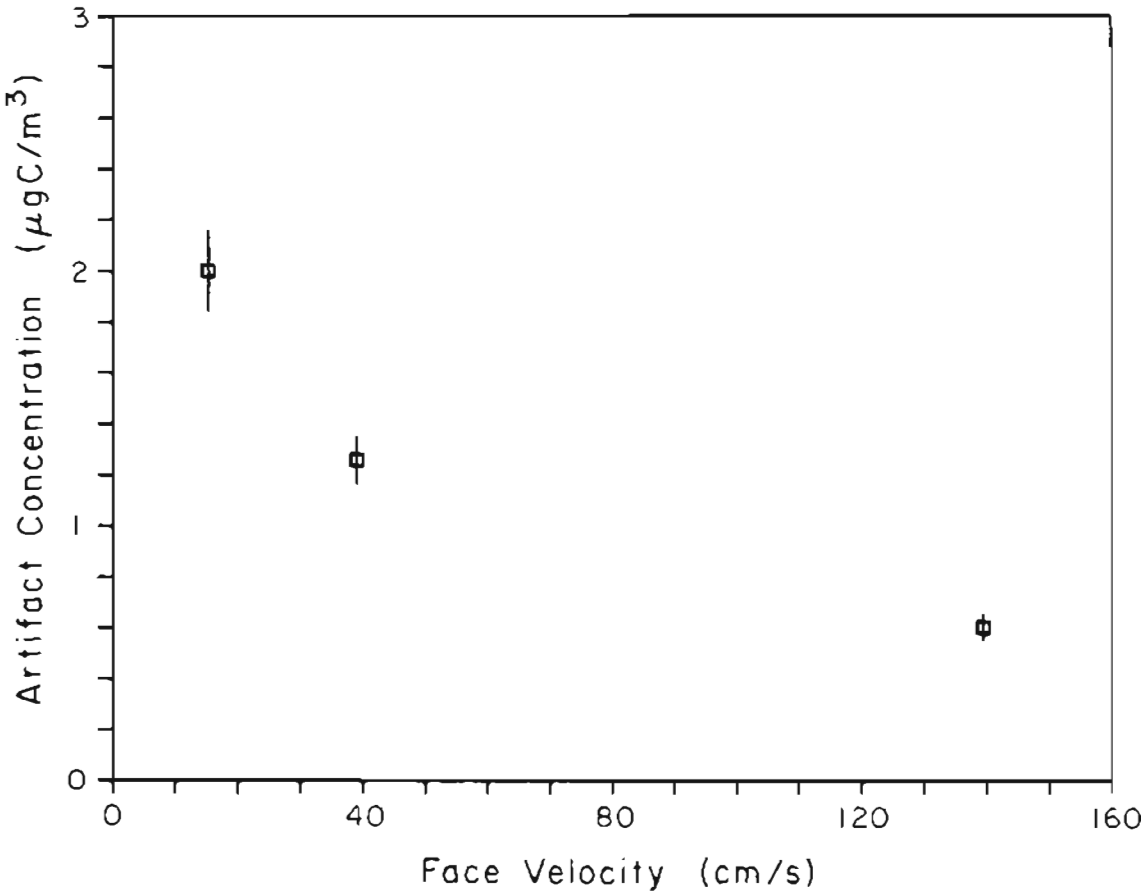

Figure 3.8c. Variation of adsorption artifact concentration with face velocity for Experiment 3.7. Adsorption artifact concentrations were estimated from carbon collected on quartz filters behind Teflon prefilters.

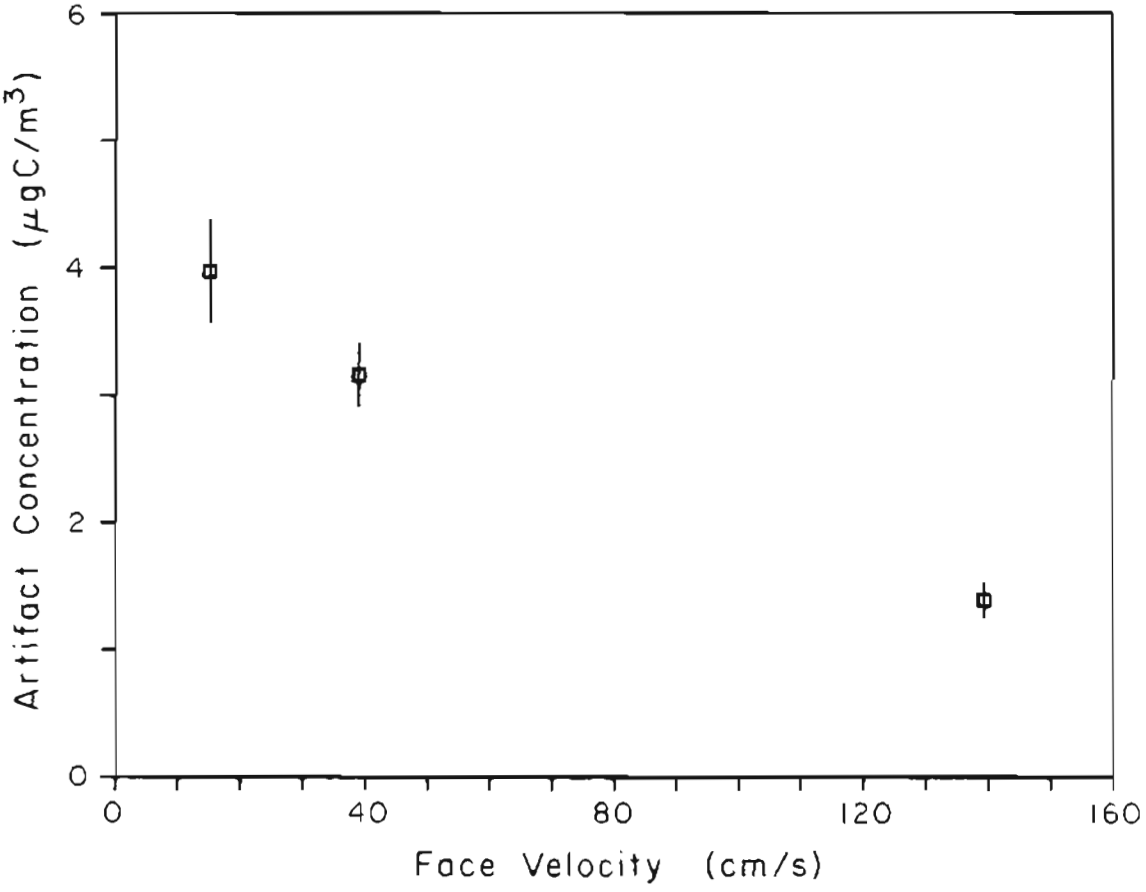

Figure 3.8d. Variation of adsorption artifact concentration with face velocity for Experiment 3.8. Adsorption artifact concentrations were estimated from carbon collected on quartz filters behind Teflon prefilters.

TABLE 3.5 - VARIATION OF ARTIFACT CONCENTRATION (FROM B2Q FILTERS) WITH FACE VELOCITY

	EXPERIMENT				
	3.5	3.6	3.7	3.8	MEAN
SAMPLING PERIOD (hrs.)	24	24	24	8.75	
CARBON MASS ADSORBED PER CUBIC METER OF AIR SAMPLED ($\mu gC/m^3$)					
LOWEST FACE VELOCITY*	2.44	1.77	2.00	3.98	
HIGHEST FACE VELOCITY**	1.31	0.78	0.60	1.39	
DIFFERENCE (uncertainty)	-1.13 (0.42)	-0.99 (0.17)	-1.40 (0.17)	-2.59 (0.43)	-1.53 (0.73)

* 15 cm/s for all experiments

** 80 cm/s for Experiments 3.5 and 3.6; 140 cm/s for 3.7 and 3.8.

TABLE 3.6 - FRACTION OF PRIMARY FILTER ORGANIC CARBON ACCOUNTED FOR BY VAPOR ADSORPTION

EXPERIMENT	FACE VELOCITY	CARBON MASS COLLECTED: AEROSOL PRIMARY FILTER $\mu gC/cm^2$	BEHIND TEFLON FILTER $\mu gC/cm^2$	BEHIND TEFLON FILTER as % of primary	BEHIND QUARTZ FIBER FILTER $\mu gC/cm^2$	BEHIND QUARTZ FIBER FILTER as % of primary
3.5	15 cm/s	15.9	3.15	20%	1.64	10%
	40 cm/s	38.7	4.95	13%	3.46	9%
	80 cm/s	72.3	5.67	8%	5.61	8%
3.6	15 cm/s	4.3	2.28	53%	0.94	22%
	40 cm/s	9.1	3.68	40%	1.98	22%
	80 cm/s	14.6	5.24	36%	3.12	21%
3.7	15 cm/s	3.8	2.58	67%	1.00	26%
	40 cm/s	7.2	4.18	58%	2.11	29%
	140 cm/s	16.8	7.27	43%	5.40	32%
3.8	15 cm/s	2.6	1.76	68%	0.62	24%
	40 cm/s	5.6	3.68	65%	1.21	22%
	140 cm/s	12.6	5.53	44%	3.14	25%
MEAN				43%		21%
STANDARD DEV.				21%		8%

The efficiency with which adsorptive vapors are removed by quartz fiber primary filters can be estimated by comparing carbon collected on the quartz filter (B2Q in Fig. 3.1) behind a Teflon prefilter (B1T) to that collected on a second quartz fiber back-up filter (B2Q) behind a Teflon prefilter (B1T) and a quartz fiber back-up filter (B2Q). For the twelve samples an average of 82% more carbon was collected on the B2Q filters than on the B3Q filters. This indicates that organic vapor adsorption decreases with downstream filter position for a quartz fiber filter series, and consequently that quartz back-up filters positioned immediately downstream of quartz primary filters can seriously underestimate the extent of adsorption artifact on primary filters. The ratio of carbon mass collected between these two filters generally decreased with increasing face velocity, as shown in Fig. 3.9. This could be an indication that the higher face velocity samples were closer to steady-state adsorption.

The extent to which adsorptive vapors are removed by Teflon membrane filters can be determined by comparing organic carbon collected on filters A2Q and B3Q (see Fig. 3.1). The only systematic difference between the two filters is the insertion of a Teflon prefilter (B1T in Fig. 3.1b). An average of 18% more carbon was observed on A2Q than on B3Q.

A simple experiment was designed to determine whether Teflon membrane filters were a source of organic contamination of downstream quartz fiber filters. In one sampling port filter configuration A (Fig. 3.1a) was used. In a second sampling port a Teflon membrane

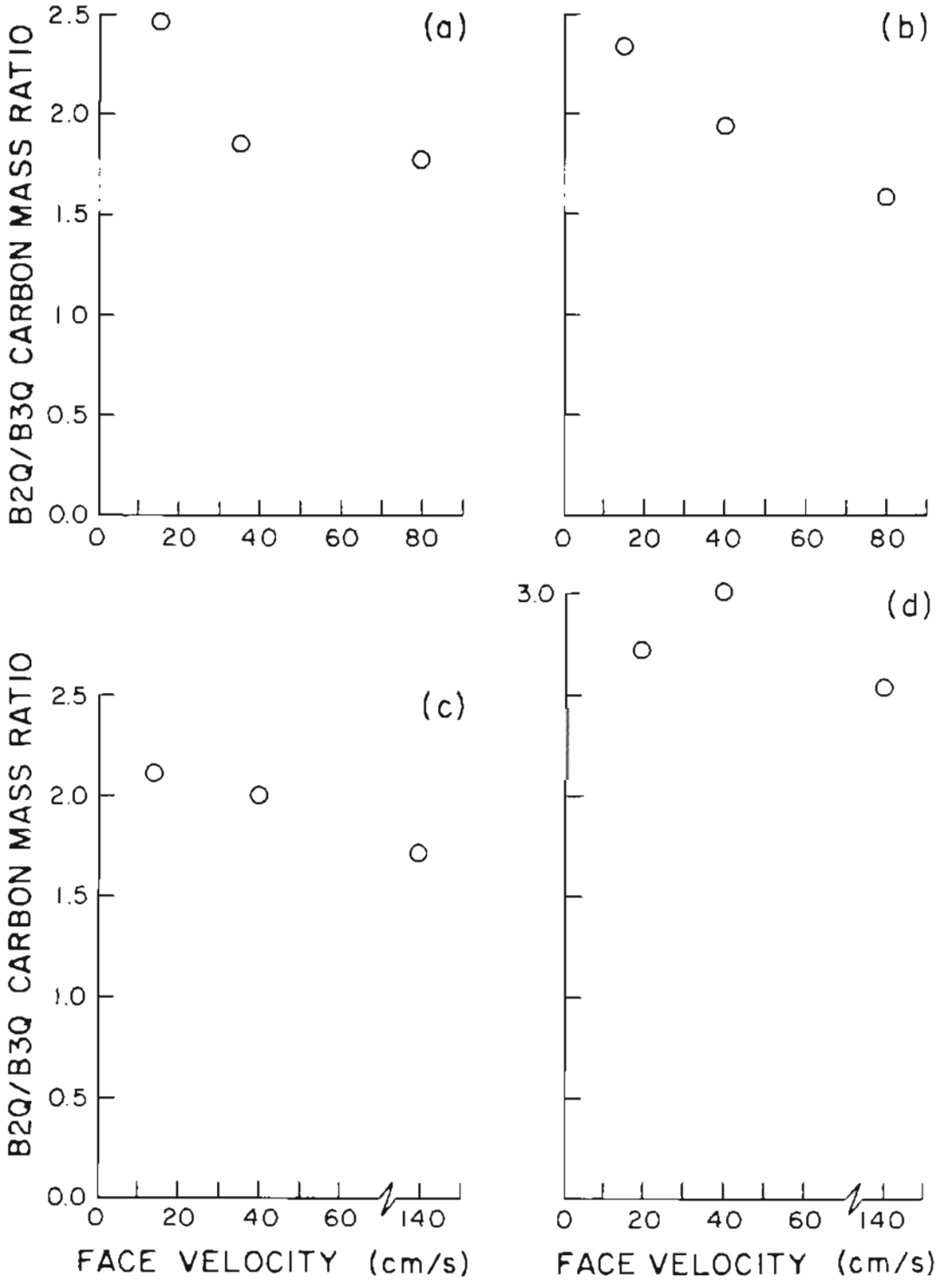

Figure 3.9. Ratio of adsorbed carbon collected on B2Q:B3Q. (See Fig. 3.1)

filter was placed between two quartz fiber filters. The only controllable difference upstream of these filters was the Teflon membrane filter. Carbon collected on the furthest downstream filters from each sampling port was compared. In two experiments of this type, carbon loadings agreed within 0.10 $\mu gC/cm^3$. This difference is much lower than the differences between carbon mass loadings on back-up filters behind quartz fiber and Teflon prefilters. Consequently contamination from Teflon can be ruled out as a cause of higher carbon loadings on the back-up filters behind Teflon prefilters.

These experiments indicate that although adsorption of organic vapors on Teflon filters is not zero, it is small in comparison to adsorption on quartz fiber filters. Thus, an improved measure of the concentration of aerosol organic carbon can be obtained by subtracting the organic carbon concentration on the quartz fiber back-up filter behind a Teflon prefilter from the organic carbon concentration on the corresponding quartz fiber aerosol filter. As shown in Figures 3.10a - 3.10d, the velocity dependence of the corrected concentrations is considerably reduced (compare with Figures 3.7a - 3.7d). Table 3.7 shows that after correction for adsorption artifact the average difference between samples collected at the highest and lowest face velocity was only -0.2 $\mu gC/m^3$. Vapor correction accounted for an average of 88% of the difference in apparent organic carbon concentration. Uncertainties reported in Table 3.7 were determined in the same manner as for Table 3.2.

Data from all four experiments are combined in Figs. 3.11 - 3.13. Results are expressed as a fraction of the quantities derived from samples collected at 15 cm/s, and uncertainties correspond to one

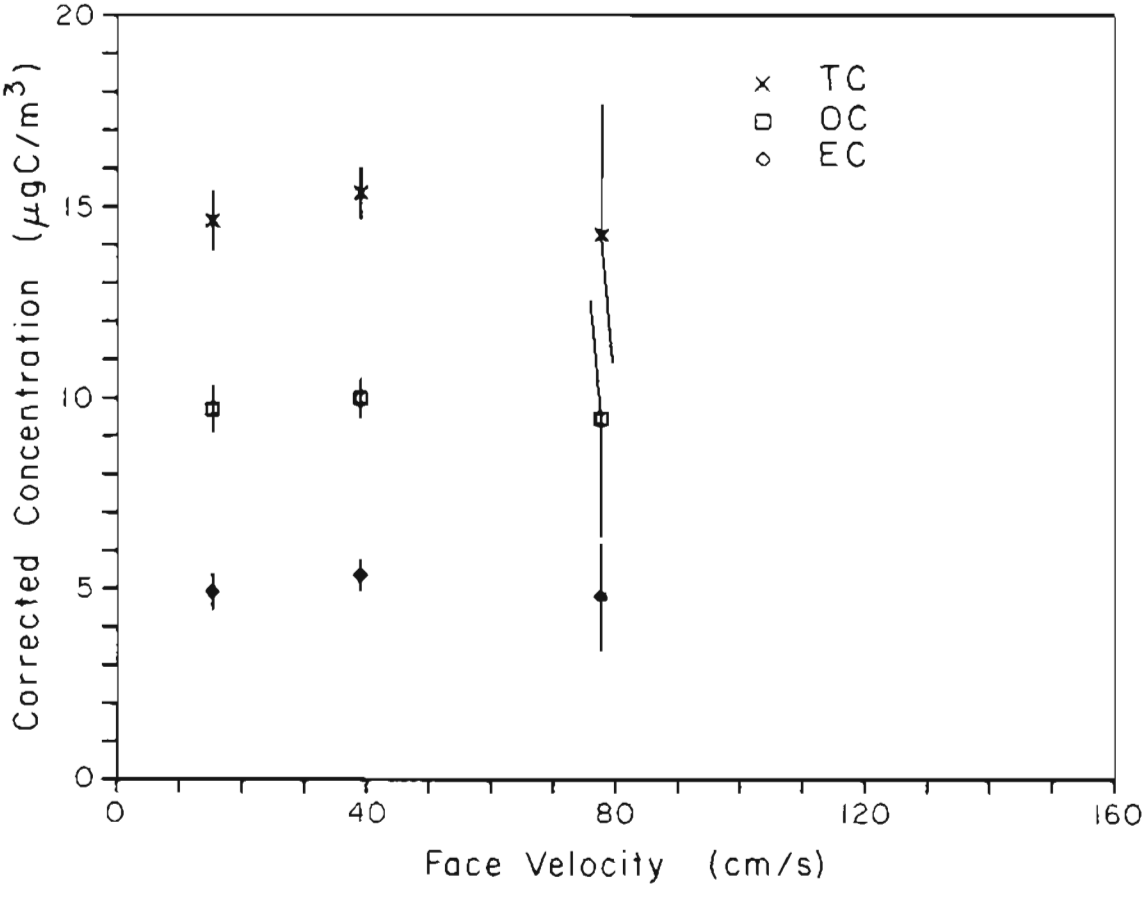

Figure 3.10a. Variation with face velocity of apparent organic carbon concentration after correction for adsorption artifact concentration for Experiment 3.5.

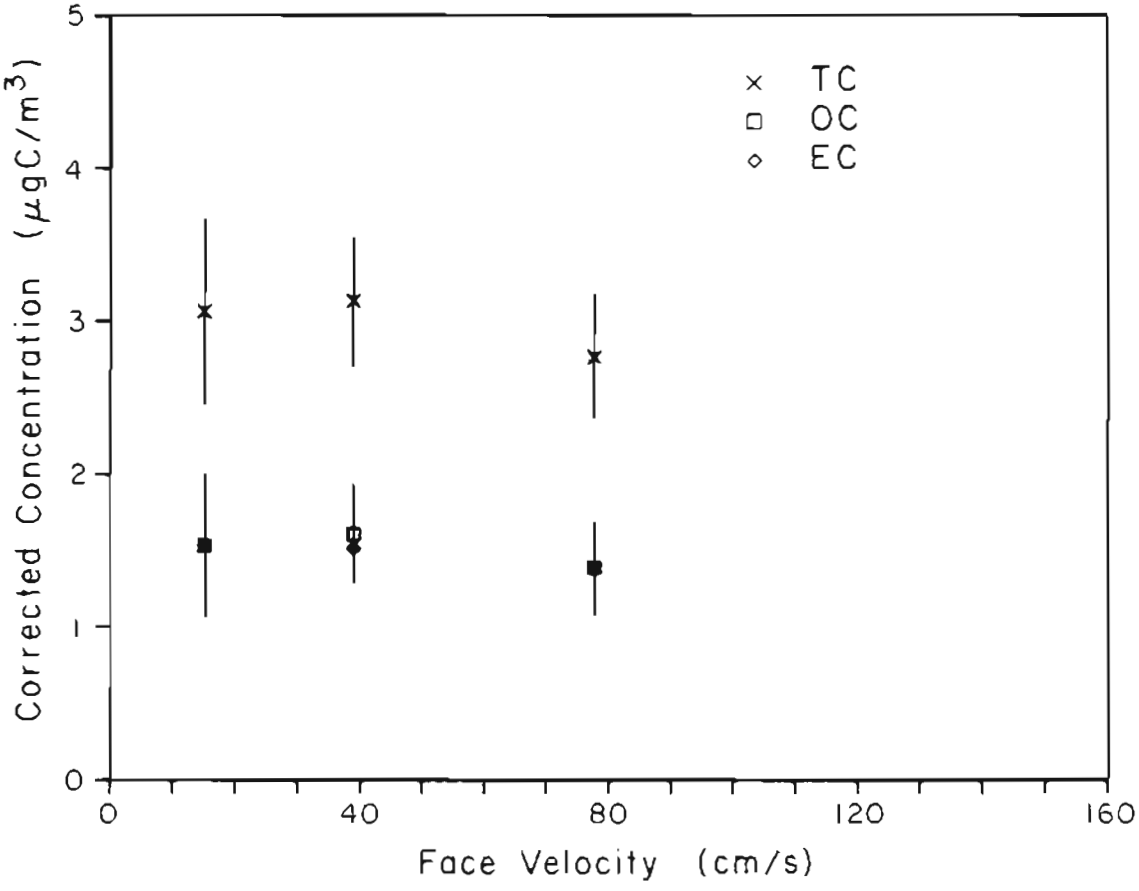

Figure 3.10b. Variation with face velocity of apparent organic carbon concentration after correction for adsorption artifact concentration for Experiment 3.6.

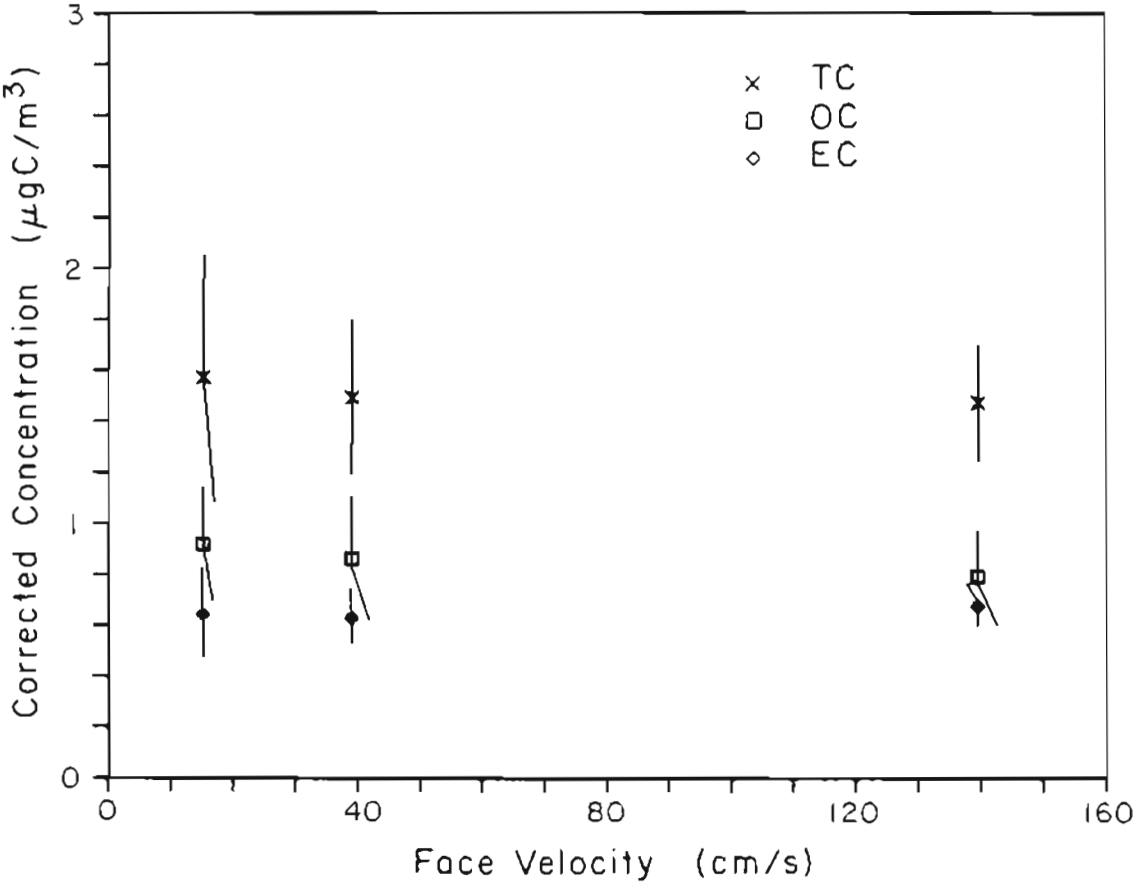

Figure 3.10c. Variation with face velocity of apparent organic carbon concentration after correction for adsorption artifact concentration for Experiment 3.7.

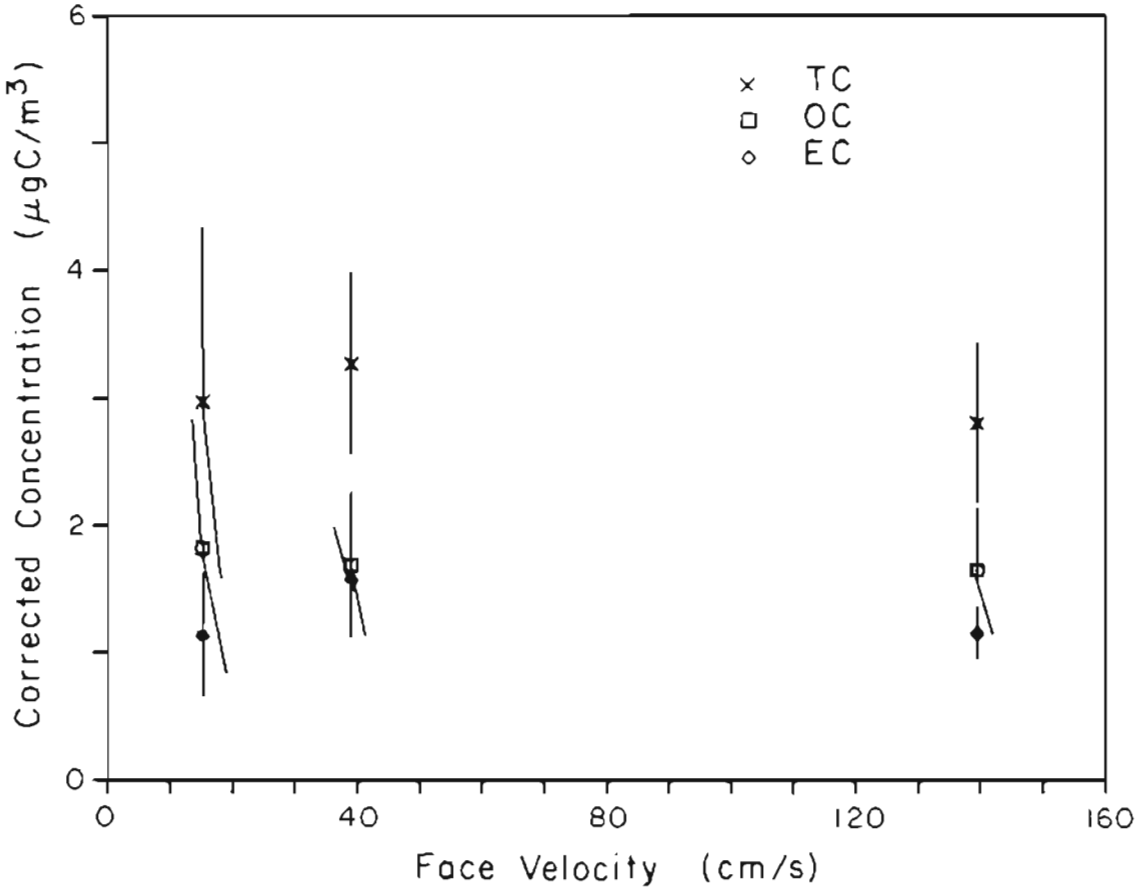

Figure 3.10d. Variation with face velocity of apparent organic carbon concentration after correction for adsorption artifact concentration for Experiment 3.8.

TABLE 3.7 - VARIATION OF APPARENT ORGANIC CARBON CONCENTRATION WITH FACE VELOCITY AFTER SUBTRACTION OF ADSORPTION ARTIFACT

	EXPERIMENT				
	3.5	3.6	3.7	3.8	MEAN
SAMPLING PERIOD (hrs.)	24	24	24	8.75	
CORRECTED ORGANIC CARBON CONCENTRATION ($\mu gC/m^3$)					
LOWEST FACE VELOCITY*	9.71	1.54	0.92	1.82	
HIGHEST FACE VELOCITY**	9.46	1.39	0.79	1.64	
DIFFERENCE (uncertainty)	-0.25 (3.15)	-0.15 (0.56)	-0.13 (0.42)	-0.18 (1.16)	-0.18 (0.05)
FRACTION OF DIFFERENCE EXPLAINED BY ADSORPTION	82%	87%	91%	93%	88%

* 15 cm/s for all experiments

** 80 cm/s for Experiments 3.5 and 3.6; 140 cm/s for 3.7 and 3.8.

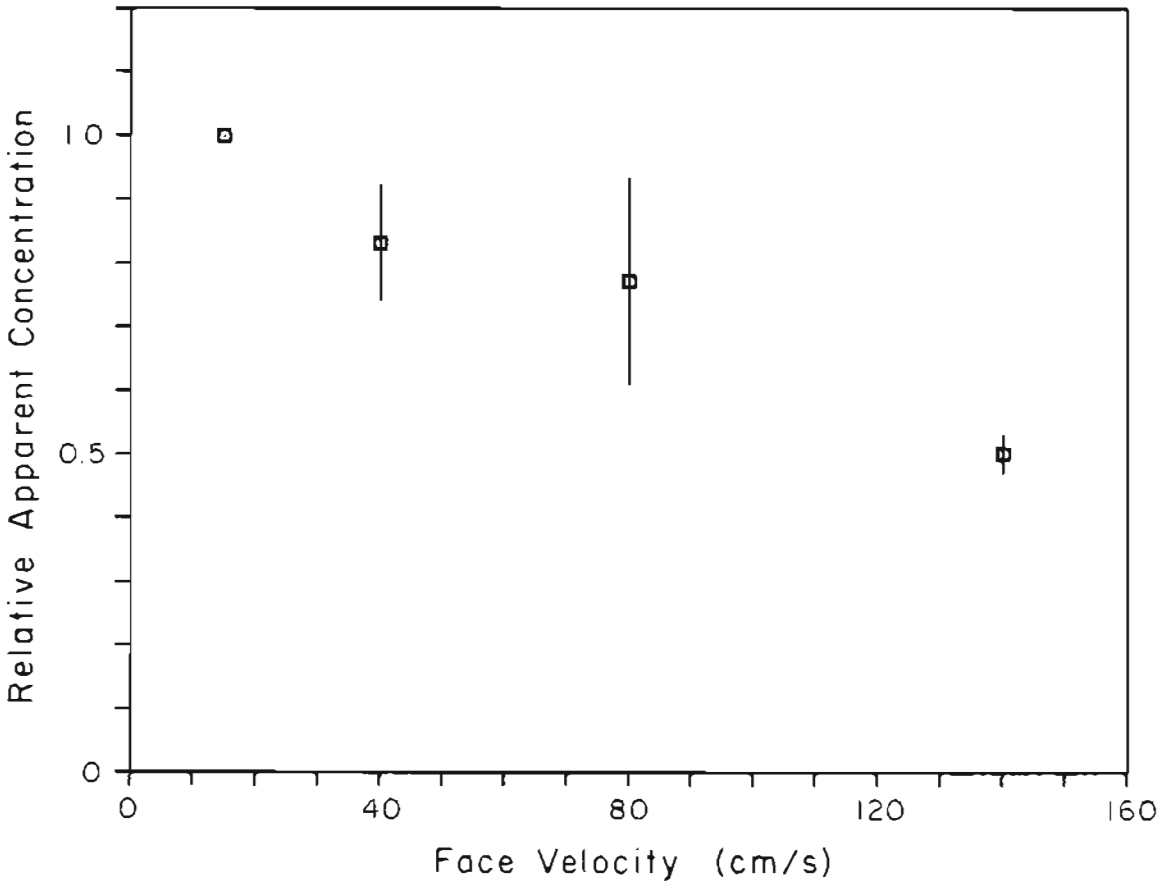

Figure 3.11. Variation of apparent particulate carbon concentration with face velocity for Experiments 3.5 through 3.8. The average apparent concentration at 15 cm/s was 6.0 $\mu g/m^3$. Relative apparent concentration refers to the ratio of the apparent concentration for a given face velocity sample to that of the sample collected at 15 cm/s.

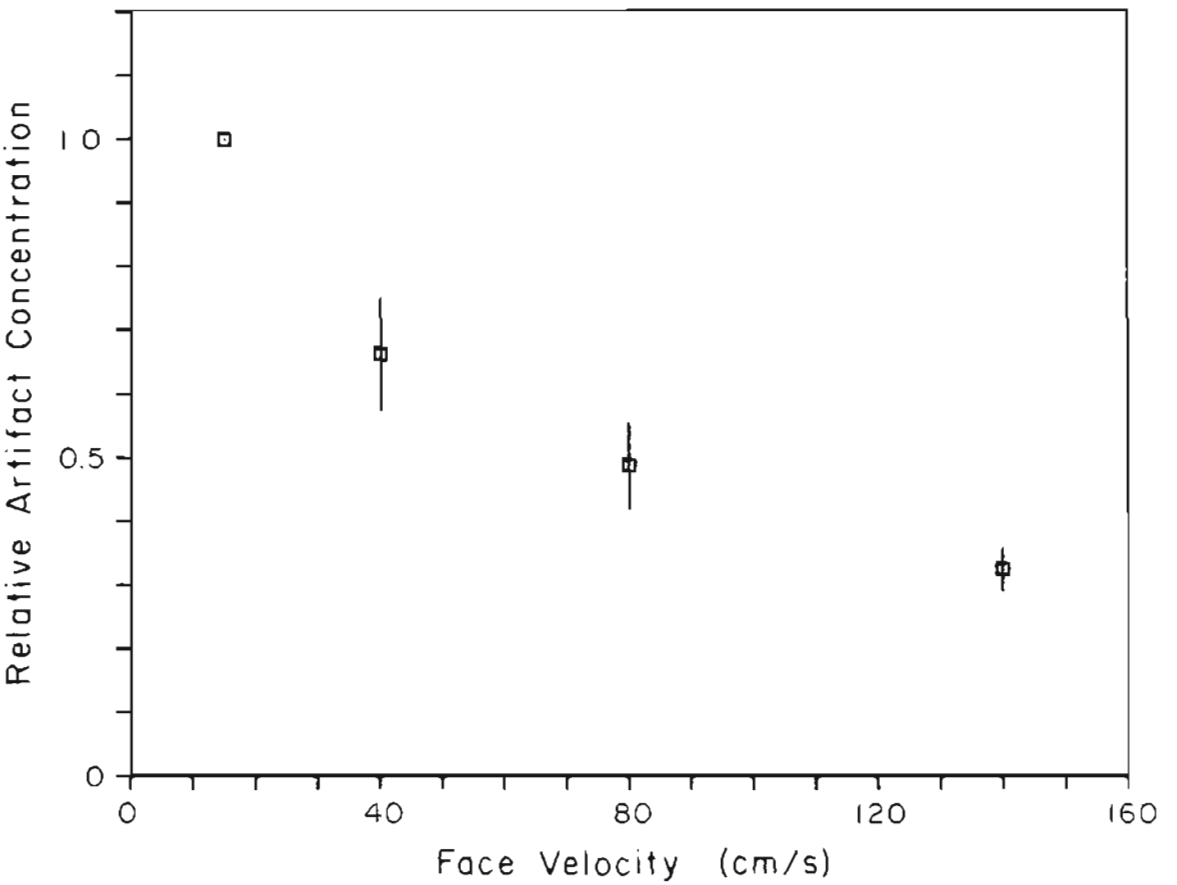

Figure 3.12. Variation of adsorption artifact concentration with face velocity for Experiments 3.5 through 3.8. The average artifact concentration at 15 cm/s was 2.55 $\mu g/m^3$. Adsorption artifact concentrations were estimated from carbon collected on quartz filters behind Teflon prefilters. Relative artifact concentration refers to the ratio of the artifact concentration for a given face velocity sample to that of the sample collected at 15 cm/s.

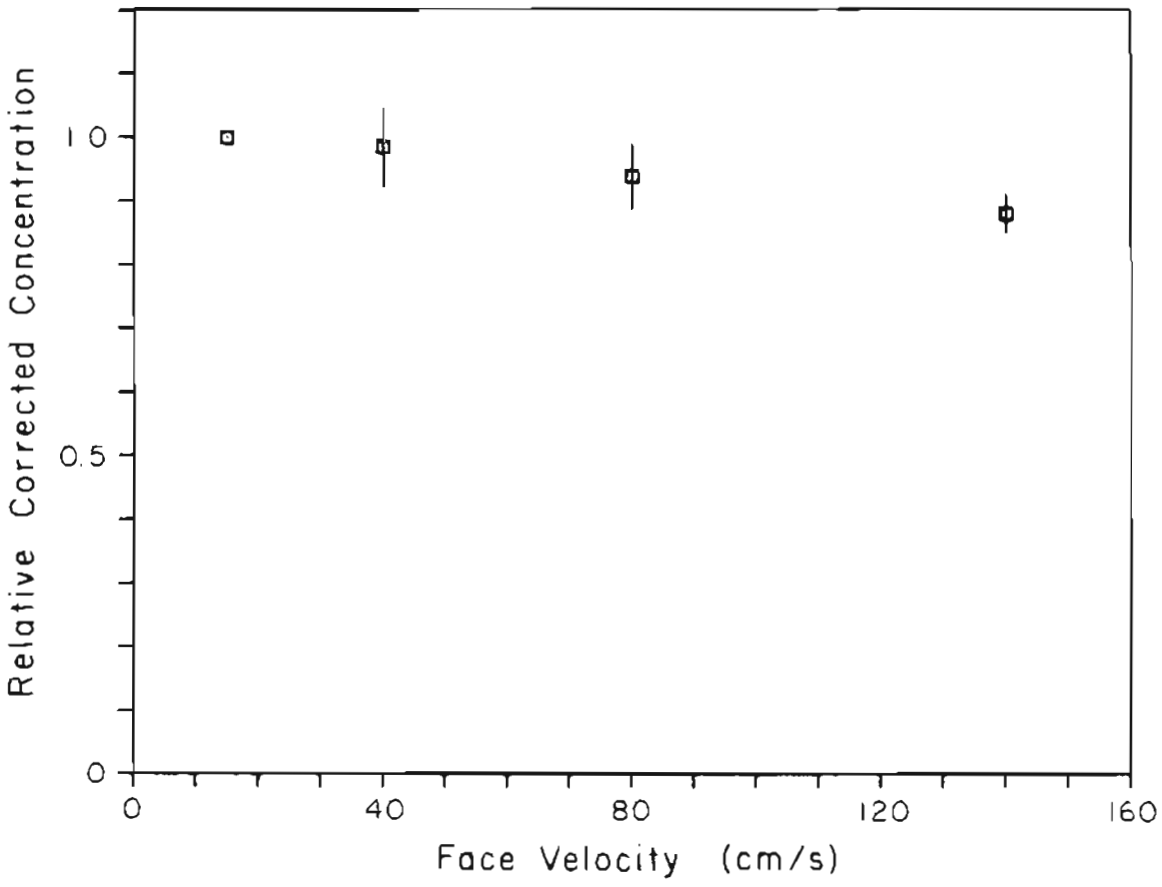

Figure 3.13. Variation with face velocity of apparent particulate organic carbon concentration after correction for adsorption artifact concentration from Experiments 3.5 through 3.8. The average corrected organic carbon concentration at 15 cm/s was 3.5 $\mu g/m^3$. Relative corrected concentration refers to the ratio of the corrected concentration for a given face velocity sample to that of the sample collected at 15 cm/s.

standard deviation of the fractions observed at each face velocity. The decreasing trend with face velocity of apparent organic carbon concentration and artifact concentration are observed in Figs. 3.11 and 3.12 respectively. The corrected concentrations are plotted in Fig. 3.12 which shows that the face velocity dependence of the organic aerosol concentration is largely removed by this procedure.

B.3. Results: Volatilization Artifact

In Experiments 3.9 and 3.10 the effect of face velocity on volatilization artifact was investigated. It should be noted that volatilization from both collected organic particulate matter and organic vapors adsorbed on the primary filter is possible. During ambient sampling, atmospheric equilibrium can favor either volatilization or adsorption of organic vapors on collected particulate matter (see Section I.C). Consequently, volatilization of sample into purified air is not representative of ambient sampling conditions. However, if adsorptive vapor concentrations decrease during sampling, the effect should be similar though less extreme. Volatilization artifacts are expressed as carbon mass lost per unit volume of purified air drawn through the filter. Volatilization artifacts are plotted against face velocity in Figs. 3.14a and 3.14b. The increasing trend of volatilization artifact with increasing face velocity is in direct contrast with the observed decreasing trend of adsorption artifact errors with increasing face velocity.

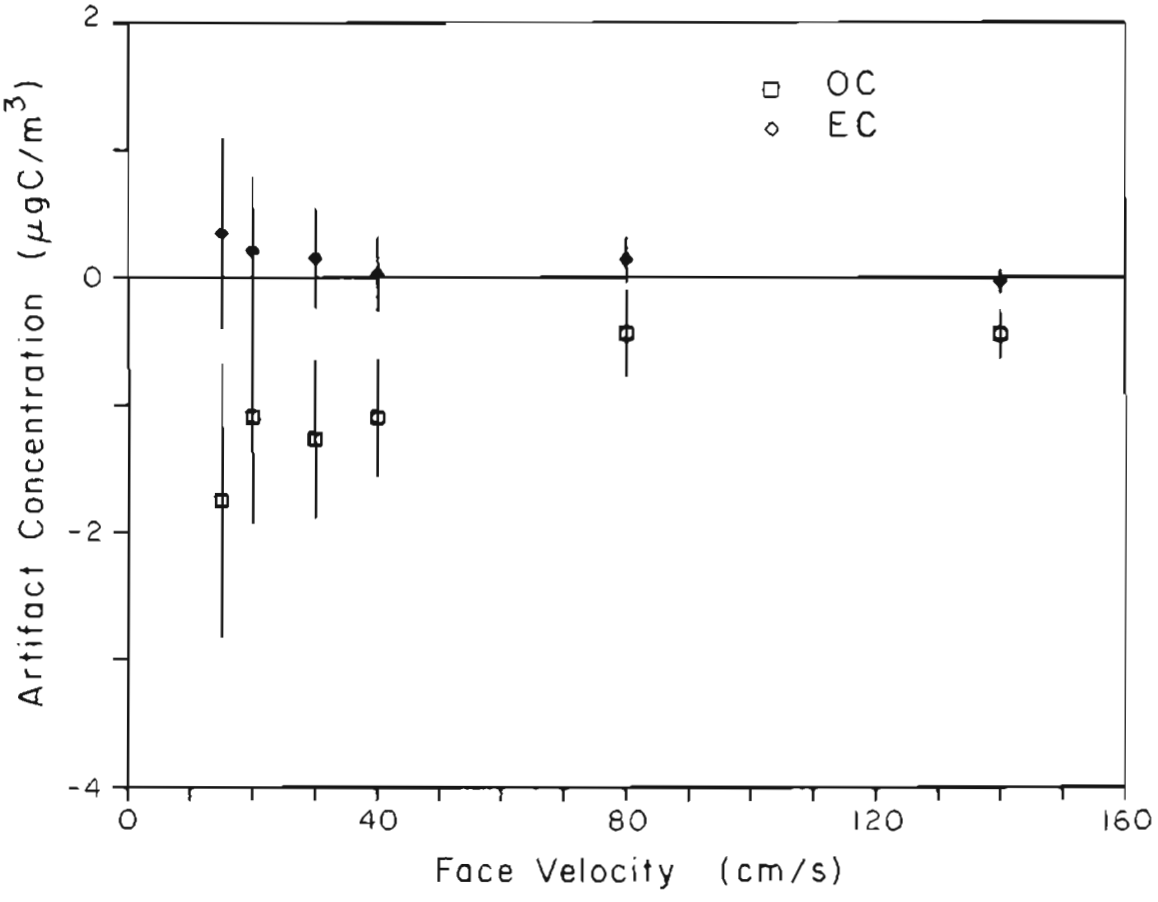

Figure 3.14a. Variation of volatilization artifact concentration with face velocity for Experiment 3.9. The volatilization artifact concentration is expressed as carbon mass lost per unit volume of pure air throughput.

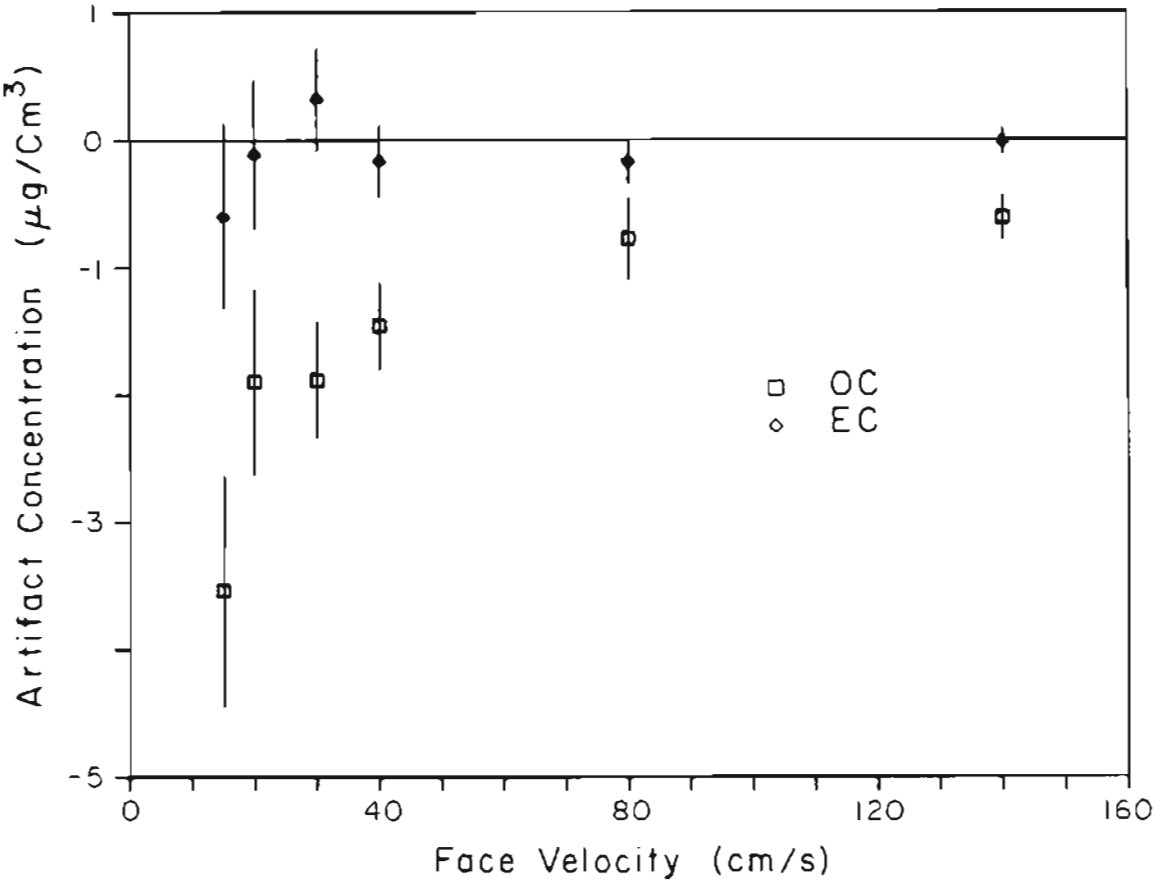

Figure 3.14b. Variation of volatilization artifact concentration with face velocity for Experiment 3.10. The volatilization artifact concentration is expressed as carbon mass lost per unit volume of pure air throughput.

The possibility that volatilization loss could be explained by the loss of organic vapor adsorbed during sampling was also addressed. Volatilization of carbon collected on quartz fiber aerosol filters (A1Q) was compared to volatilization of carbon collected on back-up filters (B2Q) behind Teflon prefilters in Experiment 3.11. In this experiment purified air was passed through both filters at the same face velocity. The carbon mass observed on the B2Q filters was used as an estimate of adsorbed carbon on the quartz fiber aerosol filters. All samples were analyzed three times for total carbon only. Comparison of mean carbon mass observed from three pairs of samples collected in this manner agreed within 8% for aerosol filters and 9% for back-up filters with 95% confidence.

Results of Experiment 3.11 given in Table 3.8 should be considered preliminary since the experiment has not been repeated. Total carbon refers to carbon collected on the aerosol filters. Vapor carbon refers to carbon collected on back-up filters. Differences between exposed and reference filters (i.e., filters not exposed to purified air) were calculated for both total and vapor carbon, and represent the mass of carbon lost per unit area of filter from volatilization. The vapor fraction is the ratio of the mass of vapor carbon lost to the mass of total carbon lost. Uncertainties refer to one standard deviation of the three analyses for each sample. Uncertainties in differences between samples as well as the vapor fraction uncertainty were propagated from the sample carbon mass uncertainties.

TABLE 3.8 - THE ROLE OF ADSORBED VAPOR IN VOLATILIZATION OBSERVATIONS

	CARBON COLLECTED ($\mu gC/cm^2$)		
	TOTAL CARBON	VAPOR CARBON	VAPOR FRACTION
CARBON COLLECTED DURING AMBIENT SAMPLING	10.77 (0.17)	2.77 (0.03)	
NO BLANK SUBTRACTION			
CARBON REMAINING AFTER VOLATILIZATION	9.99 (0.18)	2.31 (0.05)	
DIFFERENCE	0.78 (0.25)	0.46 (0.06)	59% (20%)
BLANK SUBTRACTED (0.65 ± .17 $\mu gC/cm^2$)			
CARBON REMAINING AFTER VOLATILIZATION	9.34 (0.25)	1.66 (0.18)	
DIFFERENCE	1.43 (0.30)	1.11 (0.18)	78% (20%)

Numbers in parentheses are uncertainties expressed as one standard deviation.

Blank levels were improved by placing two quartz fiber filters upstream of the samples to remove residual organic vapors in the purified air. However, the blank was not negligible in comparison to the mass of organic carbon lost from both the primary and vapor filters. It is not clear whether the blank should be subtracted because adsorption might not occur as readily on sample filters with several $\mu gC/cm^2$ already adsorbed as on clean blank filters. If the adsorption sites available to the impurities on clean filters are occupied on sample filters by organic vapors adsorbed during sampling, impurities could pass through sample filters more readily than through blank filters. In this case only a fraction, if any, of the blank should be subtracted.

The vapor fraction was calculated both with and without blank subtraction. The two calculations indicated that between 58 ± 20% and 73 ± 20% of the carbon removed from the primary filter was explained by carbon removed from the vapor filter. The difference in calculations occurs because carbon on the blank filter represents a significant fraction of the carbon lost from the primary and vapor filters. However, both estimates suggest that the majority of carbon lost is from volatilization of organic vapor adsorbed on filter material.

C. Variations with Sampling Period

C.1. Results: Apparent Concentration

From sampling duration Experiments 3.12 through 3.14 nine pairs of long duration and short duration samples were obtained. Results are summarized in Table 3.9. In all nine samples higher

TABLE 3.9 - EFFECT OF SAMPLING DURATION ON APPARENT CONCENTRATION

EXPERIMENT	DURATIONS COMPARED	FACE VELOCITY	SHORT DURATION	LONG DURATION	RATIO
ORGANIC CARBON		(cm/s)	($\mu gC/m^3$)	($\mu gC/m^3$)	
3.12	3/6 HRS.	15	1.48	1.32	1.12
		40	1.30	1.19	1.09
		80	1.13	1.02	1.11
3.13	24/48 HRS.	15	3.79	2.93	1.29
		40	2.64	2.37	1.11
		140	2.18	1.89	1.15
3.14	24/48 HRS.	15	4.10	3.03	1.35
		40	3.01	2.69	1.12
		140	2.23	2.02	1.10
MEAN					1.16
STANDARD DEV.					0.09
ELEMENTAL CARBON					
3.12	3/6 HRS.	15	0.24	0.29	0.83
		40	0.36	0.42	0.86
		80	0.33	0.33	1.00
3.13	24/48 HRS.	15	1.49	1.33	1.12
		40	1.25	1.42	0.88
		140	1.24	1.24	1.00
3.14	24/48 HRS.	15	1.46	1.35	1.08
		40	1.41	1.45	0.97
		140	1.26	1.27	0.99
MEAN					0.97
STANDARD DEV.					0.09

apparent organic carbon concentrations were observed for the composite of short samples than for the long duration samples. A paired t-test indicated a significant difference (p=0.05) between apparent concentrations from the two sampling durations. Apparent concentrations were an average of 16% higher for the short duration samples. When only 24/48-hour comparisons were considered, apparent concentrations were 19% higher for the 24-hour samples. In contrast, a negligible difference was observed for elemental carbon.

C.2. Results: Adsorption Artifact

Adsorbed vapor concentrations estimated from back-up filter analysis also varied with sampling period. The effect of sampling period on adsorption artifact error is examined in Table 3.10. On the average 28% more adsorbed vapor was collected for short than for long sampling durations. A paired t-test indicated the difference was significant (p=0.05). With two exceptions, more carbon was collected for short than for long sampling durations. Consequently, adsorption of organic vapor by the filter substrate must be at least partially responsible for difference in apparent organic aerosol concentration between different sampling durations.

The exceptions corresponded to the samples in Experiment 3.12 collected at the two lowest face velocities. This experiment compared three-hour to six-hour sampling durations in contrast to the 24 and 48-hour comparisons of Experiments 3.13 and 3.14. Thus the two samples which did not exhibit variations of apparent concentration with sampling

TABLE 3.10 - EFFECT OF SAMPLING DURATION ON ADSORPTION ARTIFACT

EXPERIMENT	DURATIONS COMPARED	FACE VELOCITY	SHORT DURATION	LONG DURATION	RATIO
ORGANIC CARBON		(cm/s)	($\mu gC/m^3$)	($\mu gC/m^3$)	
3.12	3/6 HRS.	15	0.25	0.25	1.00
		40	0.23	0.24	0.96
		80	0.28	0.22	1.27
3.13	24/48 HRS.	15	1.36	0.73	1.86
		40	0.65	0.57	1.14
		140	0.44	*	
3.14	24/48 HRS.	15	1.00	0.66	1.52
		40	0.68	0.55	1.24
		140	0.44	0.35	1.26
MEAN					1.28
STANDARD DEV.					0.27

* denotes contaminated sample

period were also the samples for which the smallest volume of air was sampled per unit filter area.

A decreasing trend of the ratio of short to long sampling duration apparent concentrations with increasing face velocity is observed for the 24/48-hour experiments, but not for the 3/6-hour experiment in Table 3.10.

D. Filter Type Differences

D.1. Results: Comparison of Glass and Quartz Fiber Filters

Significant face velocity-dependent adsorption of organic vapor was also observed on glass fiber as well as quartz fiber filters (Fig. 3.15). Apparent organic aerosol concentrations from glass and quartz fiber filters from Experiments 3.15 and 3.16 are compared in Table 3.11 both with and without blank subtraction for glass fiber filters. One blank filter was cleaned at the same time as the sample filters for each experiment and stored immediately. The blank was analyzed on the same day as the samples. Since blanks for glass fiber filters were significantly higher after storage than before storage (see Section II.D), adsorption of organic vapors during storage was probably responsible for blank levels observed. However, it is not clear whether adsorption during storage occurs to the same extent on sample filters which have already collected a significant mass of adsorbed vapor during sampling.

Without blank subtraction, 24-75% more organic carbon was observed on glass fiber than on quartz fiber filters. In both experi-

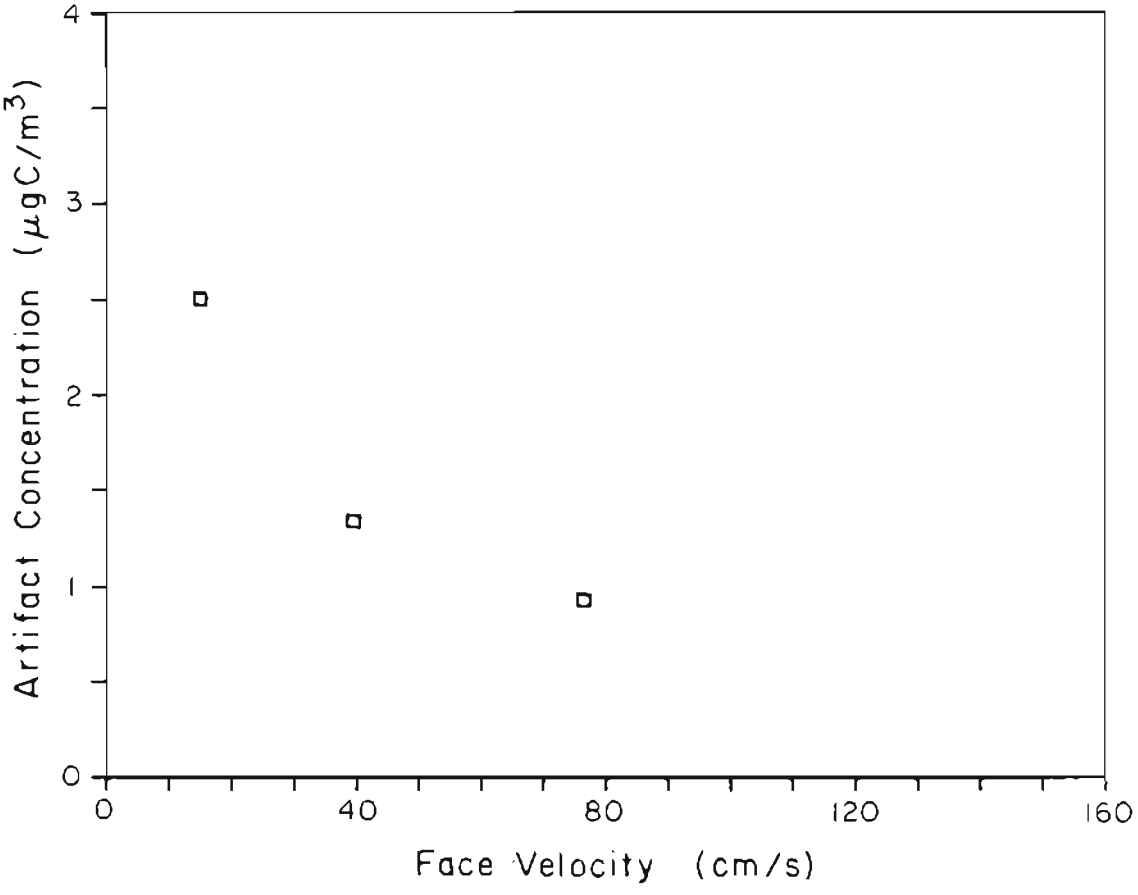

Figure 3.15. Variation of adsorption artifact concentration with face velocity for glass fiber filters (Experiment 3.7). Artifact concentrations were estimated from carbon collected on glass filters behind Teflon prefilters.

TABLE 3.11 - EFFECT OF FILTER TYPE ON ORGANIC CARBON COLLECTED:
GLASS FIBER VS. QUARTZ FIBER FILTERS
ALL VALUES IN MICROGRAMS PER SQUARE CENTIMETER

	#1	#2	#3	MEAN	UNCER-TAINTY
ORGANIC CARBON NO STORAGE BLANK SUBTRACTION					
EXPERIMENT 3.15					
GLASS	7.79	7.60	7.77	7.72	0.63
QUARTZ	6.33	5.89	6.39	6.20	0.61
RATIO (GLASS/QUARTZ)				1.24	0.16
EXPERIMENT 3.16					
GLASS	6.26	5.86	5.92	6.01	0.60
QUARTZ	3.23	3.12	3.94	3.43	0.57
RATIO (GLASS/QUARTZ)				1.75	0.34
ORGANIC CARBON STORAGE BLANK SUBTRACTED					
EXPERIMENT 3.15					
GLASS	6.69	6.50	6.67	6.62	0.61
QUARTZ	6.16	5.72	6.22	6.03	0.60
RATIO (GLASS/QUARTZ)				1.10	0.15
EXPERIMENT 3.16					
GLASS	5.99	5.59	5.65	5.74	0.60
QUARTZ	3.06	2.95	3.77	3.26	0.57
RATIO (GLASS/QUARTZ)				1.76	0.36
ELEMENTAL CARBON					
EXPERIMENT 3.15					
GLASS	1.09	1.08	1.24	1.13	0.26
QUARTZ	1.39	1.34	1.42	1.38	0.27
RATIO (GLASS/QUARTZ)				0.82	0.25
EXPERIMENT 3.16					
GLASS	1.39	0.90	1.15	1.15	0.26
QUARTZ	0.65	0.56	1.31	0.84	0.26
RATIO (GLASS/QUARTZ)				1.37	0.53

ments the organic carbon mass collected with glass fiber filters exceeded that on quartz fiber filters by more than 1.5 $\mu gC/cm^2$. In both experiments t-tests indicated a significant difference (p=0.05) in carbon collected between filter types. A substantial portion of the difference is accounted for by storage effects. Elemental carbon agreed within 0.3 $\mu gC/cm^2$ for both experiments.

Table 3.12 compares adsorbed carbon mass between quartz and glass fiber filters behind Teflon prefilters (Experiment 3.17). Organic carbon collection is compared both before and after blank subtraction. Blank filters experienced the same storage conditions as sample filters. An average of 14% more carbon was observed on glass than on quartz fiber filters before blank subtraction. A paired t-test indicated this difference was significant (p=.05). However, after blank subtraction all quartz fiber filters exhibited slightly higher loadings of organic carbon than their corresponding glass fiber counterparts, and the average glass/quartz ratio was 0.96 ± 0.04.

Significant adsorption of organic vapor can be concluded for glass fiber filters. The adsorption artifact is presumably responsible for differences in organic mass collected between different filter types. It is not clear whether more adsorption occurs during sampling on glass than on quartz fiber filters or as a result of greater adsorption during storage for glass fiber filters. Storage adsorption problems can be avoided by using quartz fiber filters (see Section II.D).

TABLE 3.12 - EFFECT OF FILTER TYPE ON ADSORPTION ARTIFACT:
GLASS FIBER VS. QUARTZ FIBER FILTERS

EXPERIMENT 3.17

ALL VALUES IN MICROGRAMS PER SQUARE CENTIMETER

NO BLANK SUBTRACTION	GLASS	QUARTZ	RATIO (GLASS/QUARTZ)
15 cm/s	3.58	3.67	1.25
40 cm/s	5.92	5.39	1.10
140 cm/s	7.50	6.89	1.09
MEAN	6.00	5.32	1.14
STANDARD DEV.			0.09
STORAGE BLANK SUBTRACTED			
15 cm/s	3.43	3.47	0.99
40 cm/s	4.77	5.19	0.92
140 cm/s	6.38	6.59	0.97
MEAN	4.86	5.08	0.96
STANDARD DEV.			0.04

D.2. Results: Comparison of Teflon and Quartz Filters

Indirect evidence of less vapor adsorption on Teflon filters than on quartz fiber filters has been discussed in connection with adsorption artifact estimates in Section III.B.2. Further evidence for this was obtained by direct carbon analysis of Teflon and quartz fiber filters collected under identical sampling conditions. Because the Teflon filters were thermally unstable above 300°C, however, the carbon analysis procedure was modified such that only carbon volatilized at 275°C in O_2-He was measured. The results of this experiment are given in Table 3.13. This can only be considered a qualitative comparison because organic carbon removal is not complete at this temperature, and the fraction removed may not be representative of the total carbon collected. For quartz fiber filters the fraction of organic carbon removed at 275°C averaged 48% and 35% for Experiments 3.18 and 3.19 respectively. For eighteen back-up filters (A2Q, C3Q, C4Q) from both experiments an average and standard deviation of 63 ± 7% of the total carbon removed at 750°C was removed at 275°C.

Moreover, removal temperatures can vary between filter types, and pyrolytically generated elemental carbon during analysis has been observed on both filter types at 275°C. The relationship between the extent of organic carbon pyrolysis and filter type is not clear. Consequently, a difference in organic carbon collection is only one of a variety of factors which could be responsible for differences in analytical response between filter types.

TABLE 3.13 - EFFECT OF FILTER TYPE ON TOTAL CARBON MEASURED BETWEEN QUARTZ FIBER AND TEFLON MEMBRANE FILTERS

EXPERIMENT	FACE VELOCITY	QUARTZ	TEFLON	RATIO
	cm/s	$\mu gC/cm^2$	$\mu gC/cm^2$	(QUARTZ/TEFLON)
3.8	15	4.3	3.5	1.22
	40	9.5	8.5	1.12
	80	16.1	15.2	1.06
3.9	15	6.6	5.6	1.16
	80	22.7	14.9	1.52
MEAN				1.21
STAN. DEV.				0.18

Ratios of carbon measured on quartz and Teflon aerosol filters are listed in Table 3.13. An average of 21% more organic carbon removable at 275°C was observed for samples collected on quartz fiber filters than from those collected on the Teflon membrane filters.

The amount of carbon observed on Teflon back-up filters (C2T) in six samples from two sampling periods never exceeded 1 $\mu gC/cm^2$. The relative adsorption artifact estimated for each filter type by the ratio of back-up to primary filters (A2Q/A1Q and C2T/C1T of Fig. 3.1) is reported in Table 3.14. 23% as much carbon was observed on quartz fiber back-up (A2Q) as on primary quartz fiber filters (A1Q). In contrast, only 9% as much carbon was present on Teflon back-up filters (C2T) as on Teflon primary filters (C1T).

Variations of adsorption artifact error with face velocity were observed for both filter types. Adsorption artifact errors were calculated from the mass loadings of Table 3.14. The average ratios of adsorption artifact error from samples collected at 15 cm/s to those collected at 80 cm/s were 2.7 and 2.2 for Teflon and quartz filters, respectively. Adsorption artifact error for Teflon filters never exceeded 0.5 $\mu gC/m^3$.

The adsorption artifact between the two filter types was directly compared using C3Q/C2T ratios (see Fig. 3.1) in Table 3.15. An average of 5.5 times as much carbon was observed on quartz fiber filters (C3Q) as on Teflon membrane filters (C2T) immediately upstream. These results suggest the possibility that more organic vapor adsorption occurs on quartz fiber filters than on Teflon membrane filters. This is consistent with the observation of lower apparent carbon con-

TABLE 3.14 - COMPARISON OF RELATIVE ADSORPTION ARTIFACT BETWEEN QUARTZ FIBER AND TEFLON MEMBRANE FILTERS AT 275°C

ALL VALUES IN MICROGRAMS PER SQUARE CENTIMETER

FACE VELOCITY	QUARTZ PRIMARY (A1Q)	QUARTZ BACK-UP (A2Q)	QUARTZ RATIO (A2Q/A1Q)	TEFLON PRIMARY (C1T)	TEFLON BACK-UP (C2T)	TEFLON RATIO (C2T/C1T)
EXPERIMENT 3.18						
15 cm/s	4.16	1.22	0.29	3.14	0.52	0.17
40 cm/s	9.37	2.18	0.23	8.11	0.93	0.11
80 cm/s	15.96	3.13	0.20	14.75	0.97	0.07
EXPERIMENT 3.19						
15 cm/s	6.56	1.91	0.30	5.43	0.41	0.08
40 cm/s				14.34	0.60	0.04
80 cm/s	22.66	3.56	0.16	14.71	0.89	0.06
MEAN			0.23			0.09
STANDARD DEV.			0.06			0.05

TABLE 3.15 - COMPARISON OF ADSORPTION ARTIFACT BETWEEN QUARTZ FIBER AND TEFLON MEMBRANE FILTERS AT 275°C

FACE VELOCITY	CARBON ADSORBED ($\mu gC/cm^2$) QUARTZ (C3Q)	TEFLON (C2T)	RATIO (C3Q/C2T)
EXPERIMENT 3.18			
15 cm/s	2.73	0.52	5.25
40 cm/s	4.41	0.93	4.74
80 cm/s	6.06	0.97	6.25
EXPERIMENT 3.19			
15 cm/s	2.58	0.41	6.29
40 cm/s	3.50	0.60	5.83
80 cm/s	4.11	0.89	4.62

centration for Teflon than for quartz filters, and with the observations of poorer efficiency for removal of adsorptive organic vapors for Teflon filters in section III.B.2.

E. Adsorption Artifact Estimates

A significant organic vapor adsorption artifact has been observed which appears to almost completely account for observed differences in apparent particulate organic carbon concentration with face velocity. The adsorption artifact is also at least partially responsible for observed differences in apparent concentration with sampling period and filter type. An average estimate of relative adsorption artifact for all face velocities calculated from adsorbate filters (B2Q) from Experiments 3.5 through 3.8 has already been presented in Table 3.7. An average and standard deviation of 43 ± 20% of primary filter organic carbon (average apparent concentration = 5.2 ± 4.0 $\mu gC/m^3$) is accounted for by adsorbed vapor estimates. This indicates that for these experiments almost half of the apparent organic aerosol collected was really adsorbed vapor. In five of the twelve samples, artifact concentrations exceeded 50% of the apparent concentrations calculated, indicating that more organic vapor than aerosol was collected.

A strong correlation of organic vapor adsorption with concentration was observed. Artifact concentrations were calculated from 13 back-up filters behind quartz fiber primary filters for 24 hours at 40 cm/s and are plotted against apparent concentrations in Fig. 3.16. The adsorption artifact error appears to increase with increasing apparent concentration. However, when expressed as a percentage of apparent

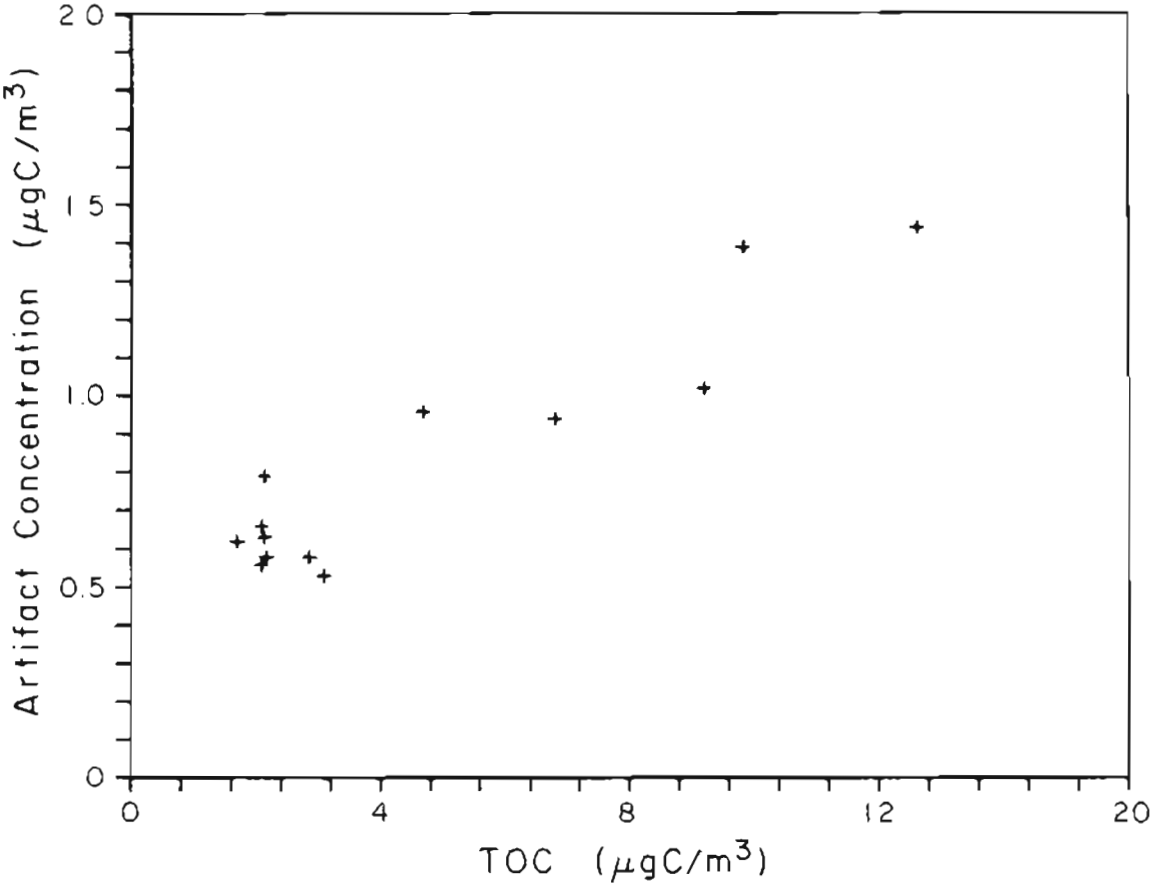

Figure 3.16. Variation of adsorption artifact concentration with apparent particulate organic carbon concentration. Adsorption artifact concentrations were estimated from quartz back-up filters behind quartz primary filters. TOC refers to total carbon collected from both the particulate and vapor phase.

concentration in Fig. 3.17, a decreasing trend of relative adsorption artifact and apparent concentration is observed which is especially pronounced at lower concentrations. For a typical urban concentration of 6.6 $\mu gC/m^3$ (Shah et al., 1986) a lower limit of 10-15% of the apparent concentration can be accounted for by organic vapor adsorption. However, at lower concentrations significantly more apparent organic aerosol concentration is accounted for by the adsorption artifact.

The actual adsorption artifact errors are probably higher than indicated in Fig. 3.16 since quartz fiber filters underestimate organic vapor adsorption (see Section III.B.2). From Table 3.7 an average of 1.8 times as much adsorbed vapor is estimated from the Teflon prefilter method than from the back-up filter method for the three experiments with 24-hour sampling periods (Experiments 3.5, 3.6 and 3.7). Although this ratio also appears to be a function of concentration, the average carbon mass loading is within 1 $\mu gC/m^3$ of the U.S. urban average. Thus a factor of 1.8 can be multiplied by artifact concentration as a rough correction for estimated differences between vapor carbon collected on primary and back-up filters at the average urban concentration. After correction more than 20% of the primary filter organic carbon can be attributed to vapor adsorption. At lower concentrations, adsorbed vapor could account for more than 50% of the apparent organic aerosol concentration.

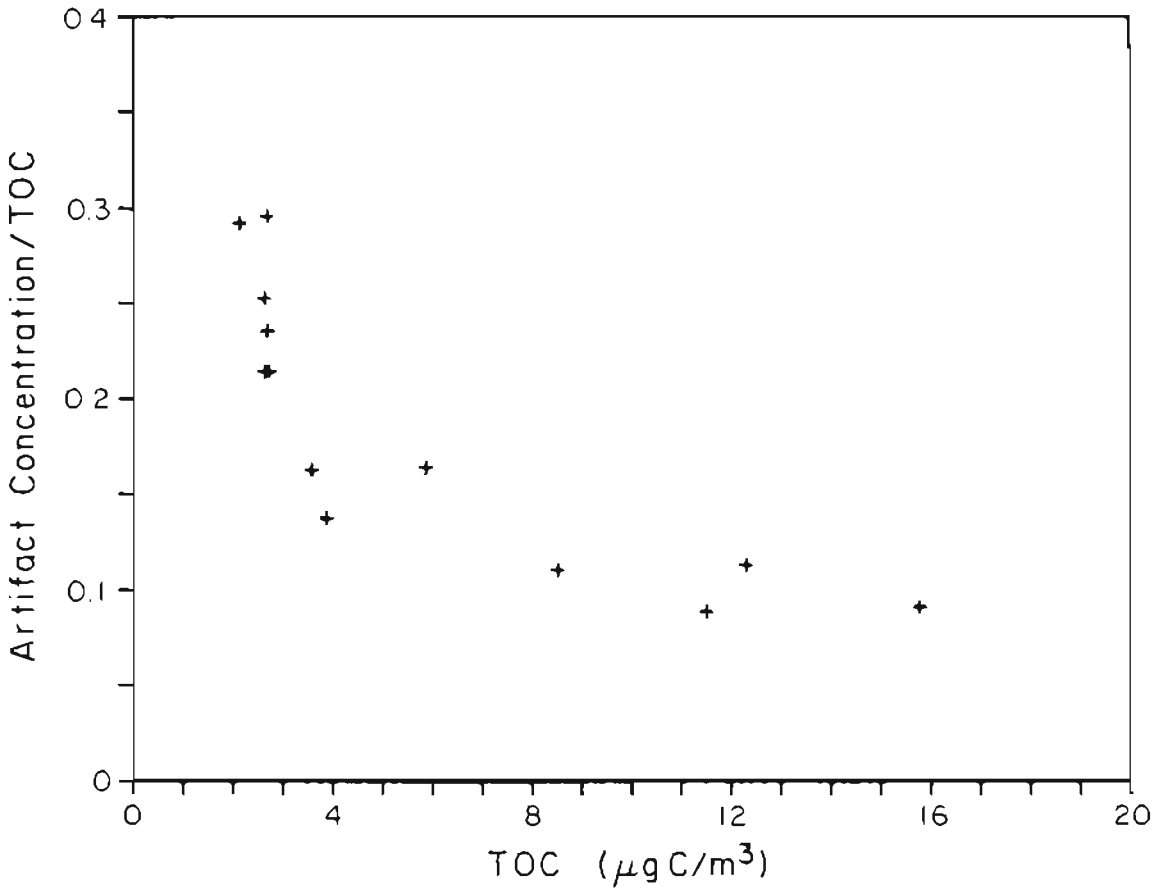

Figure 3.17. Variation of the adsorption artifact concentration: apparent particulate organic carbon concentration ratio with apparent particulate organic carbon concentration. Adsorption artifact concentrations were estimated from carbon collected on quartz back-up filters behind quartz primary filters. TOC refers to total carbon collected from both the particulate and vapor phase.

F. Summary

Significant variations in apparent particulate organic carbon concentrations with face velocity, sampling period and filter type can be concluded. Apparent concentrations were observed to decrease with increasing face velocity and sampling duration. Of the three filter types investigated, the greatest apparent concentrations were calculated from glass and quartz fiber filters and the lowest from Teflon membrane filters. The lack of substantial variation in elemental carbon with face velocity and sampling period indicates that variations in apparent concentration are unique to organic carbon and not representative of general aerosol sampling problems. A significant organic vapor adsorption artifact can be concluded, which is especially important at low face velocities, short sampling period, and low concentrations. Volatilization results are not conclusive, but do not appear to explain apparent concentration variations.

CHAPTER IV - THE COMPOSITION OF ADSORBED ORGANIC VAPOR

Structural identification of specific organic compounds associated with the adsorption artifact was pursued using gas chromatography/mass spectrometry with samples introduced by thermal desorption. Thermal desorption from low-volume aerosol samples has the advantages of higher sensitivity and minimal sample handling with respect to solvent extraction techniques (Greaves et al., 1985). These were considered important advantages in view of the low mass loadings and volatile nature of adsorbed vapor samples.

Only one set of samples was analyzed. A systematic study of the vapor composition was not attempted. The purpose of the experiment was to obtain preliminary information on the classes of compounds present and to determine whether thermal desorption and gas chromatography/mass spectrometry warranted further investigation as techniques for studying the composition of the adsorption artifact.

Samples were collected with the sampling apparatus of Fig. 2.1 for 24 hours at the Central Fire Station located at 55 S. W. Ash Street in downtown Portland, Oregon. Each sampling port was equipped with a primary and back-up quartz fiber filter and operated with a face velocity of 15 cm/s. All six sampling ports were used so that several filters could be combined for analysis. A primary, a back-up and a blank filter sample were analyzed.

0.25 cm^2 diameter disks were removed from the sample filters until 5 cm^2 of filter material was obtained and placed in a desorption

cartridge. The desorption cartridge was a modified form of a cartridge designed for collection of atmospheric organic vapor on a bed of Tenax-GC adsorbent (Ligocki and Pankow, 1985). The reported dimensions for the original design were 1.1 cm o.d., 8.0 cm bed length and 5.7 cm^3 bed volume. The ends of the cartridge were of 0.25 in. (0.64 cm) precision o.d. glass tubing.

For desorption of the filter samples, the filter disks replaced Tenax-GC in the cartridge bed. To accomplish this, a length of 0.375 in. (0.92 cm) precision o.d. glass tubing replaced the 0.25 in. tubing at one end of the cartridge so that the filters could be inserted through the tubing into the cartridge body. The filter disks occupied only a small portion of the bed volume. This cartridge was not ideal for desorption from filters but was used for convenience because it was compatible with an existing desorption apparatus. A more specialized design has been devised for desorption from filters which minimizes the unoccupied cartridge volume and eliminates extensive sample handling (Greaves et al., 1985).

For analysis, the cartridge was placed in a desorption block used by Ligocki et al. (1985). This consisted of an aluminum block containing a 200 W heater. The cartridge was sealed into the desorption block with Vespel-graphite ferrules. The desorber and its interface to the gas chromatograph were similar to that described by Pankow and Kristensen (1983) and Pankow and Isabelle (1982). Desorptions were carried out at a pressure of 30 psi.

Samples were desorbed onto an SE-54 fused silica capillary column of 30 m length and 0.32 mm diameter mounted in a HP5790A gas

chromatograph. The gas chromatograph was interfaced to a Finnigan 4000 mass spectrometer/data system as described by Pankow and Isabelle (1984). During desorption the oven temperature was maintained at -80°C to trap desorbed compounds at the head of the column. The chromatograph was temperature programmed from -10°C to 250°C at 10°C/min. The carrier gas linear velocity was 50 cm/s.

Mass spectra were obtained by scanning from 50-450 amu at 1.0 seconds/scan with the electron multiplier set at 1.8 kV. The temperatures of the transfer line, source and manifold were 250°C, 250°C, and 100°C respectively. Conditions for desorption, gas chromatography and mass spectrometry were only slightly modified from those of Ligocki et al. (1985) for analysis of vapors collected by Tenax-GC. No attempt was made to optimize these procedures for filter desorption.

The reconstructed ion chromatogram of the primary filter is given in Fig. 4.1. Although several sharp peaks are present, these are largely unidentified and much of the signal is present as a broad region of unresolved mass with retention time between 7-32 minutes.

Figure 4.2 shows the chromatogram for the back-up filter. The intensity scale is about 90% of that for the primary filter. As for the primary filter, several unidentified sharp peaks were observed, but much of the desorbed mass was not resolved. In particular, a relatively intense response was observed in the retention time range from about 19-25 minutes. This portion of the chromatogram is amplified in Fig. 4.3.

In Table 4.1 the major peaks of Figs. 4.1 through 4.3 are listed. Only n-alkanes from n-tetradecane to n-pentacosane were positively

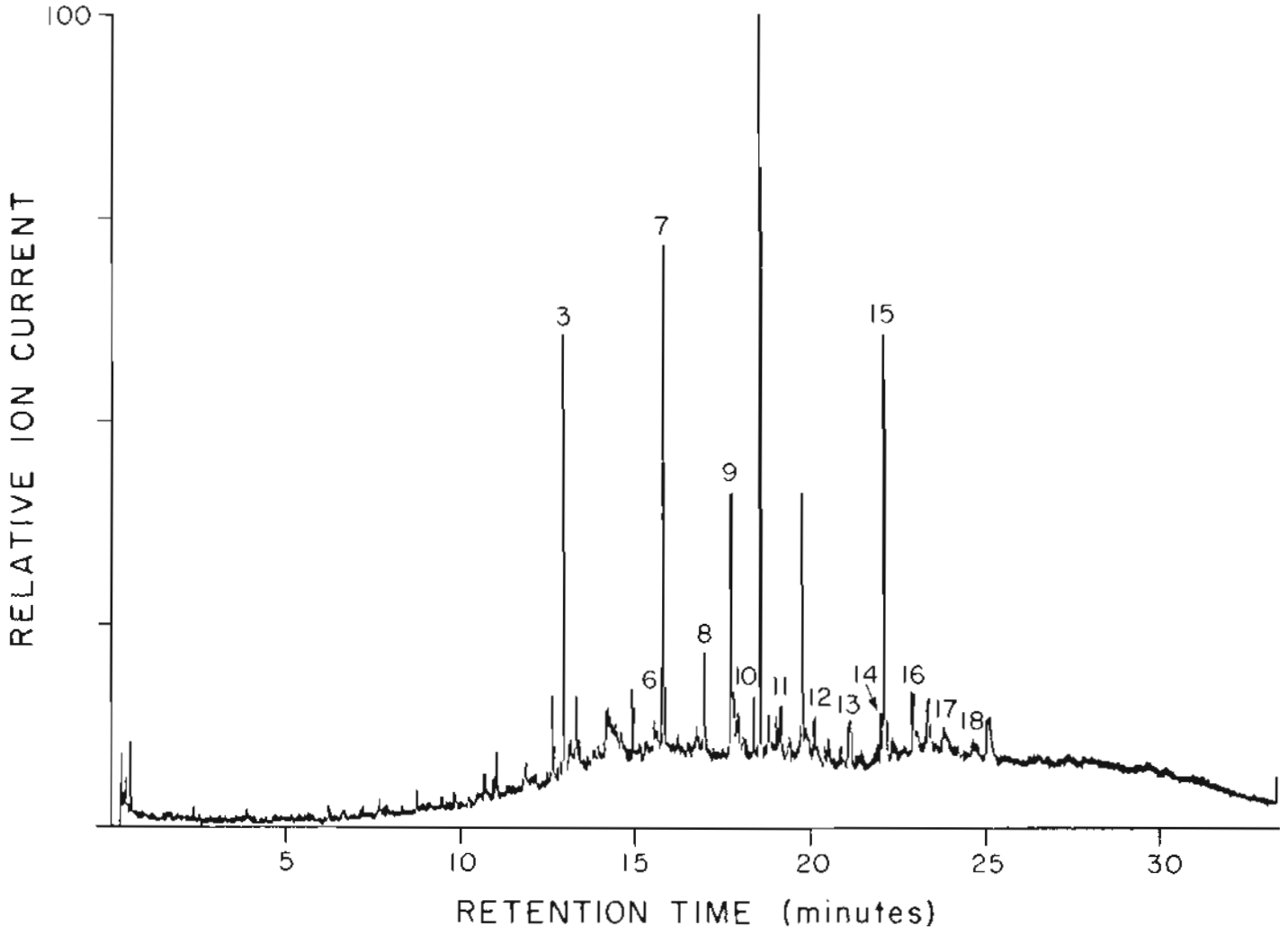

Figure 4.1. Total ion chromatogram of primary filters. The peak numbers refer to compounds listed in Table 4.1.

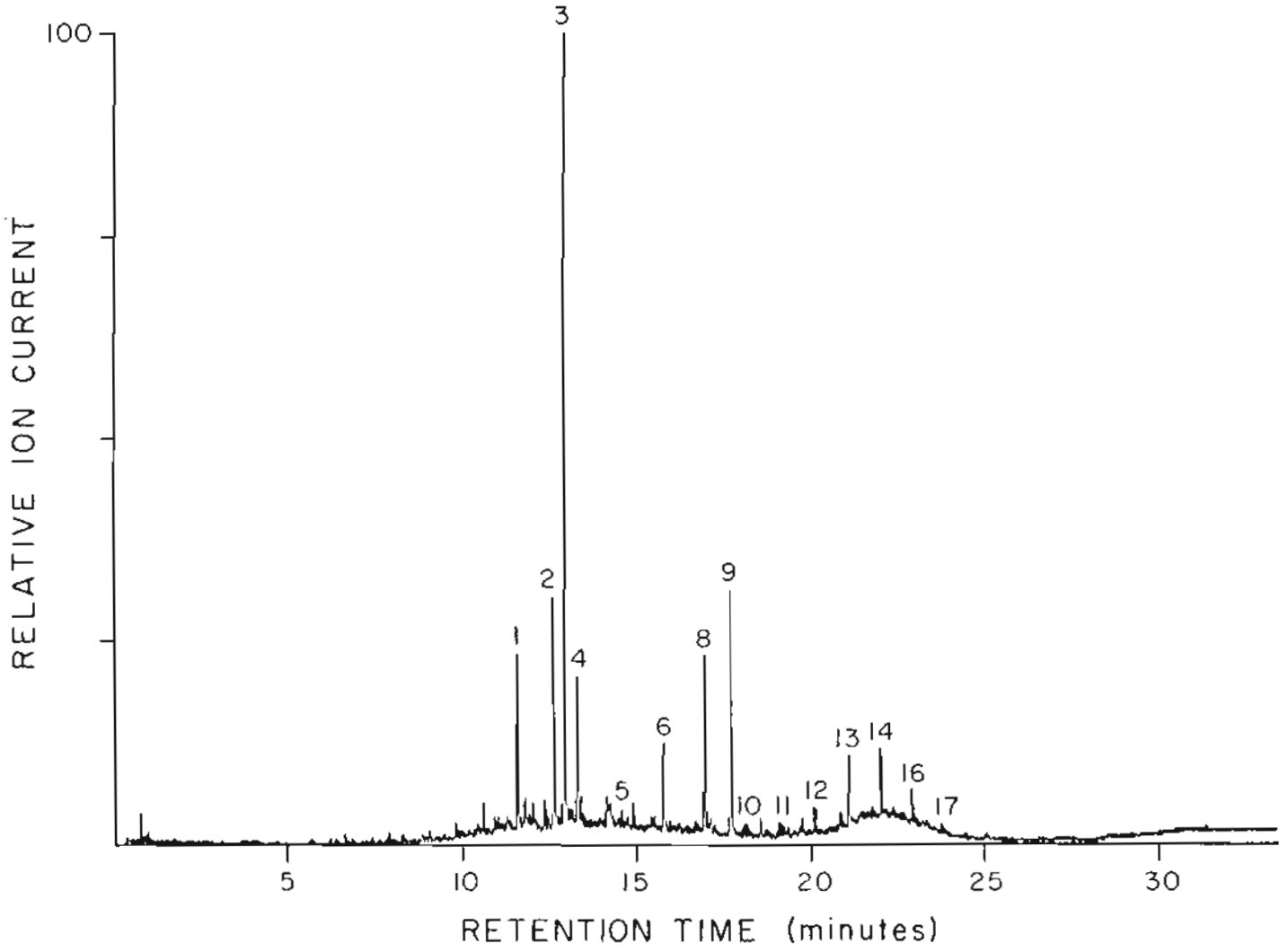

Figure 4.2. Total ion chromatogram of back-up filter. The peak numbers refer to compounds listed in Table 4.1.

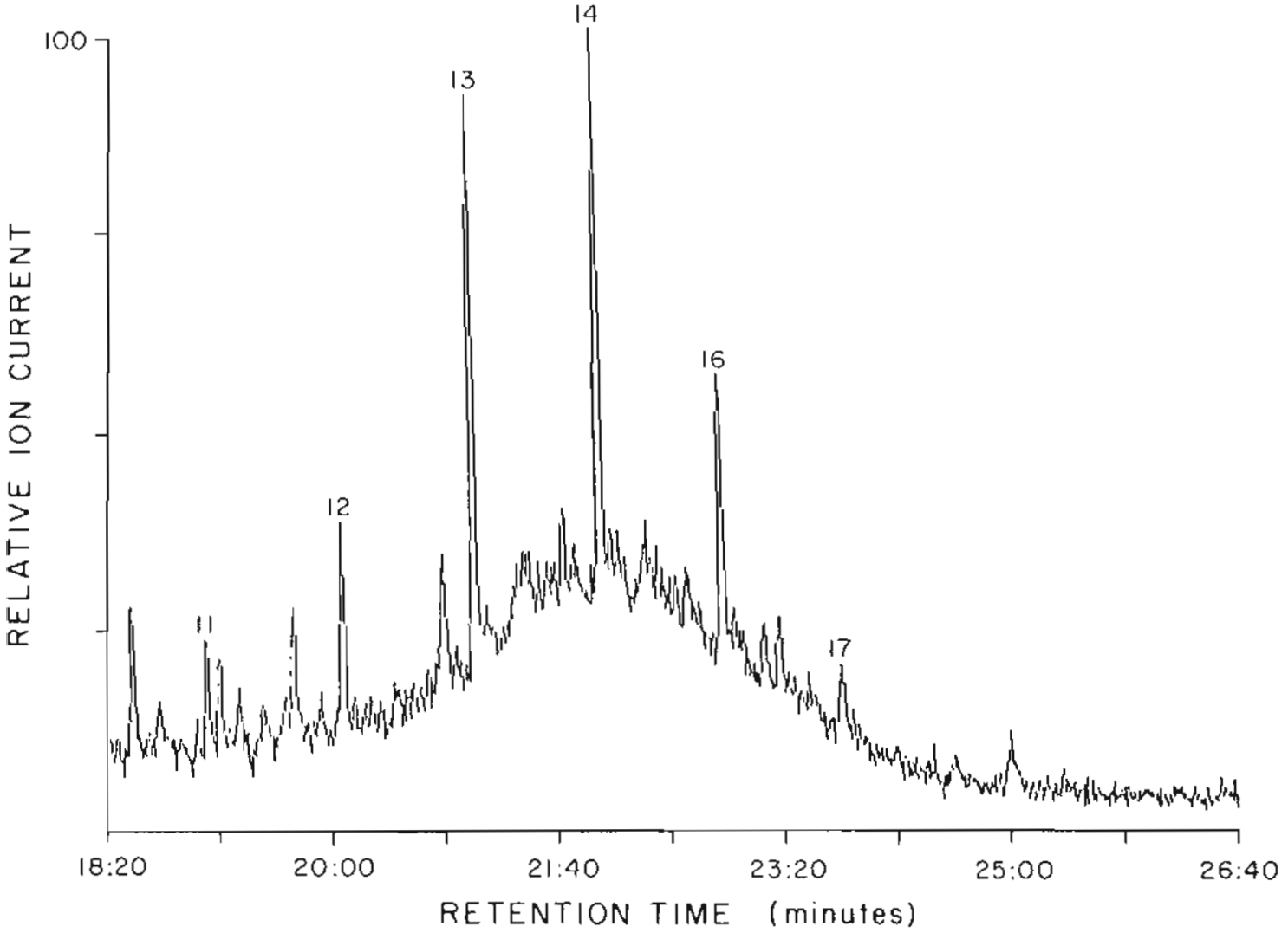

Figure 4.3. Total ion chromatogram of back-up filter for retention times between 18 and 26 minutes. The peak numbers refer to compounds listed in Table 4.1.

TABLE 4.1 - IDENTIFICATION OF ADSORBED ORGANIC VAPORS

COMPOUND	FRONT FILTER	BACK-UP FILTER	BLANK FILTER	IDENTIFICATION
1		X		83,69,55,98
2		X		71,56,83
3	X	X	X	71,56,89
4		X	X	tetradecane
5		X	X	pentadecane
6	X	X	X	hexadecane
7	X			149 (phthalate)
8	X	X	X	heptadecane
9	X	X	X	anthracene-d_{10}*
10	X	X		octadecane
11	X	X		nonadecane
12	X	X		eicosane
13	X	X		heneicosane
14	X	X		docosane
15	X			(phthalate)
16	X	X		tricosane
17	X	X		tetracosane
18	X			pentacosane

*internal standard

identified by comparison of both retention time and mass spectra to those observed from a standard n-alkane mixture. Some of the n-alkanes (i.e., n-hexadecane and n-docosane, peaks 6 and 12 of Fig. 4.1) coeluted with other compounds. These were resolved by reconstructing the chromatogram of the characteristic ions m/e=57 and m/e=71. Other compounds in Table 4.1 were identified by their base peak and other prominent peaks in order of their intensity. If a good match with an NBS library compound was observed, the compound is included in parentheses. Anthracene-d_{10} was included as an internal standard. However, quantitative analysis could not be confidently accomplished for the n-alkanes because of considerable interference from unresolved hydrocarbons. Chromatograms were also reconstructed for characteristic ions of polycyclic aromatic hydrocarbons (m/e=178, 192, 202, 216, 228, 252) but there was no indication of their presence on either primary or back-up filters.

n-Alkanes from n-hexadecane (C-16) to n-pentacosane (C-25) were observed on the primary filter sample. Back-up filter n-alkanes were slightly more volatile, ranging from n-tetradecane (C-14) to n-tetracosane (C-24). Blank filter n-alkanes ranged from n-tetradecane (C-14) to n-heptadecane (C-17).

These results suggest the possibility that adsorbed n-alkanes are displaced by their less volatile homologs during sampling. Similar results were obtained by Appel et al. (1979) for samples collected with different sampling durations. Their results showed that for longer sampling durations the volatility range of the n-alkanes collected decreased with increasing sampling duration.

The unresolved mass of hydrocarbons displays similar characteristics. For back-up filters the ion current drops to a low intensity after a retention time of 25 min., but for primary filter characteristic hydrocarbon ions are observed for the duration of the chromatogram.

The mass spectra of the unresolved mass in both chromatograms were similar and did not vary substantially with retention time. Fig. 4.4 provides a typical example. The clusters of mass peaks centering around m/e=55 to 57 and repeating every 14 amu with lower intensity are characteristic of aliphatic hydrocarbons.

Carbon analysis indicated that for the primary and back-up filter respectively, 29% and 70% of the organic carbon removed at 750°C was removed at the 250°C desorption temperature. 1.6 times as much organic carbon was removed from the primary as from the back-up filters at 250°C. This is within the range of typical ratios between the two filters of adsorbed carbon (see Section III.E.). Consequently, at this temperature it is possible that most of the primary filter organic carbon observed after desorption had been collected as organic vapor.

Although it is not clear what fraction of the adsorption artifact is accounted for by aliphatic hydrocarbons, the presence of neutral hydrocarbons on the back-up filter indicates that some fraction of organic vapor adsorption can be attributed to physical adsorption and is not analogous to acid-base interactions responsible for adsorption of inorganic gas-phase artifacts. This is presumably also true for other high molecular weight hydrocarbons, (e.g. PAHs and carboxylic acids). However, these compounds were apparently present at concentrations too low to detect for the sampling and analytical

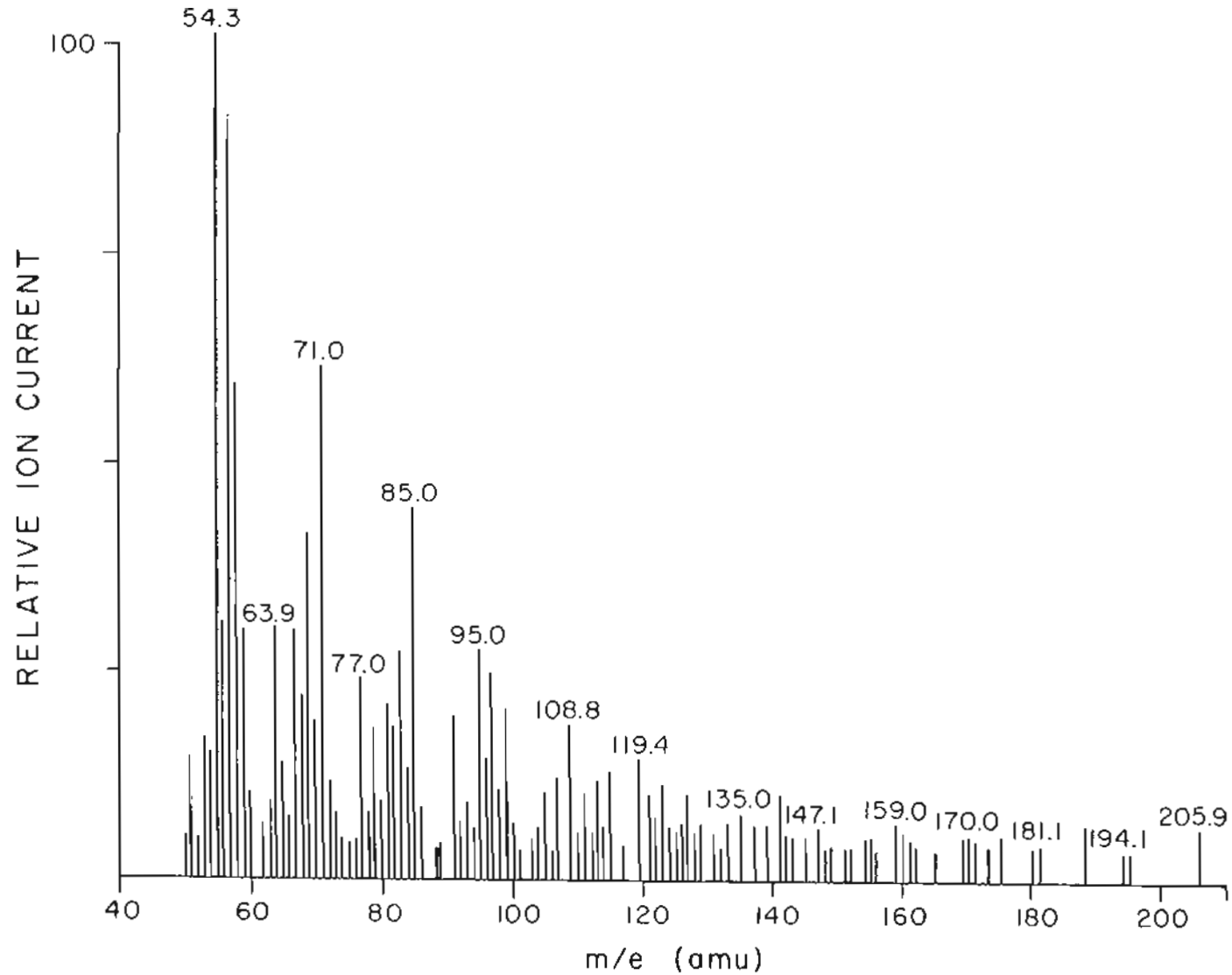

Figure 4.4. Mass spectrum typical of the unresolved region of the chromatograms.

procedures used.

Volatilization of n-alkanes from n-octadecane (C-18) to n-pentacosane (C-25) has been observed for experiments in which samples were exposed to a stream of nitrogen in the laboratory (Van Vaeck and Van Cauwenberghe, 1984). The presence of n-alkanes on the back-up filter indicates that it is possible that n-alkanes are collected as adsorbed vapor and volatilized from the filter rather than from particulate matter. n-Alkanes could therefore represent an adsorption artifact rather than a volatilization artifact.

Thermal desorption of aerosol filters followed by gas chromatographic/mass spectral analysis appears to be a promising technique for the study of the organic vapor adsorption artifact. It is possible that the majority of organic mass collected on the primary filters is adsorbed vapor. Consequently, a comparison of adsorption artifact and aerosol composition should also include solvent extraction of high-volume primary filters. Although limited here to aliphatic compounds, it can be used for PAHs and monocarboxylic acids as well (Greaves et al., 1985). Evidence for these classes of compounds was not apparent from back-up filter or primary filter analysis from this preliminary work. Further analysis of back-up filters associated with aerosol samples shown to contain PAHs and monocarboxylic acids would be of great interest.

CHAPTER V - A MODEL FOR ADSORPTION OF ORGANIC VAPORS BY FILTERS DURING SAMPLING

Two possible explanations for variations of apparent concentration with face velocity are 1) that adsorption of organic vapor varies with face velocity (see Section III.B.2) and 2) that volatilization of collected particulate matter during sampling varies with face velocity due to the face velocity dependence of the pressure drop across the filter.

A. The Organic Vapor Adsorption Model

A large number of both natural and anthropogenic vapors have been observed in the atmosphere (Lamb et al., 1980). It is not known which of these compounds are adsorbed by sampling media and to what extent they are depleted from sampled air. Moreover, information on heats of adsorption for most of these compounds on substances similar to quartz fiber filters have not been obtained. However, variations of apparent concentration and adsorption artifact error with face velocity observed in Chapter III are consistent with a simple fluid dynamics-adsorption kinetics model using the system described in Fig. 5.1. For each adsorptive species i, a mass balance can be expressed by Equation 5.1, which is analogous to the Langmuir adsorption model:

$$\frac{dM_i}{dt} = \rho_i v - \frac{1}{\tau_i} M_i \qquad 5.1$$

where:

M_i = mass collected per unit area of filter (g/cm^2)

ρ_i = adsorptive vapor concentration (g/cm^3)

v = air velocity (face velocity)

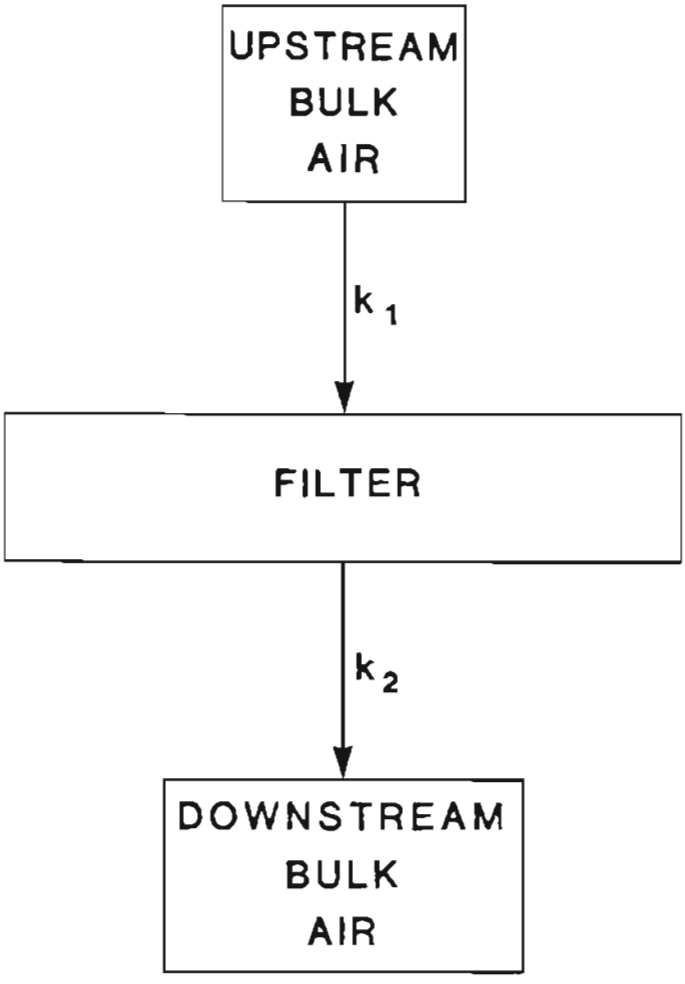

Figure 5.1. Schematic representation for the filter adsorption model.

τ_i = lifetime in filter (s)

Within the filter, an adsorptive compound can be in either the gas phase or the adsorbed state. Consequently, the residence time in the filter is the sum of the residence times for both of these states:

$$\tau_i = \tau_G + \tau_A \qquad 5.2$$

where τ_G is the residence time in the gas phase and τ_A in the adsorbed state. In the gas phase, the residence time is:

$$\tau_G = \ell / v \qquad 5.3$$

where ℓ is the effective filter thickness, (i.e., the average gas-phase path length traveled between entry into and exit from the filter).

The residence time in the adsorbed state can be expressed as:

$$\tau_A = Nf(t)\tau_A^* \qquad 5.4$$

where:

N = number of vapor-adsorbent collisions which result in adsorption;

τ_A^* = average adsorption time for a single adsorbate-adsorbent interaction;

and f(t) is a factor to account for the decreasing ability with sampling duration to adsorb vapors as more of the filter surface area becomes covered by adsorbed vapor.

The number of vapor-fiber collisions in Equation 5.4 can be expressed as:

$$N = \frac{\ell \beta}{v} \qquad 5.5$$

β represents the number of vapor-fiber collisions per molecule per unit

time and is dependent on molecular weight, temperature, and concentration of adsorbate molecules. For transport through the filter the Peclet number is much less than one. Consequently, vapor-fiber collisions will be the result of Brownian motion (Friedlander, 1977), and to a first approximation β will not be a function of face velocity.

The adsorption time for a single interaction, τ_A^* of Equation 5.6, is related to the heat of adsorption, Q_A (Adamson, 1976):

$$\tau_A^* = \tau_o \exp(Q_A/RT) \qquad 5.6$$

where τ_0 is a constant.

By substituting Equations 5.5 and 5.6 into Equation 5.4, an expression for the residence time in the adsorbed state is obtained:

$$\tau_A = \frac{\ell\beta}{v} f(t)\, \tau_o \exp(Q_A/RT) \qquad 5.7$$

Finally, the expression for total residence time in the filter τ_i is obtained by substituting the expressions for τ_G (Equation 5.3) and τ_A (Equation 5.7) into Equation 5.2:

$$\tau_i = \frac{\ell}{v} [\beta f(t) \tau_o \exp(Q_A/RT) + 1] \qquad 5.8$$

Since the fraction f(t) of surface area available for adsorption is an unknown decreasing function of time, Equation 5.8 cannot be solved unless its change over the course of the sampling period is negligible. To obtain a first approximation of the solution, f(t) is therefore assumed constant. This assumption is also a reasonable physical possibility. For constant f(t), a new constant can be defined as:

$$\varepsilon_i = \frac{1}{\ell} [\beta f(t) \tau_o \exp(Q_A/RT) + 1] \qquad 5.9$$

By substituting Equation 5.9 into Equation 5.8 a simplified expression

for filter residence time in terms of face velocity is obtained:

$$\tau_i = \frac{1}{\varepsilon_i v} \qquad 5.10$$

The original mass balance equation, Equation 5.1, now can be expressed in terms of face velocity as:

$$\frac{dM_i}{dt} = \rho_i v - \varepsilon_i v M_i \qquad 5.11$$

The solution of this equation is:

$$M_i = \frac{\rho_i}{\varepsilon_i} (1-e^{-\varepsilon_i vt}) + M_{oi} e^{-\varepsilon_i vt} \qquad 5.12$$

where M_{oi} is the initial (i.e., at t=0) mass of adsorbed vapor, and t the sampling duration.

Finally, a predicted lower limit for artifact error can be calculated from the sum of all adsorptive vapors using Equation 5.13:

$$C = \Sigma_i \frac{M_i}{vt} \qquad 5.13$$

This equation is identical to Equation 2.1, but without blank subtraction. Substituting the mass loading predicted from Equation 5.12 into Equation 5.13 yields:

$$C = \Sigma_i \frac{\rho_i (1-e^{-\varepsilon_i vt})}{\varepsilon_i vt} + \Sigma_i \frac{M_{oi} e^{-\varepsilon_i vt}}{vt} \qquad 5.14$$

B. Applications

B.1. Face Velocity and Sampling Period

For ambient sampling experiments, the initial mass loading (i.e., the sample blanks of Table 2.2 and 2.3) will be negligible, and the adsorption artifact concentration will vary with face velocity and sampling period according to Equation 5.15:

$$C_{art} = \Sigma_i \frac{\rho_i(1-e^{-\varepsilon_i vt})}{\varepsilon_i vt} \qquad 5.15$$

This equation predicts a decreasing trend of artifact concentration with increasing face velocity and sampling duration as indicated by the plot in Fig. 5.2. This plot is similar to the observed decreasing trend of artifact concentration with face velocity (Figs. 3.4, 3.5, and 3.8; Section III.B.2) and is also consistent with the greater observed artifact concentrations for shorter sampling periods. (Table 3.10; Section III.C.2).

For particles an infinite filter residence time can be assumed and Eq. 5.1 becomes

$$\frac{dM_p}{dt} = \rho_p v \qquad 5.16$$

where the subscript p designates a particulate quantity. It follows that

$$M_p = \rho_p vt \qquad 5.17$$

and

$$C_p = \rho_p \qquad 5.18$$

Equation 5.18 predicts that for particles in the absence of adsorptive vapor the observed concentration C will equal the actual concentration ρ and will consequently be independent of face velocity and sampling period, as observed for elemental carbon.

For organic carbon the apparent particulate concentration C_A is the sum of the actual particulate concentration and adsorption

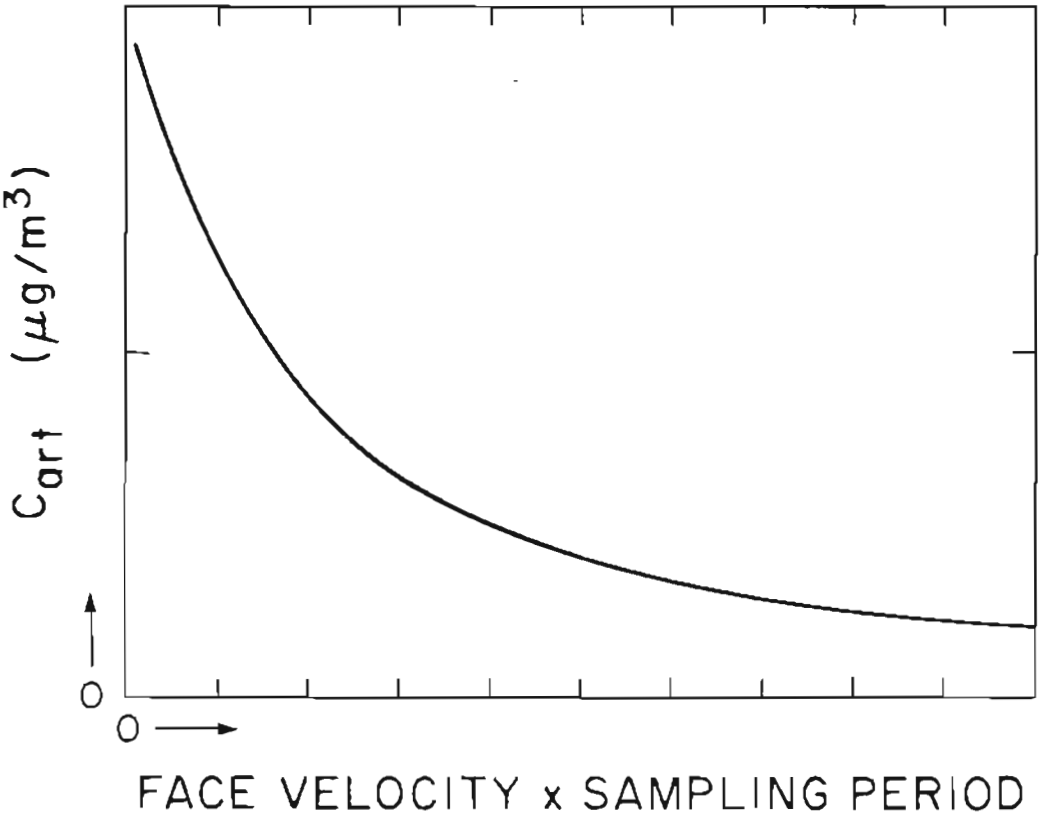

Figure 5.2. Variation of adsorption artifact concentration with face velocity predicted from Equation 5.15.

artifact concentration, or

$$C_A = \rho_p + \Sigma_i \frac{\rho_i(1-e^{-\varepsilon_i vt})}{\varepsilon_i vt} \qquad 5.19$$

The apparent concentration predicted from Equation 5.19 is plotted against face velocity in Fig. 5.3 for arbitrary values of ρ_i and ε_i. A decreasing trend of apparent concentration with face velocity and sampling duration is predicted. This is consistent with the observed decreasing trend of apparent particulate organic carbon concentration with both face velocity (Figs. 3.2 and 3.4; Section III.B.1) and sampling period (Table 3.9; Section III.C.1).

If the ith term of Equation 5.15 is divided by the gas phase concentration of species i, ρ_i, the following equation is obtained:

$$\eta_i = \frac{(1-e^{-\varepsilon_i vt})}{\varepsilon_i vt} \qquad 5.20$$

where η_i is the collection efficiency for species i by the filter. Equation 5.20 was evaluated for n-docosane. This compound appeared to be the most abundant of the chromatographically resolved n-alkanes on the back-up filter (see Chapter IV, Figs. 4.2 and 4.3).

The constant ε_i was predicted for n-docosane from Equation 5.9. The fraction of surface area available for adsorption, f(t), was assumed equal to one. The effective filter thickness, ℓ, was approximately 0.03 cm. A value of 10^{-13} sec was assumed for the constant τ_o (Adamson, 1976).

The number of collisions per vapor molecule per unit time, β_i of Equation 5.9, was estimated from gas-kinetic theory. For n_i

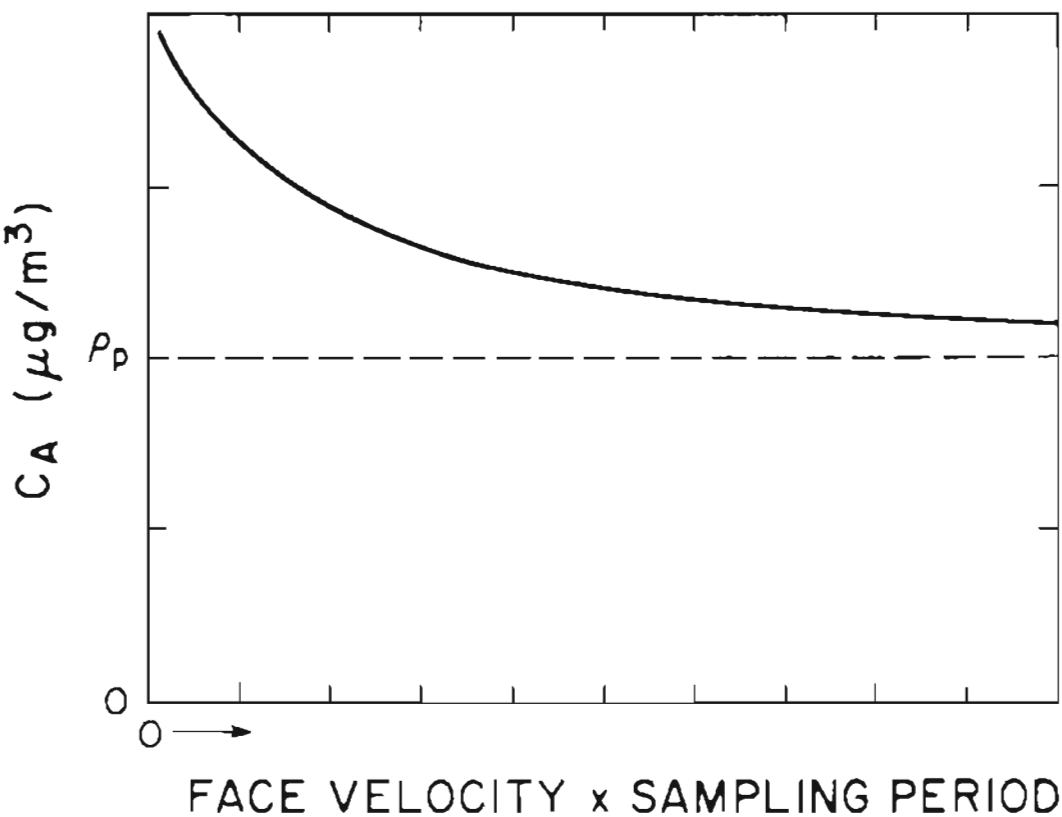

Figure 5.3. Variation of apparent particulate concentration (C_A) from Equation 5.18.

molecules per unit volume, the number of collisions with a surface per unit time per unit surface area, ν_i, is (Present, 1958):

$$\nu_i = \frac{n_i}{4}\left(\frac{8RT}{\pi MW_i}\right)^{\frac{1}{2}} \qquad 5.21$$

where MW_i is the molecular weight of species i.

The collision frequency expressed as a function of unit cross-sectional filter area, ν_{fi}, was obtained by multiplying Equation 5.21 by the unit surface area per unit cross-sectional filter area:

$$\nu_{fi} = \nu_i \times \frac{A_s}{A_f} = \frac{n_i}{4}\left(\frac{8RT}{\pi MW_i}\right)^{\frac{1}{2}} \times \frac{A_s}{A_f} \qquad 5.22$$

where A_s is the surface area of the filter and A_f is the cross-sectional area.

The number of molecules of vapor i per unit volume, n_i, is:

$$n_i = \frac{\chi_i P N_A}{RT} \qquad 5.23$$

where χ_i is the mole fraction of species i and N_A is Avogadro's number. P is the total pressure within the filter. A negligible pressure gradient through the filter was assumed. Usually, pressures upstream and downstream of the quartz fiber filters differed by less than 10%.

Substitution of Equation 5.23 into Equation 5.22 leads to:

$$\nu_{fi} = \frac{\chi_i P N_A}{4RT}\left(\frac{8RT}{\pi MW_i}\right)^{\frac{1}{2}} \times \frac{A_s}{A_f} \qquad 5.24$$

β_i was obtained by dividing ν_{fi} by the number of molecules of species i, q_i, in the gas phase within the filter at a given time:

$$\beta_i = \frac{\nu_i}{q_i} \qquad 5.25$$

q_i was estimated by multiplying the concentration, $\chi_i \Sigma n_i$ by the total volume of air space available per unit cross-sectional filter area:

$$q_i = \chi_i \Sigma n_i \frac{V_f}{A_f} = \chi_i \Sigma n_i \ell \qquad 5.26$$

Finally, β_i was expressed entirely in terms of parameters which could be easily measured or evaluated, by substituting Equations 5.24 and 5.26 into Equation 5.25:

$$\beta_i = \frac{\frac{1}{4}\left(\frac{8RT}{\pi MW_i}\right)^{\frac{1}{2}} \frac{A_s}{A_f}}{\ell} \qquad 5.27$$

From the filter surface area of 20 m^2/g (see Table 5.1), a typical weight of 105 mg per filter for a 47 mm diameter filter, a value for surface area per unit cross-sectional filter area of $1.2 \times 10^3 cm^2/cm^2$ was obtained. For the filter thickness ℓ of 0.03 cm, and molecular weight for n-docosane of 310 g/mole at a temperature of 10°C, the estimated number of vapor-fiber collisions, β_i, was 1.5×10^8 collisions $molecule^{-1} sec^{-1}$.

BET theory assumes that for multilayer adsorption, the heat of adsorption for the first adsorbate layer is determined by adsorbent-adsorbate interactions, while adsorption heats of additional layers can be approximated by the adsorbate's heat of condensation. (Brunauer et al., 1938). Consequently, two different estimates of the heat of adsorption, Q_A, were obtained. For submonolayer adsorption, a heat of

TABLE 5.1 - SURFACE AREA MEASUREMENTS

FILTER TYPE	SURFACE AREA (m^2/g)	SURFACE AREA PER UNIT FILTER AREA (cm^2/cm^2)
Quartz	20.08	1200
Teflon	1.00	130
Glass	1.76	130

adsorption for n-docosane was extrapolated from heat of adsorption measurements of the more volatile n-alkane homologs on silica using Equation 5.28 (Kiselev, 1957):

$$Q_A = 1.5 + 1.23z \text{ Kcal/mole} \qquad 5.28$$

where z is the number of carbon atoms. However, when this equation was used to estimate the n-docosane heat of adsorption, the resulting ε_i values from Equation 5.9 predicted effectively no desorption at the face velocities and sampling durations used.

For multilayer adsorption, the n-docosane heat of adsorption was approximated by the heat of condensation of 16.9 Kcal/mole. For this case an ε_i value of 2.2×10^{-7} cm^{-1} was estimated. With this value the collection efficiency, η_i, was calculated as a function of face velocity for a 24-hour sampling duration. A plot of this function is reported in Fig. 5.4. It agrees in form with the aribtrary plot of Fig. 5.2 and with the observed variations of apparent particulate organic carbon with face velocity (see Section III.B.2).

Equation 5.14 was derived by assuming a negligible decrease in the fraction of surface area available for adsorption f(t) and that the number of collisions per unit time (β) was approximately constant with face velocity and sampling duration. However, it is likely that these quantities will also decrease with increasing adsorbate mass, and adsorbed carbon has been observed to increase with both face velocity and sampling duration. As more adsorptive vapor is brought into the filter it is possible that f(t) will decrease as more of the filter surface occupied by adsorbate becomes less receptive to further adsorp-

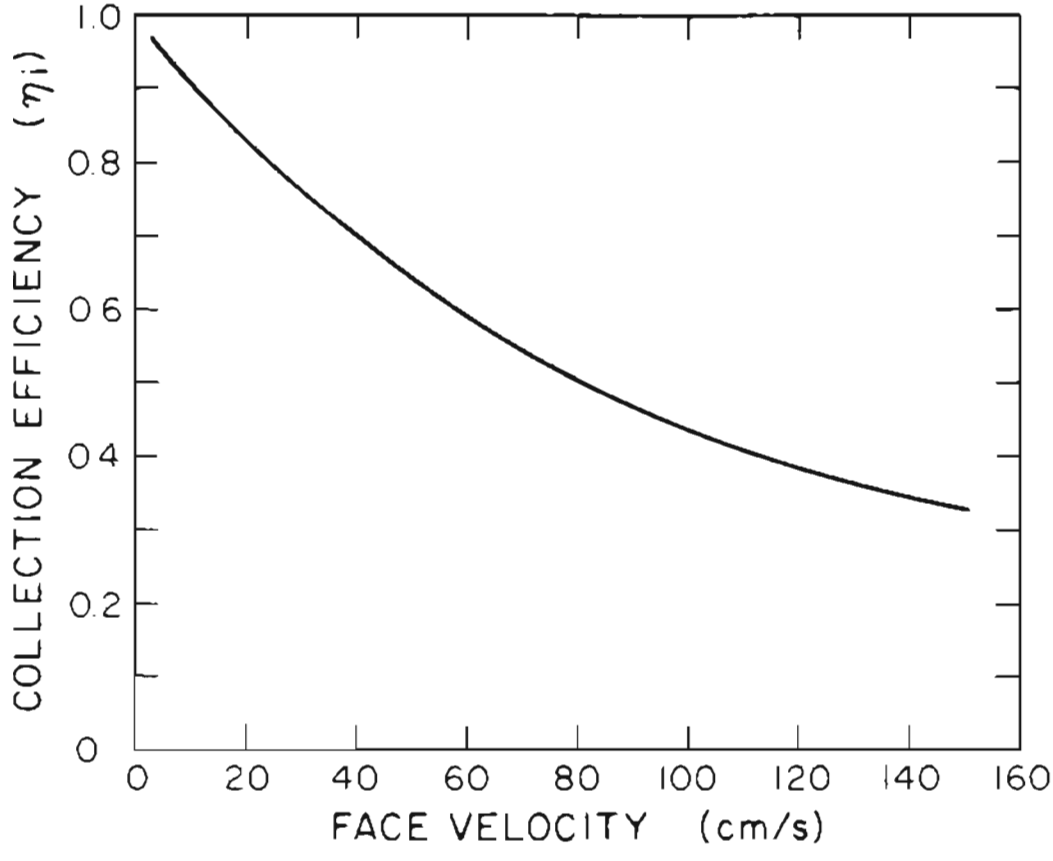

Figure 5.4. Predicted collection efficiency as a function of face velocity for n-docosane. Sampling time is 24 hr.

B.2. Volatilization

The results of the volatilization experiments of Section III.B.3 can also be explained using Equation 5.14. Here, the initial vapor concentration of the purified air is negligible and the initial carbon mass M_o is equal to that collected during ambient sampling. Under these conditions Equation 5.14 becomes

$$C = \Sigma_i \frac{M_{oi} e^{-\varepsilon v t}}{vt} \qquad 5.29$$

Equation 5.29 predicts that the loss of adsorbed vapor during exposure to purified air will decrease with increasing face velocity. The volatilization artifact concentration predicted from Equation 5.30 is plotted against face velocity and sampling duration in Fig. 5.5. This plot is similar to experimental observations plotted in Fig. 3.14 (see Section III.B.3.).

B.3. Filter Type

Variation of filter resistence time with filter types are expected because of differences in heats of adsorption of organic vapors for different filter media. This will, in turn, affect the magnitude of adsorption artifact.

For n-alkanes for methane to n-heptane, observed heats of adsorption on silica are greater than heats of condensation (Kiselev, 1957). BET type III isotherms (Brunauer et al., 1940) have been observed for hexane and octane on Teflon (Whalen, 1968). Since type III isotherms are characteristic of adsorbates with lower heats of

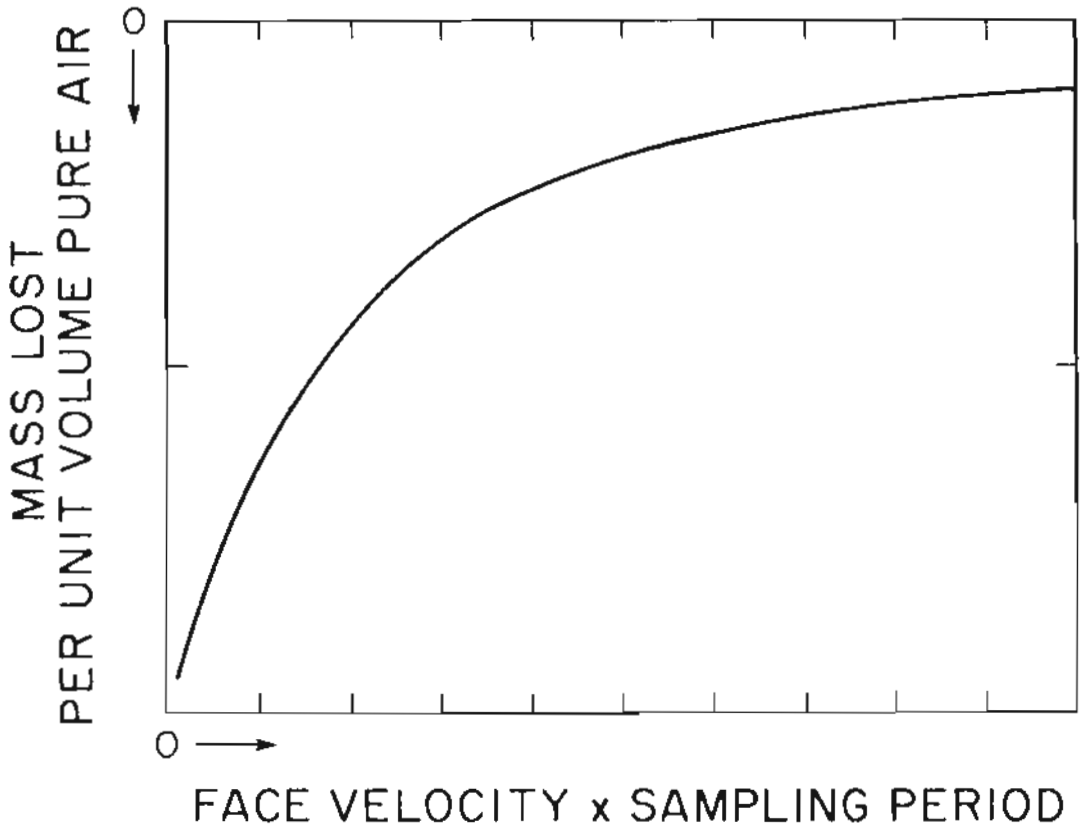

Figure 5.5. Variation of volatilization artifact with face velocity predicted from Equation 5.29.

adsorption than condensation, it follows that heats of adsorption for n-alkanes are greater on silica than on Teflon and consequently that greater artifact concentrations are predicted for quartz fiber filters.

Differences in filter type could also be explained by differences in effective path length through the filter or by differences in surface area. Teflon membrane filters are thinner and have smaller surface areas than quartz fiber filters, both of which would lead to smaller apparent concentrations on Teflon membrane filters. Surface areas measured for Teflon, quartz and glass filters are given in Table 5.1.

C. The Possibility of Volatilization Artifact

An alternative explanation for the variation of apparent organic carbon concentration with face velocity is volatilization of collected particulate matter. Since volatilization is expected to vary with pressure and the pressure drop across the filter varies with face velocity, it follows that the mass of collected particulate matter would also vary with face velocity. Organic carbon collected on back-up filters could then be partly due to adsorption of organic vapor volatilized from collected particulate matter and should not be used to correct for adsorption artifact. This is probably not an important mechanism for explaining the variation of artifact concentration with face velocity for the following reasons.

First, little pressure difference is observed in the portion of the face velocity range where the greatest differences in apparent concentrations with face velocity are observed. Typical pressure drops

are listed in Table 5.2. A much smaller difference in pressure drop across the filter is observed between samples collected at 15 and 40 cm/s than between those collected at 40 and 150 cm/s. These observations can be compared with those presented in Fig. 3.4a, which indicates that the average difference between apparent concentration between the 15 cm/s and 40 cm/s samples and between the 40 cm/s and 150 cm/s samples are similar.

Second, there is probably very little filter pressure drop variation between samples collected at different face velocities, at least for low face velocities. Most of the aerosol mass is collected in the furthest upstream fraction of the filter. Consequently, the actual pressure drop across the fraction of the filter containing most of the aerosol mass is probably overestimated by Table 5.2 and actually varies only slightly with face velocity.

TABLE 5.2 - VARIATION WITH FACE VELOCITY OF PRESSURE DROP ACROSS IMPACTOR AND TWO QUARTZ FIBER FILTERS

FACE VELOCITY (cm/s)	PRESSURE DROP (psi)	(kPa)
15	0.65	4.5
20	0.71	4.9
30	0.83	5.7
40	1.05	7.2
80	1.30	9.0
150	2.71	18.7

CHAPTER VI - CONCLUSIONS

Of the three sampling procedures investigated, face velocity, sampling duration, and filter type, all appeared to have a significant influence on the apparent concentration of organic particulate matter. An average of 41% more organic carbon was collected at 15 cm/s than at 150 cm/s face velocity for the atmospheric conditions existing during the sampling. At sampling durations of 48 hours an average of 19% more organic carbon was collected than for consecutive 24-hour sampling durations.

These differences appear to be accounted for by adsorption artifact. An average of 3.1 times as much carbon was collected on quartz fiber back-up filters behind Teflon prefilters at 15 cm/s than at 80 or 140 cm/s face velocity. This difference accounted for an average of 88% of the difference in apparent organic carbon concentration observed between these face velocities. An average of 28% more carbon was collected on back-up filters during consecutive 24-hour samples than for 48-hour samples. The observation of higher carbon loadings on quartz back-up filters behind Teflon prefilters than on those behind quartz primary filters indicated that more organic vapor adsorption probably occurs on quartz than on Teflon filters. Finally, a significant fraction of organic carbon collected on quartz fiber primary filters was generally accounted for by adsorbed vapor, especially at low organic aerosol concentrations. In five of twenty-four samples this fraction exceeded 50%, indicating that the majority of organic carbon collected was probably adsorbed from the vapor phase.

The adsorption artifact is probably more important than the volatilization artifact. This latter artifact has previously been interpreted to be responsible for results of experiments which measured "blow-off" into a clean air stream or nitrogen and for variations of apparent concentration with face velocity and sampling period. In this research all three of these phenomena were also observed for organic vapor adsorbed on back-up filters. Compounds susceptible to "blow-off" were measured on back-up filters, and adsorbed vapor accounted for the major fraction of "blow-off" from primary filters.

Several remaining questions must be answered before an optimum organic aerosol sampling procedure can be determined with confidence:

(1) Because all of the ambient samples were collected at one location in Portland, Oregon, under conditions of light to moderate air pollution, it is not clear how important the adsorption artifact would be under conditions of photochemical smog or heavy woodsmoke. Ambient experiments should be conducted under these conditions.

(2) A more conclusive comparison between volatilization from primary (aerosol) filters and from filters on which only adsorbed vapor are collected requires lower blank levels for the purified air. The extent of "blow-off" loss from the filter which is attributable to vapor cannot be adequately quantified until this is achieved. Also, experiments should be conducted for which the volatilization artifact is determined under ambient conditions.

(3) Loss of n-alkanes, PAHs and monocarboxylic acids has been

observed after exposure to a stream of nitrogen (Van Vaeck and Van Cauwenberghe, 1984). Of these classes of compounds, only n-alkanes were identified on back-up filters in this research. (However, PAHs and carboxylic acids were also not observed on primary filters because of the small amount of material available for analysis.) Analysis for PAHs and carboxylic acids on back-up filters associated with aerosol samples known to contain them would provide valuable information for both the comparison of adsorption and volatilization artifacts and for the composition of the adsorption artifact. For these applications thermal desorption followed by gas chromatography/mass spectrometry appears to be promising. The role of low molecular weight organic ions such as formate or acetate should also be assessed to determine whether there is some component of organic vapor adsorption which is analogous to sulfate or nitrate adsorption artifact.

(4) Finally, there is some evidence that the composition of the adsorption artifact can change during sampling. For example, n-alkanes could be replaced by their heavier homologs. This phenomenon should be further explored.

Although more research is necessary, it is clear that an important priority in an organic aerosol sampling scheme should be the minimization of the adsorption artifact. The recommended sampling procedure for this purpose is to sample with Teflon membrane filters at the highest practical face velocity for the longest practical sampling period. In more general terms, the greatest possible sampled air volume and the most inert sampling surface obtainable should be used.

Although this might be practical for analytical techniques which remove organic carbon by solvent extraction, Teflon filters are not suitable for thermal-optical carbon analysis. For samples collected for thermal-optical analysis, quartz fiber filters can be used and the adsorption artifact estimated from a quartz back-up filter behind a Teflon prefilter sampled simultaneously under otherwise identical sampling conditions. The use of glass fiber filters appears to be a poor choice for organic sample collection because of high blank levels.

REFERENCES

Adamson, A. W. (1976), Physical Chemistry of Surfaces, Third Edition, John Wiley and Sons, New York.

American Chemical Society (1980), Subcommittee on Environmental Analytical Chemistry. Guidelines for data acquisition and data evaluation in environmental chemistry. Anal. Chem. 52, 2242-2249.

American Public Health Association (1977), Methods of Air Sampling and Analysis, Second edition (edited by M. Katz). American Public Health Association, Washington, D.C., 1977.

Appel, B. R., Colodny, P. and Wesolowski, J. J. (1976). Analysis of carbonaceous materials in Southern California aerosols. Environ. Sci. Tech. 10, 359-363.

Appel, B. R., Hoffer, E. M., Kothny, E. L., Wall, S. M., Haik, M. and Knights, R. L. (1979). Analysis of carbonaceous material in Southern California aerosols 2. Environ. Sci. Tech. 13, 98-104.

Appel, B. R., Tokiwa, Y. and Kothny, E. L. (1983). Sampling of carbonaceous particles in the atmosphere. Atmos. Environ. 17, 1787-1796.

Brockhaus, A. (1974). Sampling of tetracyclic aromatic hydrocarbons under atmospheric conditions. Atmos. Environ. 8, 521.

Broddin, G., Cautreels, W. and Van Cauwenberghe, K. (1980). On the aliphatic and aromatic hydrocarbon levels in the urban background aerosols from Belgium and the Netherlands. Atmos. Environ. 14, 895-910.

Brunauer, S., Emmett, P. H. and Teller, E. (1938). Adsorption of gases in multimolecular layers. J. Am. Chem. Soc. 60, 309-319.

Brunauer, S., Deming, L. S., Deming, W. E. and Teller, E. (1940). On a theory of the van der Waals adsorption of gases. J. Am. Chem. Soc. 62, 1723-1732.

Cadle, S. H., Groblicki, P. J. and Stroup, D. B. (1980). Automated carbon analyzer for particulate samples. Anal. Chem. 52, 2201-2206.

Cadle, S. H., Groblicki, P. J. and Mulawa, P. A. (1983). Problems in the sampling and analysis of carbon particulate. Atmos. Environ. 17, 593-600.

Cautreels, W. and Van Cauwenberghe, K. (1978). Experiments on the distribution of organic pollutants between airborne particulate matter and the corresponding gas phase. Atmos. Environ. 12, 1133-1141.

Commins, B. T. (1962). Interim report on the study of techniques for determination of polycyclic aromatic hydrocarbons in air. National Cancer Institute Monograph 9, 225-233.

Coutant, R. W. (1977). Effect of environmental variables on collection of atmospheric sulfate. Environ. Sci. Tech. 11, 873-878.

David, D. J. (1974). Gas Chromatographic Detectors. John Wiley and Sons, New York.

Davies, O. L. and Goldsmith, P. L. (1972). Statistical Methods in Research and Production, Fourth Edition. Longman Group Limited, London.

Della Fiorentina, H., De Wiest, F. and De Graeve, J. (1975). Determination par spectrometrie infrarouge de la matiere organique non volatile associee aux particules en suspension dans l'air - II. Facteurs influencant l'indice aliphatique. Atmos. Environ. 9, 517-522.

De Wiest, F. and Della Fiorentina, H. (1975). Suggestions for a realistic definition of an air quality index relative to hydrocarbonaceous matter associated with airborne particles. Atmos. Environ. 9, 951-954.

Eichmann, R., Neuling, P., Ketseridis, G., Hahn, J., Jaenicke, R. and Junge, C. (1979). n-Alkane studies in the troposphere - I. Gas and particulate concentrations in North Atlantic air. Atmos. Environ. 13, 587-599.

Friedlander, S. K. (1977). Smoke, Dust and Haze: Fundamentals of Aerosol Behavior. John Wiley and Sons, New York.

Goldberg, E. D. (1985). Black Carbon in the Environment: Properties and Distribution. Wiley Interscience, New York.

Greaves, R. C., Barkley, R. M., and Sievers, R. E. (1985). Rapid sampling and analysis of volatile constituents of airborne particulate matter. Anal. Chem. 57, 2807-2815.

Grosjean, D. (1975). Solvent extraction and organic carbon determination in atmospheric particulate matter: the organic extraction-organic carbon analyzer technique. Anal. Chem. 47, 797-805.

Hieger, I. (1946). Carcinogenic substances in human tissues. Cancer 6, 657-667.

Hoffman, D. and Wynder, E. L. (1968). Chemical analysis and carcinogenic bioassays of organic particulate pollutants. In Air Pollution, Volume II: Analysis, Monitoring and Surveying (edited by Stern, A. C.), pp. 187-247. Academic Press, New York.

Huntzicker, J. J., Johnson, R. L., Shah, J. J. and Cary, R. A. (1982). Analysis of organic and elemental carbon in ambient aerosols by a thermal-optical method. In Particulate Carbon: Atmospheric Life Cycle (edited by Wolff, G. T. and Klimisch, R. L.)., pp. 79-88. Plenum Press, New York.

Japar, S. M., Szkarlat, A. C., Gorse, R. A., Heyerdahl, E. K., Johnson, R. L., Rau, J. A. and Huntzicker, J. J. (1984). Comparison of solvent extraction and thermal-optical carbon analysis methods: applications to diesel vehicle exhaust. Environ. Sci. Tech. 18, 231-234.

Johnson, R. L. (1981). Development and evaluation of a thermal-optical method for the analysis of carbonaceous aerosol. M. S. Thesis, Oregon Graduate Center.

Johnson, R. L., Shah, J. J., Cary, R. A. and Huntzicker, J. J. (1982). An automated thermal-optical method for the analysis of carbonceous aerosol. In American Chemical Society Symposium Series No. 167, Atmospheric Aerosol: Source/Air Quality Relationships (edited by Macias, E. S. and Hopke, P. K.), pp. 223-233. American Chemical Society, Washington, D.C.

Kawamura, K., Ng, L.-L. and Kaplan, I. R. (1985). Determination of organic acids (C_1-C_{10}) in the atmosphere, motor exhausts, and engine oils, Environ, Sci. Tech. 19, 1082-1086.

Keith, L. H., Crummet, W., Deegan, J., Libby, R. A., Taylor, J. K. and Wentler, G. (1983). Principles of environmental analysis. Anal. Chem. 55, 2210-2218.

Kiselev, A. V., in Proceedings of the Second International Conference on Surface Activity, Butterworths, London 1957, pp. 179-188.

Klippel, W. and Warneck P. (1980). The formaldehyde content of the atmospheric aerosol. Atmos. Environ. 14, 809-818.

Konig, J., Funcke, W., Balfanz, E., Grosch, B. and Pott, F. (1980). Testing a high volume air sampler for quantitative collection of polycyclic aromatic hydrocarbons. Atmos. Environ. 14, 609-613.

Lamb, S. I., Petrowski, C., Kaplan, I. R. and Simoneit, B. R. T. (1980). Organic compounds in urban atmospheres: a review of distribution, collection and analysis. J. Air Pollution Control Assoc. 30, 1098-1115.

Lee, F. S.-C., Pierson, W. R. and Ezike, J. (1980). The problem of PAH degradation on several commonly used filter media. In Polynuclear Aromatic Hydrocarbons: Fourth International Symposium on Analysis, Chemistry, and Biology, pp. 543-563. Batelle Press, Columbus, Ohio.

Leiter, J. and Shear, M. J. (1942). J. National Cancer Inst. 3, 167.

Ligocki, M. P., Leuenberger, C. and Pankow, J. F. (1985). Trace organic compounds in rain-II. Gas scavenging of neutral organic compounds. Atmos. Environ. 19, 1609-1617.

Ligocki, M. P. and Pankow, J. F. (1985). Assessment of adsorption/solvent extraction with polyurethane foam and adsorption/thermal desorption with Tenax-GC for the collection and analysis of ambient organic vapors. Anal. Chem. 57, 1138-1144.

McNair, H. M. and Bonelli, E. J. (1968). Basic Gas Chromatography. Varian Aerograph, Walnut Creek, California.

Pankow, J. F. and Isabelle, L. M. (1982). Adsorption-thermal desorption as a method for the determination of low levels of aqueous organics. J. Chromatography 237, 25-39.

Pankow, J. F. and Kristensen, T. J. (1983). Effects of flow rate and thermal desorbability of polycyclic aromatic hydrocarbons and pesticides from Tenax-GC. Anal. Chem. 55, 2187-2192.

Pankow, J. F. and Isabelle, L. M. (1984). Interface for the direct coupling of a second gas chromatograph to a gas chromatograph/mass spectrometer for use with a fused silica capillary column. Anal. Chem. 56, 2997-2999.

Peters, J. and Seifert, B. (1980). Losses of benzo(a)pyrene under conditions of high-volume sampling. Atmos. Environ. 14, 117-119.

Pitts, J. N., Van Cauwenberghe, K. A., Grosjean, D., Schmid, J. P., Fitz, D. R., Belser, W. L., Knudson, G. B. and Hynds, P. M. (1978). Atmospheric reactions of polycyclic aromatic hydrocarbons: facile formation of mutagenic nitro derivatives. Science 202, 515-519.

Pitts, J. N., Lokensgard, D. M., Ripley, P. S., Van Cauwenberghe, K. A., Van Vaeck, L., Shaffer, S. D., Thill, A. J. and Belser, W. L. (1980). "Atmospheric" epoxidation of benzo(a)pyrene by ozone: formation of the metabolite benzo(a)pyrene-4,5-oxide. Science 210, 1347-1349.

Present, R. D. (1958). Kinetic Theory of Gases, McGraw-Hill, New York.

Pupp, C., Lao, R. C., Murray, J. J. and Pottie, R. F. (1974). Equilibrium vapour concentrations of some polycyclic aromatic hydrocarbons, As_4O_6 and SeO_2 and the collection efficiencies of these air pollutants. Atmos. Environ. 8, 915-925.

Rondia, D. (1965). Sur la volatilite des hydrocarbures polycycliques. Int. J. Water Air Pollution 9, 113-121.

Scaringelli, F. P. and Rehme, K. A. (1969). Determination of atmospheric concentrations of sulfuric acid aerosol by spectrophotometry, coulometry and flame photometry. Anal. Chem. 41, 707-713.

Schwartz, G. P., Daisey, J. M. and Lioy, P. J. (1981). Effect of sampling duration on the concentration of particulate organics collected on glass fiber filters. Amer. Ind. Hyg. Assoc. J. 42, 258-263.

Shah, J. J., Johnson, R. L., Heyerdahl, E. K. and Huntzicker, J. J. (1986). Carbonaceous aerosol at urban and rural sites in the United States. J. Air Pollution Control Assoc. 36, 254-257.

Simoneit, B. R. T. and Mazurek, M. A. (1982). Organic matter in the troposphere-II. Natural background of biogenic lipid matter in aerosols over the rural western United States. Atmos. Environ. 16, 2139-2159.

Spicer, C. W. and Schumacher, P. M. (1977). Interferences in sampling atmospheric particulate nitrate. Atmos. Environ. 11, 873-876.

Stevens, R. K., Dzubay, T. G., Shaw, R. W., McClenny, W. A., Lewis, C. W. and Wilson, W. E. (1980). Characterization of the aerosol in the Great Smoky Mountains. Environ. Sci. Tech. 14, 1491-1498.

Tanner, R. L., Gaffney, J. S. and Phillips, M. F. (1982). Determination of organic and elemental carbon in atmospheric aerosol samples by thermal evolution. Anal. Chem. 54, 1627-1630.

Thomas, J. F., Mukai, M. and Tebbens, B. D. (1968). Fate of airborne benzo(a)pyrene. Environ. Sci. Tech. 2, 33-39.

Thrane, K. and Mikalsen, A. (1981). High volume sampling of airborne polycyclic aromatic hydrocarbons using glass fibre filters and polyurethane foam. Atmos. Environ. 15, 909-918.

Tu, K.-W. (1984). An evaluation of an ultra-high-volume airborne particulate sampler, the LEAP. Amer. Ind. Hyg. Assoc. J. 45, 360-364.

Van Vaeck, L. and Van Cauwenberghe, K. (1978). Cascade impactor measurements of the size distribution of the major classes of organic pollutants in atmospheric particulate matter. Atmos. Environ. 12, 2229-2239.

Van Vaeck, L., Van Cauwenberghe, K. and Janssens, J. (1984). The gas-particle distribution of organic aerosol constituents: measurement of the volatilization artifact in Hi-Vol Cascade Impactor Sampling. Atmos. Environ. 18, 417-430.

Van Vaeck, L. and Van Cauwenberghe, K. A. (1985). Characteristic parameters of particle size distributions of primary organic constituents of ambient aerosols. Environ. Sci. Tech. 19, 707-716.

Whalen, J. W. (1968). Adsorption on low-energy surfaces: hexane and octane adsorption on polytetrafluoroethylene. J. Colloid Interface Sci. 28, 443-448.

Witz, S. and Wendt, J. G. (1981). Artifact sulfate and nitrate formation at two sites in the South Coast Air Basin. A collaborative study between the South Coast Air Quality Management District and the California Air Resources Board. Environ. Sci. Tech. 15, 79-83.

Witz, S., Smith, M. M. and Moore, A. B. (1983). Comparative performance of glass fiber hi-vol filters. J. Air Pollut. Control Assoc. 33, 988-991.